REPUBLIC OF TURKEY
YILDIZ TECHNICAL UNIVERSITY
GRADUATE SCHOOL OF NATURAL AND APPLIED SCIENCES

A NEW METHOD FOR QT INTERVAL ANALYSIS OF ECG SIGNALS BASED ON GAUSSIAN MIXTURE MODEL AND NEURAL NETWORK

MEHMET İŞCAN

MSc. THESIS
DEPARTMENT OF MECHATRONIC ENGINEERING
PROGRAM OF MECHATRONICENGINEERING

ADVISER
PROF. DR.FARUK YİĞİT

CO-ADVISER
ASSIST. PROF. CUNEYT YILMAZ

İSTANBUL, 2016

REPUBLIC OF TURKEY
YILDIZ TECHNICAL UNIVERSITY
GRADUATE SCHOOL OF NATURAL AND APPLIED SCIENCES

A NEW METHOD FOR QT INTERVAL ANALYSIS OF ECG SIGNALS BASED ON GAUSSIAN MIXTURE MODEL AND NEURAL NETWORK

A thesis submitted by Mehmet İŞCAN in partial fulfillment of the requirements for the degree of **MASTER OF SCIENCE** is approved by the committee on 23.04.2016 in Department of Mechatronic Engineering,Mechatronic Engineering Program.

Thesis Adviser

Prof. Dr. Faruk YİĞİT

Yıldız Technical University

Co- Adviser

Assoc. Prof. Dr. Cuneyt YILMAZ

Yıldız Technical University

Approved By the Examining Committee

Prof. Dr. Faruk YİĞİT

Yıldız Technical University _____

Prof.Dr. Musa Hakan ASYALI

Yıldız Technical University _____

Prof. Dr., Volkan TUZCU

İstanbul Medipol University _____

ACKNOWLEDGEMENTS

This work would not have been possible without the support of the İstanbul Medipol University Pediatric Cardiology Department and Yıldız Technical University Mechatronic Engineering deparment. I am especially indebted to Dr. Volkan TUZCU and Dr. Musa Hakan ASYALI , who have been supportive of my career goals and who worked actively to provide me with the protected academic time to pursue those goals.

I am grateful to all of those with whom I have had the pleasure to work during this and other related projects. Each of the members of my Dissertation Committee has provided me extensive personal and professional guidance and taught me a great deal about both scientific research and life in general. I would especially like to thank Dr. Dr. Faruk YİĞİT, the one of my committee. As my teacher and mentor, he has taught me more than I could ever give him credit for here. He has shown me, by his example, what a good scientist (and person) should be.

Nobody has been more important to me in the pursuit of this project than the members of my family. I would like to thank my parents, whose love and guidance are with me in whatever I pursue. They are the ultimate role models.

June, 2016

Mehmet İŞCAN

TABLE OF CONTENTS

Page

LIST OF SYMBOLS vi

LIST OF ABBREVIATIONS vii

LIST OF FIGURES viii

LIST OF TABLES x

ABSTRACT xii

ÖZET xiv

CHAPTER 1

INTRODUCTION 1

1.1 Literature Review 1
1.2 Objective of the Thesis 1
1.3 Hypothesis 1

CHAPTER 2

HEART DISEASES 36

2.1 QT Syndrome 36
2.1.1 Short QT Syndrome 37
2.1.2 Long QT Syndrome 38

CHAPTER 3

THE QT RECOGNITION ALGORITHM WITH NOVEL METHOD 42

3.1 QT Recognition 42
3.1.1 Method 47
3.1.2 Training Algorithm 57
3.1.3 Test 60
3.1.3.1 GMM Algortihm and Back-Propagation Algorithm 60
3.1.3.2 The Novel Approach to Pattern Recognition of ECG 65
3.1.3.2.1 Heartbeat Recognition 71
3.1.3.2.1.1 One-to-One Recognition 71

3.1.3.2.1.2 One-to-Another Recognition.....79
3.1.3.2.2 QT Segment Recognition 86

CHAPTER 4

RESULTS AND DISCUSSION 124

REFERENCES.....129

CIRRUCULUM VITAE.....136

LIST OF SYMBOLS

I	Current
ϕ	Flux
r	Radius
V	Voltage
P(.)	Probability
μ	Mean Value
σ	Covariance Value
E[.]	Expectation Value I Current
$l(.)$	Likelihood
α	Membership probability ratio
Σ	Covariance Matrix
g(.)	Gauss Mixture Model Representation
J	Cost Function
η	Learning Rate

LIST OF ABBREVIATIONS

ANN	Artificial Neural Network
AHA	American Heart Assosication
CIRC	Circulation
IEEE	Institute of Electrical and Electronics Engineers
YTU	Yıldız Technical University

LIST OF FIGURES

Page

Figure 1.1 Orientation of cardiac muscle fibers....6
Figure 1.2 Electric events of the Heart....8
Figure 1.3 Electrophysiology of the heart....9
Figure 1.4 The genesis of the electrocardiogram....10
Figure 1.5 The 10 ECG leads of Waller....13
Figure 1.6 Einthoven's leads system....14
Figure 1.7 Einthoven limb leads and Einthoven triangle....15
Figure 1.8 The signal generated by the propagating activation front between a pair of extracellular electrodes....16
Figure 1.9 The vector of the electric activities in the heart - I....19
Figure 1.10 The vector of the electric activities in the heart - II....20
Figure 1.11 The vector of the electric activities in the heart - III....21
Figure 1.12 The vector of the electric activities in the heart - IIII....22
Figure 1.13 The normal electrocardiogram signal....23
Figure 1.14 Wilson Central Terminal....24
Figure 1.15 The circuit of the Wilson Central Terminal and The location of the Wilson Central Terminal in the Image Space....25
Figure 1.16 The circuit of the Goldberger augmented leads and the location of the Goldberger lead vectors in the image space....26
Figure 1.17 Precordial Leads....27
Figure 1.18 The projections of the lead vectors of the 12-Lead ECG system in three orthogonal planes with assumptions....28
Figure 3.1 The scheme for Jensen's theorem....48
Figure 3.2 Comparison of distribution modeling....53
Figure 3.3 The structure of neural network for LLGMN in [89]....58
Figure 3.4 An ideal ECG frame with typical features....60
Figure 3.5 QRS Recognition results with different input....61
Figure 3.6 The distribution of Data for different input....61
Figure 3.7 QRS Recognition results with same input....62
Figure 3.8 The distribution of Data for same input....62
Figure 3.9 QRS Recognition results with same input for different ECG signal....63
Figure 3.10 An ideal QRS complex analysis with neural network....64
Figure 3.11 An ideal QRS complex analysis with neural network for different signal 64
Figure 3.12 QRS Complex Detection with Novel Approach....68
Figure 3.13 QRS Complex Detection with different ECG signal....69
Figure 3.14 P wave detection results....70
Figure 3.15 Q wave detection results....70
Figure 3.16 S wave detection results....71

Figure 3.17 QRS complex recognition with specified parameters.....72
Figure 3.18 Classification results for the end of T wave.....87
Figure 3.19 Classification results for real ECG signal.....88
Figure 3.20 Cluster diagram for T and Artificial Wave.....89
Figure 3.21 Classification results for second (sel116) ECG signal.....94
Figure 3.22 Cluster diagram for T and Artificial Wave under sel116 training data set 95
Figure 3.23 Classification results for second (sel117) ECG signal.....98
Figure 3.24 Cluster diagram for T and Artificial Wave under sel117 training data set 98
Figure 3.25 Cluster diagram for T and Artificial Wave under sel123 training data set 101
Figure 3.26 QRS Complex - T wave incompability in sel14046.....104
Figure 3.27 Cluster diagram for T and Artificial Wave under sel14046 training data set.....107
Figure 3.28 Classification results for second (sel14046) ECG signal with the usage of subset training data of current signal.....108
Figure 3.29 The end of the T wave incompability in sel14157.....111
Figure 3.30 Classification results for (sel14157) ECG signal with changing the lengthened data set.....112
Figure 3.31 Cluster diagram for T and Artificial Wave under sel14157 training data set.....114
Figure 3.32 Classification results for second (sel14157) ECG signal with the usage of subset training data of current signal.....114
Figure 3.33 The illustration of "sel14172" QT signal.....116
Figure 3.34 Classification results for (sel4172) ECG signal.....116
Figure 3.35 Cluster diagram for T and Artificial Wave under sel14172 training data set.....118
Figure 3.36 Classification results for (sel6265) ECG signal.....120
Figure 3.37 Cluster diagram for T and Artificial Wave under sel16265 training data set.....122

LIST OF TABLES

Page

Table 3.1 The characteristic parameters of convergence algorithm.....72
Table 3.2 The recognition results for cost function values.....73
Table 3.3 The characteristic parameters of convergence algorithm for learning rate.... ……..……..……..……74
Table 3.4 The recognition results for learning rate changing..... ……..……..……74
Table 3.5 The characteristic parameters of convergence algorithm for teacher vector ……..……..……75
Table 3.6 The recognition results for teacher vector changing..... ……..……..……76
Table 3.7 The characteristic parameters of convergence algorithm for compare vector ……..……..……77
Table 3.8 The recognition results for compare vector changing..... ……..……..……78
Table 3.9 The characteristic parameters of convergence algorithm for cost value..... ……..……..……79
Table 3.10 The recognition results for cost function value changing..... ……..……..……80
Table 3.11 The characteristic parameters of convergence algorithm for learning rate ……..……..……81
Table 3.12 The recognition results for learning rate changing..... ……..……..……81
Table 3.13 The characteristic parameters of convergence algorithm for learning rate ……..……..……82
Table 3.14 The recognition results for teacher vector changing..... ……..……..……83
Table 3.15 The characteristic parameters of convergence algorithm for learning rate ……..……..……84
Table 3.16 The recognition results for compare vector changing..... ……..……..……85
Table 3.17 The characteristic parameters of the algorithm for QT recognition ……..……..……89
Table 3.18 The characteristic parameters of the algorithm for QT recognition ……..……..……89
Table 3.19 The characteristic parameters of the algorithm for first QT recognition ……..……..……91

Table 3.20 The characteristic parameters of the algorithm for second QT recognition ……..…….....94
Table 3.21 The characteristic parameters of the algorithm for second QT recognition with itself training data ……..…….....96
Table 3.22 The characteristic parameters of the algorithm for third QT recognition ……..…….....97
Table 3.23 The characteristic parameters of the algorithm for third QT recognition ……..…….....99
Table 3.24 The characteristic parameters of the algorithm for fourth QT recognition ……..…….....100
Table 3.25 The characteristic parameters of the algorithm for fourth QT recognition trained by itself……..…….....102
Table 3.26 The characteristic parameters of the algorithm for fifth QT recognition ……..…….....103
Table 3.27 The characteristic parameters of the algorithm for fifth QT recognition after applying the condition ……..…….....106
Table 3.28 The characteristic parameters of the algorithm for fifth QT recognition with the subset of training data after applying the condition ……..…….....109
Table 3.29 The characteristic parameters of the algorithm for sixth QT recognition with the subset of training data after applying the condition ……..…….....110
Table 3.30 The characteristic parameters of the algorithm for sixth QT recognition after applying the correction functions ……..…….....113
Table 3.31 The characteristic parameters of the algorithm for sixth QT recognition with the subset of training data after applying the correction functions ……..…….....115
Table 3.32 The characteristic parameters of the algorithm for sel14172 QT recognition ……..…….....117
Table 3.33 The characteristic parameters of the algorithm for sel14172 QT recognition with the subset of training data ……..…….....119
Table 3.34 The characteristic parameters of the algorithm for sel16265 QT recognition with applying threshold ……..…….....121
Table 3.35 The characteristic parameters of the algorithm for sel16265 QT recognition by using the subset of the current ECG signal with applying threshold ……..…….....123

ABSTRACT

A NEW METHOD FOR QT INTERVAL ANALYSIS OF ECG SIGNALS BASED ON GAUSSIAN MIXTURE MODEL AND NEURAL NETWORK

Mehmet İŞCAN

Department of Mechatronic Engineering

MSc. Thesis

Adviser: Prof. Dr. Faruk YİĞİT

Co-adviser: Assoc. Prof. Dr. Cüneyt YILMAZ

Nowadays, cardiac diseases are the most contributing factor to human death. With the improving technology, some of the cardiac illnesses can be treated but many of the cardiac diseases cannot be determined by experts. The recognition of the diseases on the heart is the most important problem because cardiac signal is non-stationary. To treat the disease, the experts must diagnose the kind of diseases. Several algorithms such as support vector machine, dynamic time wrapping for recognition illness in the heart have been developed but they aren't still being used effectively. Especially, the heart signal which is composed of five types of signal, P, Q, R, S and T is used as the indicator of cardiac activity. Also, the diseases can be diagnosed by analyzing this signal. Especially, in the heart signal, QT interval which is between at the beginning of the QRS complex and at the end of T wave is used to analyze some of the heart signal which is called electrocardiogram signal (ECG). A lengthened QT interval causes the potential of ventricular tachyarrhythmias and it creates a risk factor for sudden death. Because of these, QT interval calculation is very important to diagnose diseases.

In this thesis, we presented a noval approach to measure the QT interval based on expectation maximizaton algorithm with neural network. The organization of the thesis is as follows: In the first Chapter, anatomy of the heart and its electrophyscological properties are described. Major hearth diseases related to ventricular repolarization abnormalities are discussed in Chapter 2. A log linearized Gaussian mixture model

(LLGMN) for the purpose of QT interval analysis is introduced in Chapter 3. In Chapter 4, we presented an improved model that consists of a compare algorithm.

Firstly, all of the components of the heart and its functions will be described. Many types of illness in cardiology will be shown and their explanation will be given. In particular, QT interval analysis will be analyzed and its diseases will be researched by using several algorithms such as a log linearized Gaussian mixture model (LLGMN). Also, ECG circuit will be established and its application will be demonstrated. Today, QT interval isn't being found correctly. This thesis purpose is to find the QT interval measure by new method based on maximum likelihood with neural network. Finally, all of the results will be compared and the best method will be represented in conclusion.

Key words:ECG Pattern Recognition, QT Interval, Neural Network, Gauss Mixture Model

ÖZET

GAUSS KARIŞIM MODELİ VE YAPAY ZEKA TABANINDA EKG'NİN QT ZAMAN ARALIĞININ TESPİTİ ÜZERİNE YENİ BİR METHOD

Mehmet İŞCAN

Mekatronik Mühendisliği Anabilim Dalı

Yüksek Lisans Tezi

Tez Danışmanı: Prof. Dr. Faruk YİĞİT

Eş Danışman: Yrd. Doç. Dr. Cüneyt YILMAZ

Günümüzde kalp hastalıkları insan ölümleri üzerine sebep olan en önemli faktördür. Teknolojinin ilerlemesi ile bazı kalp hastalıkları iyileştirilebilmekte ancak pekçok kalp hastalığı uzmanlar tarafından tespit edilememektedir. Kalp hastalıklarının tanınması en önemli problemlerden biridir çünkü kalp sinyalleri zaman bağlı olarak değişmektedir. Hastalığı iyileştirmek için, uzmanlar hangi hastalığını olduğunu tespit etmek zorundadırlar. Şu ana kadar dinamik zaman öteleme, destek vektör mekanizması hastalıkları tanımak için geliştirilmiştir, ancak hala aktif olarak kullanılamamaktadırlar. Özellikle, P, QRS ve T dalgalarından oluşan kalp sinyali hastalık tespiti için bir indikatör olarak kullanılmaktadır. Ayrıca, hastalıklar bu sinyallerin incelenmesi ile tespit edilebilmektedir. Özellikle, kalbin elektriksel gevşemesini ve kasılmasını gösteren QT zaman aralığı kalp anomalilerinin tespiti için analiz edilmektedir. Uzayan bir QT zaman aralığı ventriküler taşikardiye potansiyel oluşturmaktadır ve bu da ani ölümlere sebep olmaktadır. Bunlardan dolayı, QT zaman aralığının hesaplanması hastalık teşhisleri için önem oluşturmaktadır.

Bu çalışmada, Gauss karışım modeli ve yapay zeka tabanında QT zaman aralığı ölçümü yapabilen bir yeni algoritma sunduk. Tezin içeriği şöyle sıralanabilir: İlk bölümde kalbin anatomik ve elektriksel yapısını açıklanmıştır. İkinci bölümde ventriküler

gevşemeye bağlı hastalıklar tartışılmıştır. Logaritmik lineerleştirilmiş Gauss karışım modeli üçüncü bölümde açıklanmıştır. Dördüncü bölümde karşılaştırılma algoritması ile verilen yeni bir algoritma sunulmuştur. Son olarak, tüm test sonuçları verilmiş ve en iyi metot sonuç bölümünde sunulmuştur.

Anahtar Kelimeler: EKG Kalıp Tanıma, QT Zaman aralığı, Yapay Zeka, Gauss Karışım Modeli,

CHAPTER 1

INTRODUCTION

1.1. Literature Review

In this section, the information about general subjects such as circulatory system, the structure of heart and its functions, the conduction system in the human heart, electrocardiography and its interpretation is given. Also, this section includes the electronic circuit design regarding biomedical devices. Especially, ECG circuit will be explained in this section and its components. Both electronic circuit design and their theoretical explanation will also be described. Apart from these, to process the signal, some of the electronic components and circuit will be suggested based on theoretical processing in this section. Finally, the analysis of the electrocardiogram signal will be described and its application in neural networks will be established for recognition the electrocardiogram signals such as P, Q, R, S and T.

The circulatory system is an organ system that permits blood and lymph circulation to transport nutrients such as amino acids and electrolytes, oxygen, carbon dioxide, hormones blood cells, etc. to and from cells in the body to nourish it and help to fight diseases, stabilize body temperature and pH, to maintain homeostasis. Homeostasis which means that is the property of a system in which variables are regulated so that internal conditions remain stable and relatively constant. For example, it includes the regulation of temperature and the balance pH. Also, the human body's internal environment changes depending on external conditions. It is a process of homeostasis.

The circulatory system in human is often seen as strictly as a blood dispersion network, but some consider the circulatory systems consist of collectively of the cardiovascular system which is composed of the distribution of the blood and lymphatic system. In cardiovascular system, blood is a fluid consisting of plasma, red blood cells, white

blood cells and platelets (thrombocytes that is circulated by the heart through the vertebrate vascular system). The cardiovascular system comprises the blood, heart and the blood vessel. The lymph, lymph nodes, and lymph vessels from the lymphatic system which returns filtered blood plasma from the interstitial fluid as lymph.

The humans have a closed cardiovascular system.Human cardiovascular system includes the pulmonary circulation which carries deoxygenated blood away from the heart to the lungs and returns oxygenated blood back to the heart; and the systematic circulation a loop through rest of the body to provide oxygenated blood.

Pulmonary circulation is the movement of blood from the heart, to the lungs, and back to the heart again. De-oxygenated blood leaves the heart, goes to the lungs, and then re-enters the heart. The only artery in the body leaves the systematic circulation when it enters the right heart, more specifically the right atrium through the superior vena cava. The blood is then pumped through the tricuspid valve which is the same as right atrioventricular valve, into the right ventricle. Blood is then pumped through the semilunar valve and into the pulmonary artery.

The human cardiovascular system is closed which means that the blood never leaves the network of blood vessels. On the other hand, the lymphatic system isn't closed. Besides these, blood vessels are an important part of the circulatory system. They are the body's highways that allow blood to flow quickly and efficiently from the heart to every region of the body and back again. All blood vessels contain a hollow area called the lumen through which blood is able to flow. Around the lumen is the wall of vessel which may be thin in the case of capillaries or very thick in the case of arteries.

All blood vessels are lined with a thin layer of simple squamous epithelium which is known as the endothelium that keeps blood cells inside of the blood vessels and prevents clots from the forming. The endothelium lines the entire circulatory system, all the way to the interior of the heart, where it is called the endocardium.

There are three major types of blood vessels: arteries, capillaries and veins. Generally, blood vessels are often named by looking the region of the body through which they carry blood or for nearby structure. For instance, the brachiocephalic artery carries blood into the brachial (arm) and cephalic (head) regions. Sequentially, they can be expressed with the explanation of its function.

Arteries and Arterioles, respectively, are blood vessels that carry blood away from the heart and are narrower arteries that branch off from the ends of arteries and carry blood to capillaries. Arteries includes highly oxygenated, because the body is feed this vessel. The pulmonary trunk and arteries of the pulmonary circulation loop are exception in this vessel. Arteries face high levels of blood pressure as they carry blood being pushed from the heart under great force. So the arteries walls are thicker, more elastic and more muscular than those of other vessels. Smaller arteries are more muscular in the structure of their walls. The smooth muscles of the arterial walls of these smaller arteries contract or expand to regulate the flow of blood through their lumen. In this way, the body controls how much blood flows to different parts of the body under varying circumstances. Arterioles face much lower blood pressures than arteries due to their greater number. Therefore, it walls are much thinner than those of arteries. Arterioles, like arteries, are able to use smooth muscle to control their aperture and regulate glow and blood pressure.

Capillaries are the smallest and thinnest of the blood vessels in the body and also the most common. They provide nutrient or blood running throughout almost every tissue of the body. The walls of capillaries consist of only a thin layer of endothelium so that there is the minimum amount of structure possible between the blood and the tissues. The endothelium acts as a filter to keep the blood cells inside of the vessels while allowing liquids, dissolved gases and other chemicals to diffuse along their concentration gradients into or out of tissues.

Veins and Venules, respectively, are the large return vessels of the body and act as the blood return counterparts of arteries and are similar to arterioles as they are small vessels that connect capillaries, but unlike arterioles, venules link to veins instead of arteries. Venules' task is to pick up blood from many capillaries and deposit it into larger veins for transport back to the heart.

Also, there is **coronary circulation** in this system. It provides that myocardium with the oxygen and nutrients necessary to pump blood throughout the body. The left and right coronary arteries branch off from the aorta and provide blood to the left and right sides of the heart. It belongs to the heart particularly.

To feed the stomach, the veins of the stomach and intestines perform a unique function: instead of carrying blood directly back to the heart, they carry blood to the liver through

the hepatic portal vein because the blood provides itself to nutrient and other chemicals from there. The liver removes the toxins, stores sugars and processes the products of digestion before they reach the other body tissue. This blood is carried through the inferior vena cava.

The critical part of the circulation system, blood is made up of red blood cells, white blood cells, platelets and liquid plasma. As a liquid, blood is used to transport nutrients, wastes, oxygen, carbon dioxide and hormones.

Red blood cells, also known as erythrocytes, are by far the most common type of blood cell and make up about 45% of blood volume. Red blood cells are produced inside of red bone marrow from stem cells at the astonishing rate of about 2 million cells every second. Erythrocytes transport oxygen in the blood through the red pigment hemoglobin. Hemoglobin contains iron and proteins joined to greatly increase the oxygen carrying capacity of erythrocytes. The high surface areas to volume ratio of erythrocytes allow oxygen to be easily transferred into the cell in the lungs and out of the cell in the capillaries of the systemic tissues.

White blood cells which are known as leukocytes make up a very small percentage of the total number of cells in the bloodstream, but have important functions in the body's immune system. It has two types of white blood cells, granular and agranular leukocytes . Granular leukocytes are used to neutralize the bacteria that invade the body. Agranular leukocytes develop into cells called macrophages that engulf and ingest pathogens and the dead cells from wounds or infections.

Thrombocytes are small cell fragments responsible for the clotting of blood and the formation of scabs.

Plasma is the non-cellular or liquid portion of the blood that makes up about 55% of the blood's volume. Plasma is a mixture of water, proteins and dissolved substances.

After that, cardiovascular system physiology can be described in three major functions: transportation materials, protection from pathogens and regulation of the body's homeostasis.

The other system of the circulation is **lymphatic system**. Lymphatic systems is an extension of the circulatory system consisting of a fluid known as lymph, capillaries called lymphatic vessels, and structures called lymph nodes. **Lymph** is a watery fluid

derived from plasma that has seeped out of the blood system capillaries and mingled with the cells. Rather than returning to the heart through the blood veins, this lymph enters a series of one-way **lymphatic vessels** that return the fluid to the circulatory system. Along the way, the ducts pass through hundreds of tiny, capsule like bodies called **lymph nodes.** Located in the neck, armpits, and groin, the lymph nodes contain cells that filter the lymph and phagocytize foreign particles.

The **spleen** is composed primarily of lymph node tissue. Lying close to the stomach, the spleen is also the site where red blood cells are destroyed. The spleen serves as a reserve blood supply for the body.

The lymph nodes are also the primary sites of the white blood cells called lymphocytes. The body has two kinds of lymphocytes: **B-lymphocytes** and **T-lymphocytes.** Both of these cells can be stimulated by microorganisms or other foreign materials called**antigens** in the blood. Antigens are picked up by phagocytes and lymph and delivered to the lymph nodes. Here, the lymphocytes are stimulated through a process called the**immune response.**

Certain antigens, primarily those of fungi and protozoa, stimulate the T-lymphocytes. After stimulation, these lymphocytes leave the lymph nodes, enter the circulation, and proceed to the site where the antigens of microorganisms were detected. The T-lymphocytes interact with the microorganisms cell to cell and destroy them. This process is called **cell-mediated immunity.**

B-lymphocytes are stimulated primarily by bacteria, viruses, and dissolved materials. On stimulation, the B-lymphocytes revert to large antibody-producing cells called **plasma cells.** The plasma cells synthesize proteins called **antibodies**, which are released into the circulation. The antibodies flow to the antigen site and destroy the microorganisms by chemically reacting with them in a highly specific manner. The reaction encourages phagocytosis, neutralizes many microbial toxins, eliminates the ability of microorganisms to move, and causes them to bind together in large masses. This process is called **antibody-mediated immunity.** After the microorganisms have been removed, the antibodies remain in the bloodstream and provide lifelong protection to the body. Thus, the body becomes immune to specific disease microorganisms.

The heart is located in the chest between the lungs behind the sternum and above the diaphragm. It is surrounded by the pericardium. Its size is about that of a fist, and its weight is about 250-300 g. Its center is located about 1.5 cm to the left of the midsagittal plane. Located above the heart are the great vessels: superior and inferior vena cava, the pulmonary artery and vein, as well as the aorta. The aortic arch lies behind the heart. The esophagus and the spine lie further behind the heart.

In order to cover the anatomy of the heart, the walls of the heart are composed of cardiac muscle, called myocardium. It also has striations similar to skeletal muscle. In addition, it should be examined that the muscle fibers are oriented spirally and are divide into four groups: Two groups of fibers wind around the outside of both ventricles. Beneath these fibers a third group winds around both ventricles. Beneath these fibers a fourth group winds on around the left ventricle. It is the fact that cardiac muscle cells are oriented more tangentially than radially, and that the resistivity of the muscle is lower in the direction of the fiber has importance in electrocardiography and magnetocardiography. The following figure illustrates the schematic of oriented fibers in the heart.

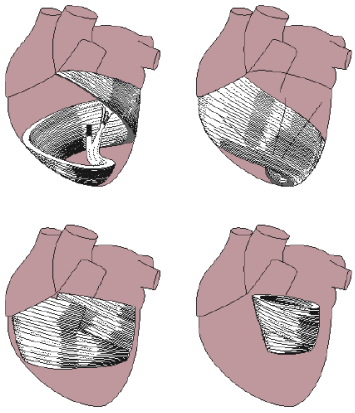


Figure. 1.1 Orientation of cardiac muscle fibers

It was described that the electricity of the heart passes through the line in the fibers. Therefore, **cardiac muscle cell** must be investigated to understand well. In the heart muscle cell, or myocyte, electric activation takes place by means of the same mechanism as in the nerve cell that is from the inflow of sodium ions across the cell membrane. The amplitude of the action potential is also similar, being about 100 mV for both nerve and muscle. The duration of the cardiac muscle impulse is, however, two orders of magnitude longer than that in either nerve cell or skeletal muscle. This is

called “plateau phase” which follows cardiac depolarization and thereafter repolarization takes place. In the nerve cells, repolarization is defined as a consequence of the outflow of potassium ions.

Associated with the electric activation of cardiac muscle cell is its mechanical contraction, which happens a little later. For the sake of comparison with the another kind of cells, the corresponding comparison is given to demonstrates the electric activity and mechanical contraction of frog Sartorius muscle, frog cardiac muscle and smooth muscle from the rat uterus [3].

Muscle cell in Frog Sartorius arises instantly and falls down immediately. However, Frog cardiac muscle cell can propagate much longer than the normal muscle. On the other hand, in Rat uterus wall smooth muscle cell is stimulated consecutively.

An important distinction between cardiac muscle tissue and skeletal muscle is that activation can propagate from one cell to another in any direction. As a result, the activation wavefronts are of rather complex shape. The only exception represents that the boundary between the atria and ventricles, which the activation wave normally cannot cross except along a special conduction system, since a nonconducting barrier of fibrous tissue is present.

As for **the conduction system of the heart**, it has been explained in the previous sections. However, there is some of the information about it. The atrioventricular node (AV Node) is placed at the boundary between the atria and ventricles, it possesses intrinsic frequency of about 50 pulses/min. However, if the AV node is triggered with a higher pulse frequency, it follows this higher frequency. In a normal heart, the AV node provides the only conducting path form the atria to the ventricles. Under normal circumstances, the latter can be excited only by pulses that propagate through it.

Propagation from the AV node to the ventricles is provided by a specialized a conduction system. Proximally, this system consists of a common bundle, called the bundle of His which is named after German physician Wilhelm His. More distally it separates into two bundle branches propagation along each side of the septum, constituting the right and left bundle branches. Even more distally the bundles ramify into Purkinje fibers that diverge to the inner sides of the ventricular walls. Propagation along the conduction system takes place at a relatively high speed once it is within the ventricular region, but prior to this the velocity is extremely slow.

From the inner side of the ventricular wall, the many activation sites cause the formation of a wavefront which propagates through the ventricular mass toward the outer wall. This process is called as “cell-to-cell activation”. After each ventricular muscle region has depolarized, repolarization occurs. Repolarization does not include the propagating phenomenon, because the duration of the action impulse much shorter at the epicardium than at the endocardium. **Epicardium** refers to as the outer side of the cardiac muscle and **endocardium** denotes the inner side of the cardiac muscle. The termination of activity appears as if it were propagating from epicardium toward the endocardium, that is, from the outer side of the cardiac muscle toward the inner side of the cardiac muscle. It is sourced due to fact that the intrinsic rate of the sinus node is the greatest; it sets the activation frequency of the whole heart. If any problems occur from the atria to the AV node, the AV node is adopted its intrinsic frequency. In addition, if the conduction system is failed at the bundle of His, the ventricles will beat at the determined frequency by their own region that has the highest frequency, that is, it equals to sinus node frequency. The electric events are given in figure (1.2).

Location in the heart	Event	Time [ms]	ECG-terminology	Conduction velocity [m/s]	Intrinsic frequency [1/min]
SA node	impulse generated	0		0.05	70–80
atrium, Right	depolarization *)	5	P	0.8–1.0	
Left	depolarization	85	P	0.8–1.0	
AV node	arrival of impulse	50	P–Q interval	0.02–0.05	
	departure of impulse	125			
bundle of His	activated	130		1.0–1.5	
bundle branches	activated	145		1.0–1.5	
Purkinje fibers	activated	150		3.0–3.5	
endocardium					
Septum	depolarization	175		0.3 (axial)	20–40
Left ventricle	depolarization	190		–	
			QRS	0.8	
epicardium	depolarization	225		(transverse)	
Left ventricle	depolarization	250			
Right ventricle					
epicardium					
Left ventricle	repolarization	400			
Right ventricle	repolarization				
			T	0.5	
endocardium					
Left ventricle	repolarization	600			

Figure. 1.2 Electric events of the Heart

All of the electric activity of the heart is illustrated as the following graph.

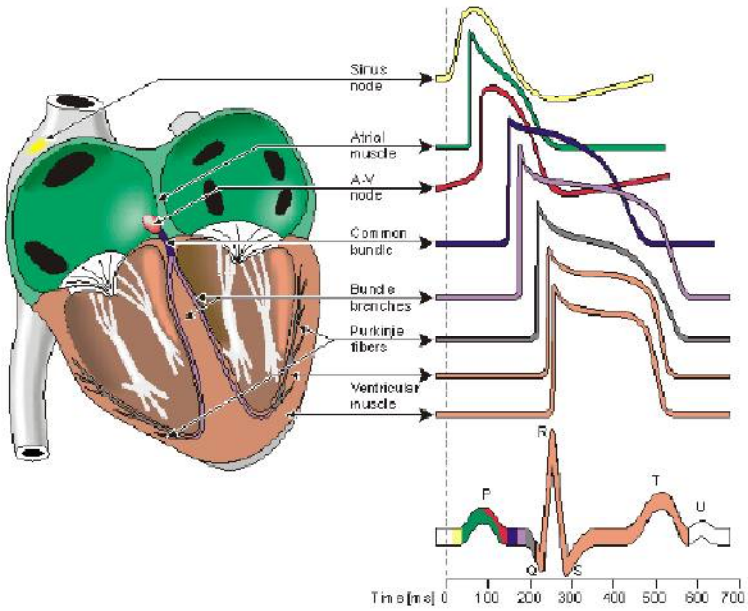


Figure. 1.3 Electrophysiology of the heart

The above explanations discuss cardiac electric events on an intracellular level. Such electric signals illustrating fig. (1.3) may be recorded with an electrode which is inserted inside a cardiac muscle cell. However, the **electrocardiogram** is a recording of the electric potential, generated by the electric activity of the heart, on the surface of the thorax. Thus the ECG refers to as **the extracellular activity of the cardiac muscle tissue**.

The following figure illustrates a segment of cardiac tissue through which propagating depolarization (A) and repolarization (B) wavefront planes are passing.

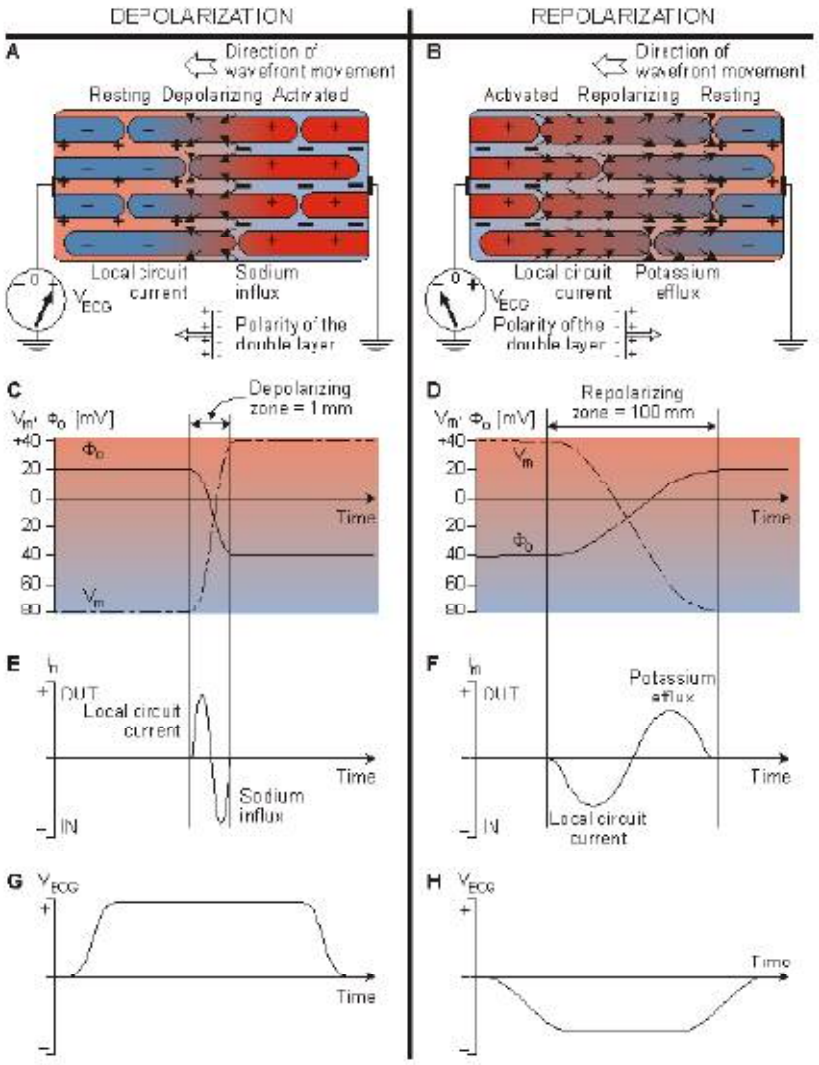


Figure. 1.4 The genesis of the electrocardiogram

The wavefronts move from right to left, which means that the time axis points to the right. There are two important properties of cardiac tissue that we shall make use of to analyze the potential and current distribution associated with these propagating waves. First, cells are interconnected by low-resistance pathways, as a result of which currents flowing in the intracellular space of one cell pass freely into the following cell. Second, the space between cells is very restrictive. As a conclusion, both intracellular and extracellular currents are confined to the direction parallel to the propagation of the plane wavefront.

It can be said that both intracellular and extracellular currents flow in a linear path by using **linear core conductor model**. Accordingly, when using the condition $I_i + I_o = 0$ and equation (1) can be derived with an appropriate **linear core conductor model**.

$$\frac{\partial \varphi_i}{\partial x} = -I_i r_i \quad , \quad \frac{\partial \varphi_0}{\partial x} = -I_0 r_0 \tag{1.1}$$

Then we can obtain the following formula.

$$\frac{\partial \varphi_i}{\partial x} = I_0 r_i \quad , \quad \frac{\partial \varphi_0}{\partial x} = -I_0 r_0 \tag{1.2}$$

Integrating from $x = -\infty, to\ x = x$ gives,

$$\varphi_i = r_i \int I_0 dx, \qquad \varphi_0 = r_0 \int I_0 dx, \tag{1.3}$$

When applying$V_m = \varphi_i - \varphi_0$, the definition of the transmembrane potential, we obtain:

$$V_m = (r_i + r_0) \int I_0 dx \tag{1.4}$$

According to the linear core conductor conditions, the important relation can be represented as the following formulas.

$$\varphi_i = \frac{r_i}{r_i + r_0} V_m \varphi_0 = -\frac{r_0}{r_i + r_0} V_m \tag{1.5}$$

Note that they depend on the validity of which requires that there are no external currents in the region under consideration [4].

The genesis of the electrocardiogram has been given in figure 4. Therefore, **depolarization wave** can be explained by using equations given. Eqn. (4) and (5) are applied to the propagating wave under investigation. The variation of $V_m(x)$ is easily inferred from figure 4 as dashed line since in the activated region it is at the **plateau voltage**, generally around +40 mV, whereas in the resting region it is around -80 mV. In figure 4, the ratio of resistors has been chosen on the basis of experimental evidence for propagation along the cardiac fiber axis as 1 [5]. According to these information, the transmembrane current $I_m$can be examinedfrom $V_m(x)$ in figure 4 by applying general cable equation as the following formula.

$$\phi_0 = \frac{r_0}{r_0 + r_i} V_m \tag{1.6}$$

The transmembrane current can be expressed by the following equation:

$$i_m = \frac{1}{r_o + r_i} \frac{\partial^2 V_m}{\partial x^2} \tag{1.7}$$

An examination of the extracellular potential ϕ_0 demonstrates it to be uniform except for a rapid change across the wavefront. Such a variation from plus to minus is what one would expect at a double layer source where the dipole direction is from right to left. It

can be concluded that **for the depolarization of cardiac tissue a double layer appears at the wavefront with the dipole orientation in the direction of propagation.** One can also approximate the source as proportional to the transmembrane current - estimated here by a lumped negative point source and a lumped positive point source which gotten together constitutea dipole in the direction of propagation.

As a result, a double layer, whose positive side is pointing to the recording electrode produces a positive ECG signal.

Secondly, **repolarization wave** is in principle very different from the depolarization wave. The repolarization is not a propagating phenomenon. Repolarization in the cell occurs because the action pulseis active restrictive duration. Thus, the cell repolarizes at a certain instant of time after its depolarization, not because of the repolarization of an adjoining cell. The repolarization would accurately follow the same sequence as depolarization when the action pulses of all cells are of equal duration. In reality, it is not the case in ventricular muscle. The action pulses of the epicardial (outer)cells are of shorter duration than those of the endocardial (inner) cells. So, the "isochrones" of repolarizing cells proceed from the epicardium (outer) to the endocardium (inner) giving the illusion that the repolarization proceeds as a wave from epicardium (outer)to endocardium (inner).

If the cardiac action pulse were always of the same shape, then following propagation of depolarization from right to left, the recovery would also proceed from right to left. This case is illustrated in the highly idealized figure 10B, where the cells that were activated earliest must recover first. The recovery of cardiac cells is relatively slow, requiring approximately 100 ms. For this reason, in figure 10B it has been depicted the recovery interval as much wider than the activation internal.

The polarity of $V_m(x)$decreases from its plateau value of +40 mV on the left to the resting value of -80 mV on the right in figure 10D. Again, equation (5) may be performed, in this case showing that the extracellular potential ϕ_0 (solid line) increases from minus to plus. In this case the double layer source is directed from left to right. Then, it is spread out over a wide region of the heart muscle.

The transmembrane current I_m can be examined from $V_m(x)$in figure 10D by applying equation (6). As shown in figure 10B, to the right of the centerline it is outward and just to the left it is inward. The outward portion reflects the potassium efflux due to the rapid

rise of potassium permeability. The current inflow is again the "local circuit"current. The course of the transmembrane current during repolarization is approximated in figure 10F. Thus, in repolarization, a double layer is formed that is similar to that observed during depolarization. The double layer in repolarization, however, has a polarity opposite to that in depolarization, and thus its negative side points toward the recording electrode; as a result, a negative (ECG) signal is recorded as figure 2H.

In real heart muscle, since the action potential duration at the epicardium is actually shorter than at the endocardium, the recovery phase appears to move from epicardium to endocardium. That is to say, the opposite to direction as the activation dipole occurs. As a consequence the recovery dipole is in the same dipoles are thus in the same direction one can describe the common observation that the normal activation and recovery ECG signal has the same polarity.

Augustus Desire Waller obtained the human electrocardiogram in 1887 using Lippman's capillaryelectrometer [6]. He used five electrode locations: the four extremities and the mouth to maximize the ECG signal. Furthermore, the electrode location is defined and the attachment of electrodes facilitated at the limb positions. The five measurement points generate altogether 10 different leads. From these 10 possibilities he selected five - designated **cardinal leads**. Two of these are identical to the **Einthoven leads I** and **III** described below. Waller's leads is illustrated in figure (1.5).

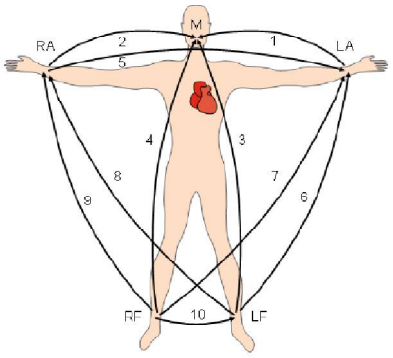


Figure. 1.5 The 10 ECG leads of Waller

Willem Einthoven also performed the capillary electrometer in his first ECG recordings. His essential contribution to ECG-recording technology was the development and application of the string galvanometer. Its sensitivity greatly exceeded the previously used capillary electrometer. It was invented by Clement Ader [7].In 1908, Einthoven

reported a description of the first clinically vital ECG measurement system. Einthoven's lead system is given in figure (1.6).

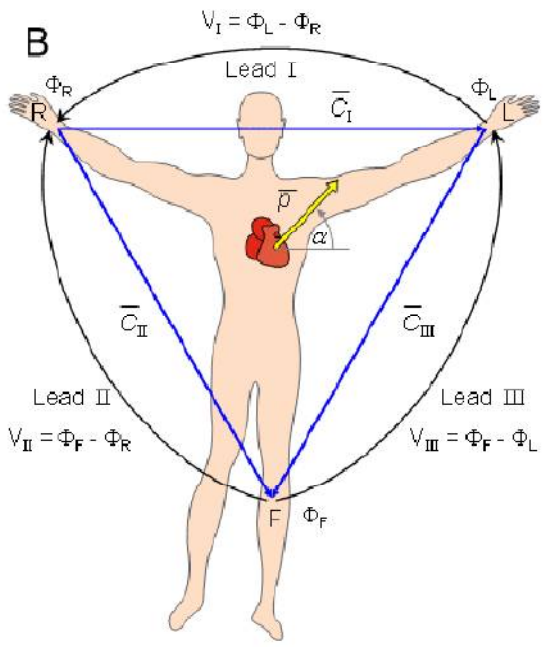


Figure. 1.6 Einthoven's leads system

In accordance with Einthoven lead system previously given in figure (1.3), **limb leads** can be derived in order to define the voltage difference between two points.

$$Lead\ I = V_1 = \phi_L - \phi_R \tag{1.7}$$

$$Lead\ II = V_2 = \phi_F - \phi_R \tag{1.8}$$

$$Lead\ III = V_3 = \phi_F - \phi_L \tag{1.9}$$

where $V_1, V_2\ and\ V_3$ denotethe voltage of Lead I, II and III, respectively. $\phi_L, \phi_R\ and\ \phi_F$ represent potential at the left arm, right arm and left foot, respectively. According to Kirchhoff's law, these lead voltages have the following relationship:

$$V_1 + V_3 = V_2 \tag{1.10}$$

hence only two of these three leads are independent.

The lead vectors associated with Einthoven's lead system are conventionally found based on the assumption that the heart is located in **an infinite, homogeneous volume conductor (or at the center of a homogeneous sphere representing torso)**. One can demonstrate that if the position of the right arm, left arm and left leg are at the vertices

of an equilateral triangle, having the heart located at its center, then the lead vectors also form an equilateral triangle.

A simple model conclusions from supposing that the cardiac sources are denoted by a dipole placed at the center of a sphere representing the torso, thus, at the center of the equilateral triangle. With these assumptions, the voltages measured by the three limb leads are proportional to the projections of the electrical heart vector on the sides of the lead vector triangle. It is shown as the following figure.

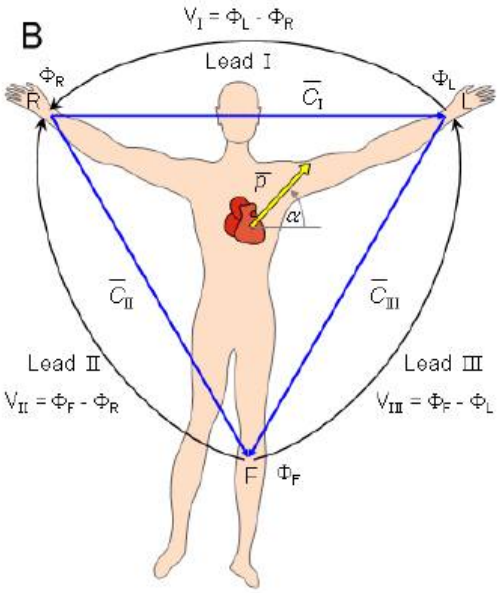


Figure. 1.7 Einthoven limb leads and Einthoven triangle

The voltages of the limb leads can be obtained as the following formula which is duplicated below [8].

$$V_I = pcos(\alpha) = p_y \tag{1.11}$$

$$V_{II} = \frac{p}{2}\cos(\alpha) - \frac{3^{\frac{1}{2}}}{2}psin(\alpha) = 0.5p_y - 0.87p_z \tag{1.12}$$

$$V_{III} = -\frac{p}{2}\cos(\alpha) - \frac{3^{\frac{1}{2}}}{2}psin(\alpha) = -0.5p_y - 0.87p_z \tag{1.13}$$

When the equations are substituted into equation (10), we obtain:

$$V_I + V_{III} = \frac{p}{2}\cos(\alpha) - \frac{3^{\frac{1}{2}}}{2}psin(\alpha) = V_{II} \tag{1.14}$$

Up to now, general equations and representations of the heart model have been evaluated and derived appropriately. Now, we can focus on the generation of the Electrocardiography signal in detail. For this purpose, it should be considered that a simple example explaining what kind of signal a propagating activation front produces in a volume conductor. Besides, a volume conductor and a pair of electrodes on its opposite surfaces should be split into four parts, A, B, C and D, respectively.

In the case **A**, when the depolarization front propagates toward a positive electrode, it generates a positive signal. In the case **B**, when propagation of activation is away from the positive electrode, the signal possesses the corresponding negative polarity. For the case **C**, it is understandable that when the repolarization front propagates toward a positive electrode, the signal is negative. Although it is known that repolarization does not actually spread, a boundary between repolarized and still active regions can be defined as function of time. Finally, for case **D**, when the direction of propagation of a repolarization front is away from the positive electrode, a positive signal is generated.

The following figure represents all of the cases in volume conductor and pair of electrodes.

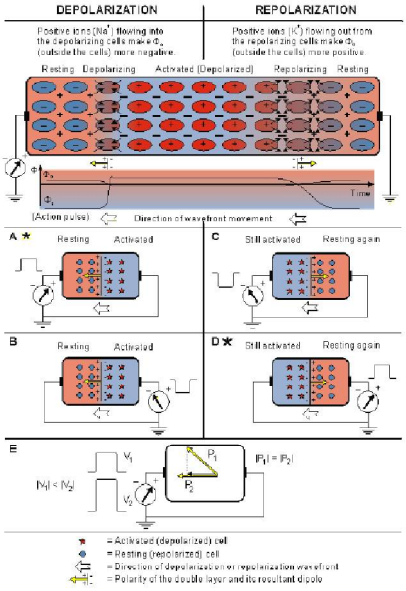


Figure. 1.8 The signal generated by the propagating activation front between a pair of extracellular electrodes

The positive polarity of the signal in case **A**can be verified in the following way. We note that the transmembrane voltage ahead of the wave is negative since this region is

still at rest. Behind the wavefront, the transmembrane voltage is in the plateau stage; thus, it is positive.

What is vital here is that the orientation of the double layer, given by the negative spatial derivative of V_m, is entirely to the left since the diploes are directed toward the positive electrode, the signal is positive.

The negative polarity of the signal in the case **C** can be confirmed in the following way. The direction of repolarization allows us to designate in which regions V_m is negative and positive. In this highly idealized example, it can be showed that repolarization as occurring instantly at the minus to plus interface. However, the source associated with this spatial distribution of V_m is still found**line dipole density source**. It is given as the following equation:

$$\varphi = \frac{1}{4\pi\sigma_0}\int\left(-\sigma_i\pi a^2\frac{\partial V_m}{\partial x}\right)\nabla\left(\frac{1}{r}\right)\overline{a_x}dx \tag{1.15}$$

Application of that equation demonstrates that the double layer, given by the negative spatial derivative, is zero everywhere except at the repolarization wavefront, where it is oriented to the right. Since the sources dipoles are directed away from the positive electrode, a negative signal will be measured.

For the case D, activation does not spread directly toward an electrode, the signal is proportional to the component of the velocity in the direction of the electrode, as shown in figure 8E. Note that the possible influence of a changing extent of the wave of activation with a change in directionare ignored. Special attention should be given to cases A and D, marked with an asterisk, since these reflect the fundamental relationships.

General structure of contraction in heart muscle has been given in order to cover the mechanism of electrical dynamics. Now, the formation of the ECG signalshould be discussed because ECG signal propagates in three directions. Therefore, it is important to show how heart signal propagates toward any direction in the heart.

The cells that constitute the ventricular myocardium are coupled together by gap junctions which, for normal healthy heart, have a very low resistance. As a result, activity from one cell to another is rapidly propagated. It can be said that the heart behaves as a syncytium which refers to having an effect on the neighboring cells. That is, a propagation wave once initiated continues to spread out uniformly into the region

that is still at rest. Now, we can apply these results to the heart if we considers it to be composed of uniform fibers. These equivalent fibers are a valid representation because they are consistent with the syncytial nature of the heart.In fact, syncytium reflects connectivity in all directions, the fiber orientation may be chosen at our convenience.

Much of what we know about the activation sequence in the heart comes from canine studies. The earlier comprehensive study in this area was made by Scher and Young [9]. Such studies were performed on the human heart, and a seminal paper describing the results was published by Durrer et al. These studies demonstrate that activation wavefronts proceed relatively uniformly, from endocardium to epicardium and from apex to base.

One way of describing cardiac activation is plotting the sequence of instantaneous depolarization wavefronts. Since these surfaces connect all points in the same temporal phase, the wavefront surfaces are also referred to as isochrones. An evaluation of dipole sources can be performed by applying generalized equation (15) to each equivalent fiber. This process contains taking the spatial gradient of V_m. If we assume that on one side cells are entirely at rest, while on the other cells are entirely in the plateau phase, the source is zero, everywhere except at the wavefront. As a conclusion, the wavefront or isochrone not only describes the activation surface but also shows the location of the double layer sources.

From the above it should be possible to evaluate the actual generation of the ECG by taking into account realistic progression of activation double layers. Such a description is contained in below figures. At the beginning of the loop, the activation of the heart has begun at the sinus node, it propagates along the atrial walls. The resultant vector of the atrial electric activity is depicted with a thick arrow. The projections of this resultant vector on each of the three Einthoven limb leads is positive, and thus, the measured signals are also positive. After the depolarization has propagated over the atrial walls, it reaches the AV node. The propagation through the AV junction is very slow and involves negligibleamount of tissue; it concludes in a delay in the progress of activation.

Once activation has received the ventricles, propagation proceeds along the Purkinje fibers to the inner walls of the ventricles. The ventricular depolarization is sourced from the left side of the interventricular septum, and therefore, the final dipole from this

septal activation points to the right. This is shown in figure 15, 16,17 and 18 as negative signal in leads I and II.

In the next phase, depolarization waves occur on both sides of the septum, and their electric forces cancel. However, early apical activation is also occurring, so the resultant vector points to the apex.

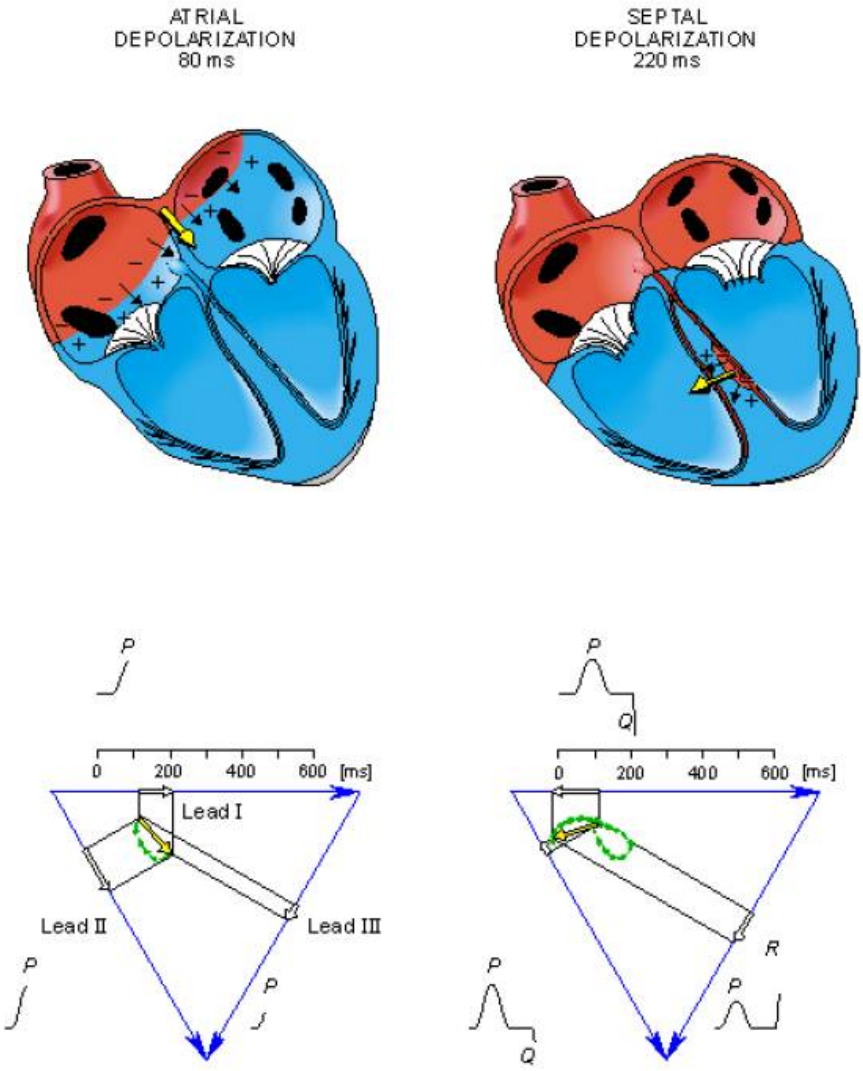


Figure. 1.9 The vector of the electric activities in the heart - I

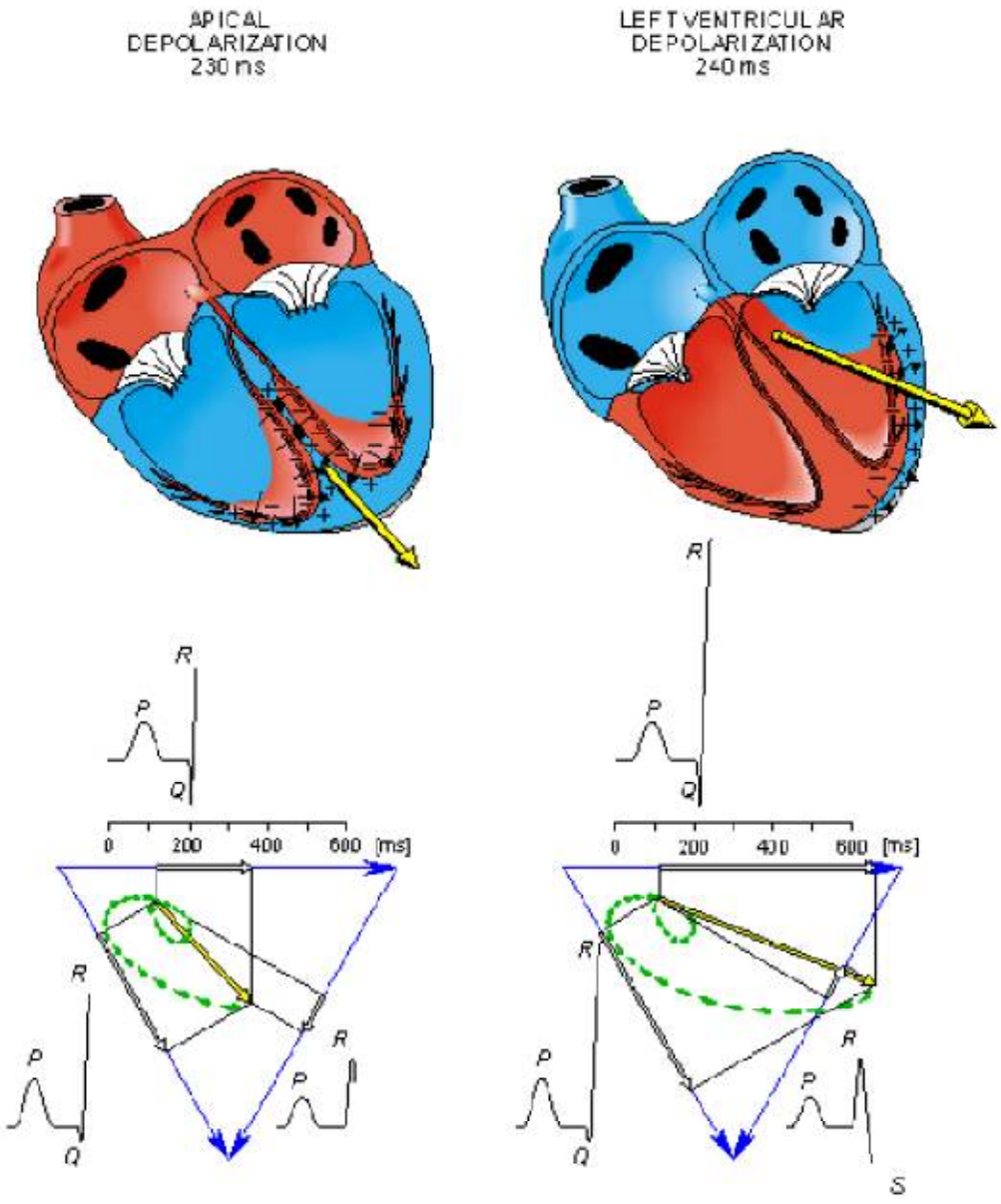


Figure. 1.10 The vector of the electric activities in the heart - II

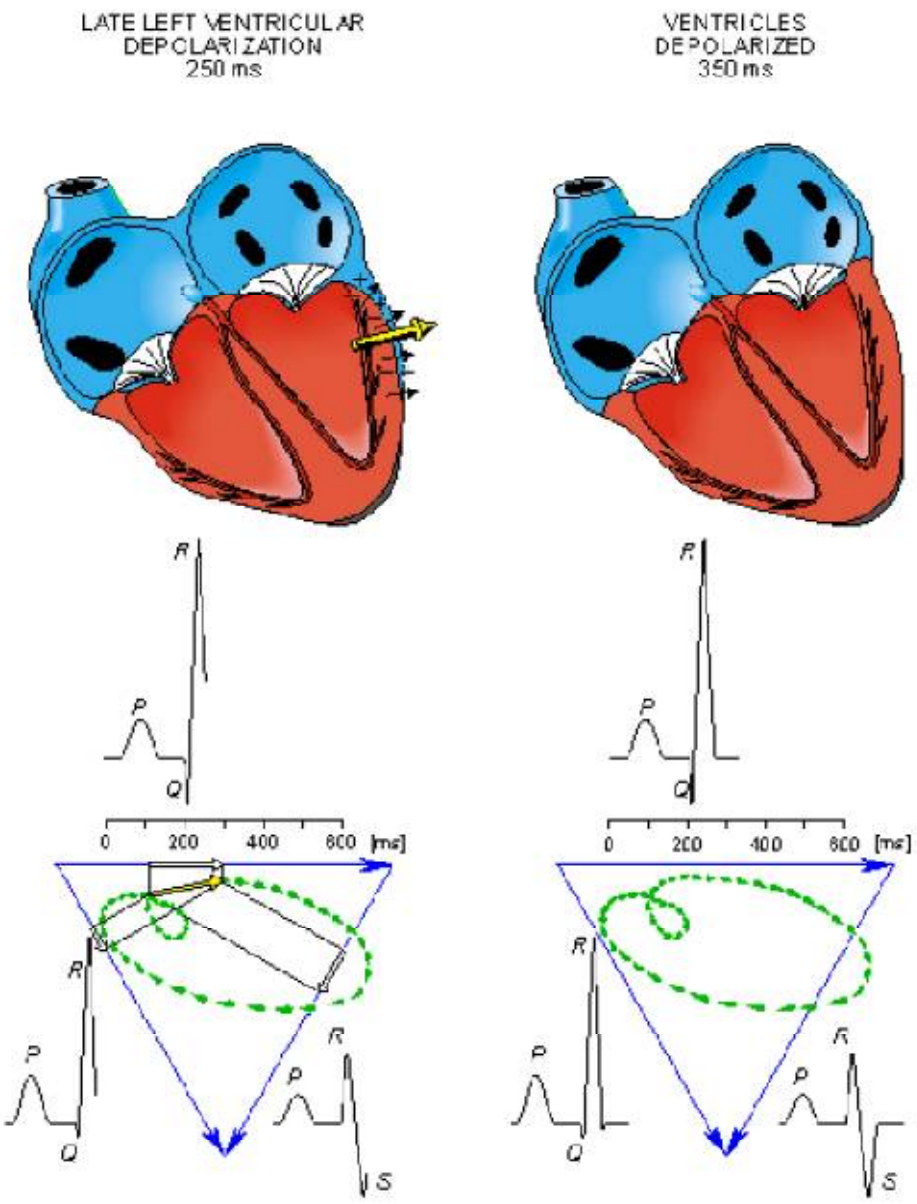


Figure. 1.11 The vector of the electric activities in the heart - III

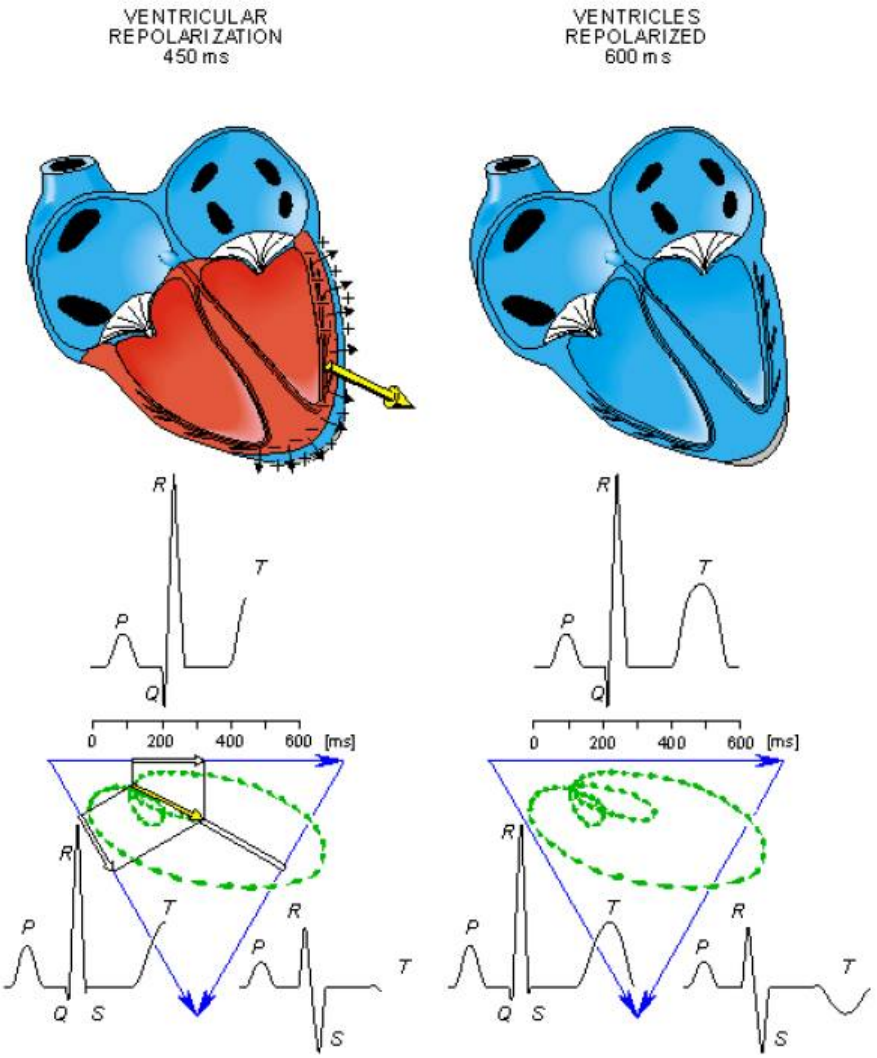


Figure. 1.12 The vector of the electric activities in the heart - IIII

After a while the depolarization front has propagated through the wall of the right ventricle; when it first arrives at the epicardial surface of the right-ventricular free wall, the event is called "breakthrough". Since the left ventricular wall is thicker, activation of the left ventricular free wall continues even after depolarization of a large part of the right ventricle. Because there are no compensating electric forces on the right, the resultant vector reaches its maximum in this phase, and it points leftward. The depolarization front carries on propagation along the left ventricular wall toward the back. Because its surface area now continuously decreases, the magnitude of the resultant vector also decreases until the whole ventricular muscle is depolarized. The last to depolarize are basal regions of both left and right ventricles. Because there is no longer a propagating activation front, there is no signal either.

Ventricular repolarization starts from the outer side of the ventricles and the repolarization front propagates inward. Thisseems paradoxical, but even though the epicardium is the last to depolarize, its action potential durations are relatively short, and it is the first to recover. Although recovery of one cell does not propagate to neighboring cells, one notices that recovery generally does move from the epicardium toward the endocardium. The inward spread of the repolarization front generates a signal with the same sign as the outward depolarization front, as pointed out in figure 8. Because of the diffuse form of the repolarization, the amplitude of the signal is much smaller than that of the depolarization wave and it lasts longer.

According to the above explanations, the normal electrocardiogram signal is illustrated in figure (1.13).

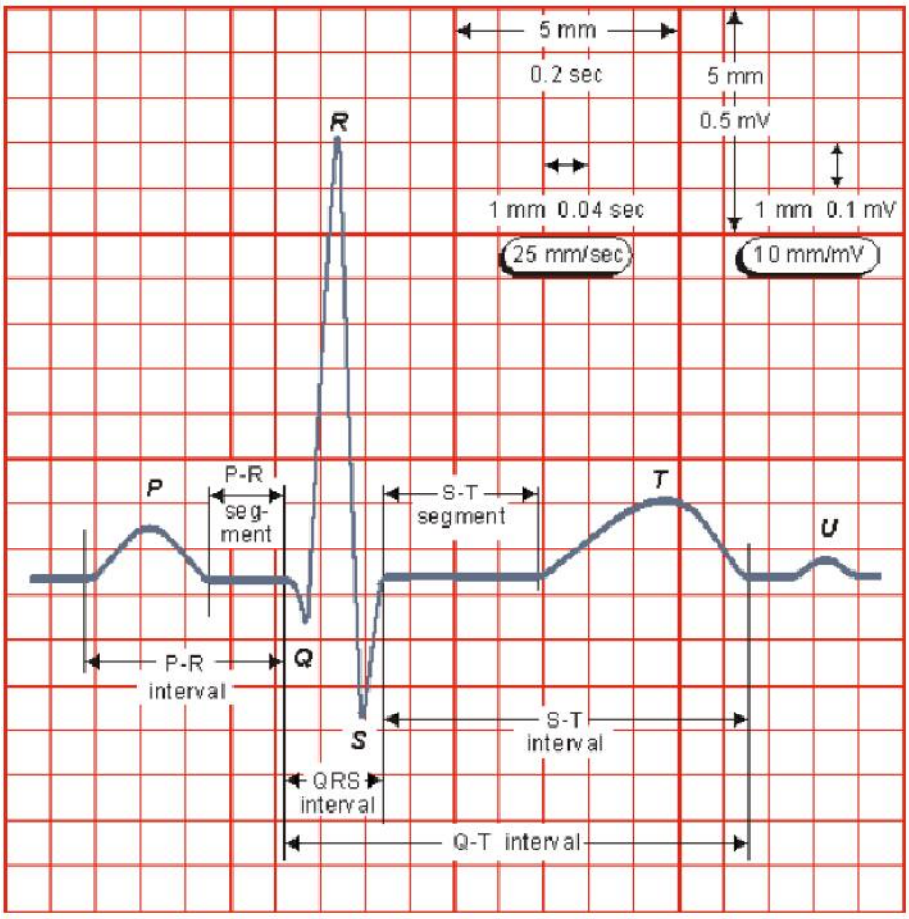


Figure. 1.13 The normal electrocardiogram signal

The figure also contains the explanations for different segments and intervals in the ECG.On the graph, every deflection has a specific name in alphabetic order. The

starting letter P, which represents atrial depolarization. The ventricular depolarization causes the QRS complex, and repolarization is responsible for the T wave. Atrial repolarization occurs during the QRS complex and generates such a low signal amplitude that it cannot be visible apart from the normal ECG.

Every component of the ECG signal has been discussed. However, researchers published some papers with their methods to obtain a good ECG signal. Now, we will discuss about it and their methods.

Frank Normal Wilson (1890-1952) invented how electrocardiographicunipolar potentials could be defined. The two types of leads are unipolar and bipolar. Bipolar leads have one positive and one negative pole [10]. In a 12-lead ECG, the limb leads (I, II and III) are bipolar leads. Unipolar leads also have two poles, as a voltage is measured; however, the negative pole is a composite pole (Wilson's Central Terminal) made up of signals from multiple other electrodes [11]. Ideally, those are measured with respect to a remote reference (infinity). But how is one to achieve this in the volume conductor of the size of the human body with electrodes already placed at the extremities? In several articles on the subject, Wilson and colleagues [12, 13] suggested the use of the central terminal as this reference. This was formed by connecting a 5 kOhm resistor from each terminal of the limb leads to a common point called the central terminal, as shown in figure 20. Wilson suggested that unipolar potentials should be measured with respect to this terminal which approximates the potential at infinity.

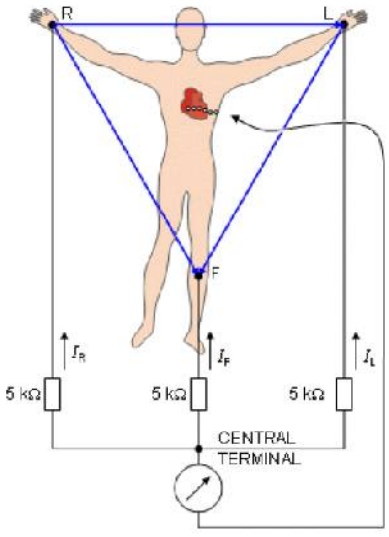


Figure. 1.14 Wilson Central Terminal

Actually, the Wilson central terminal is not independent of but, rather, is the average of the limb potentials. this is easily demonstrated by noting that in an ideal voltmeter there is no lead current. As a result, the total current into the central terminal from the limb leads must add to zero to verify the conservation of current. In accordance with this, it is required that

$$I_R + I_L + I_F = \frac{\phi_{CT}-\phi_R}{5000} + \frac{\phi_{CT}-\phi_L}{5000} + \frac{\phi_{CT}-\phi_F}{5000} \quad (1.16)$$

from which it follows that

$$\phi_{CT} = \frac{\phi_R+\phi_L+\phi_F}{3} \quad (1.17)$$

Since the central terminal potential is the average of the extremity potentials it can be discussed that it is then somewhat independent of any one in particular and therefore a satisfactory reference. In clinical practice good reproducibility of the measurement system is vital. Results coming from Einthoven's application verified these measurements as correct.

Wilson suggested 5 kOHM resistances; these are still widely used, though at present the high-input impedance of the ECG amplifiers would allow much higher resistances. A higher resistance increases the CMRR and diminishes the size of the artifact introduced by the electrode/skin resistance. It is easy to demonstrate that in the image space the Wilson central terminal is found at the center of the Einthoven triangle as shown in (1.15).

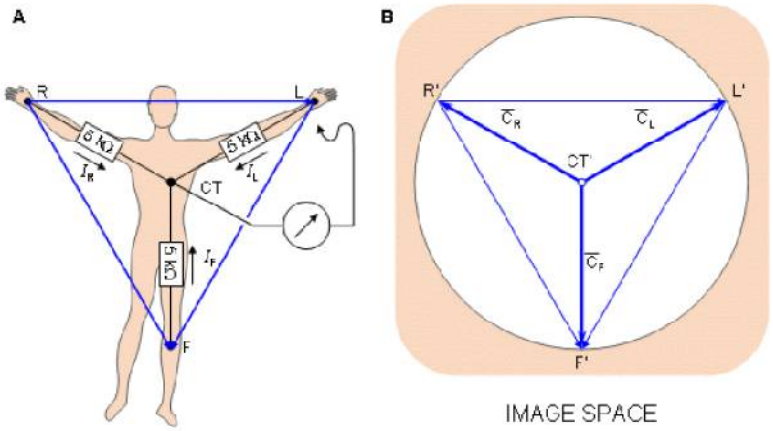


Figure. 1.15 The circuit of the Wilson Central Terminal and The location of the Wilson Central Terminal in the Image Space

In 1942, E. Goldberger observed that these signals can be augmented by omitting that resistance from the Wilson central terminal, which is connected to the measurement electrode [14, 15]. Three additional limb leads V_R, V_L *and* V_F are obtained by measuring the potential each limb electrode and the Wilson central terminal. For instance, the measurement from the left gives

$$V_F = \phi_F - \phi_{CT} = \frac{2\phi_F - \phi_R - \phi_L}{3} \tag{18}$$

In this way, the aforementioned three leads may be replaced with a new set of leads that are called augmented leads because of the augmentation of the signal as shown in figure (1.16).

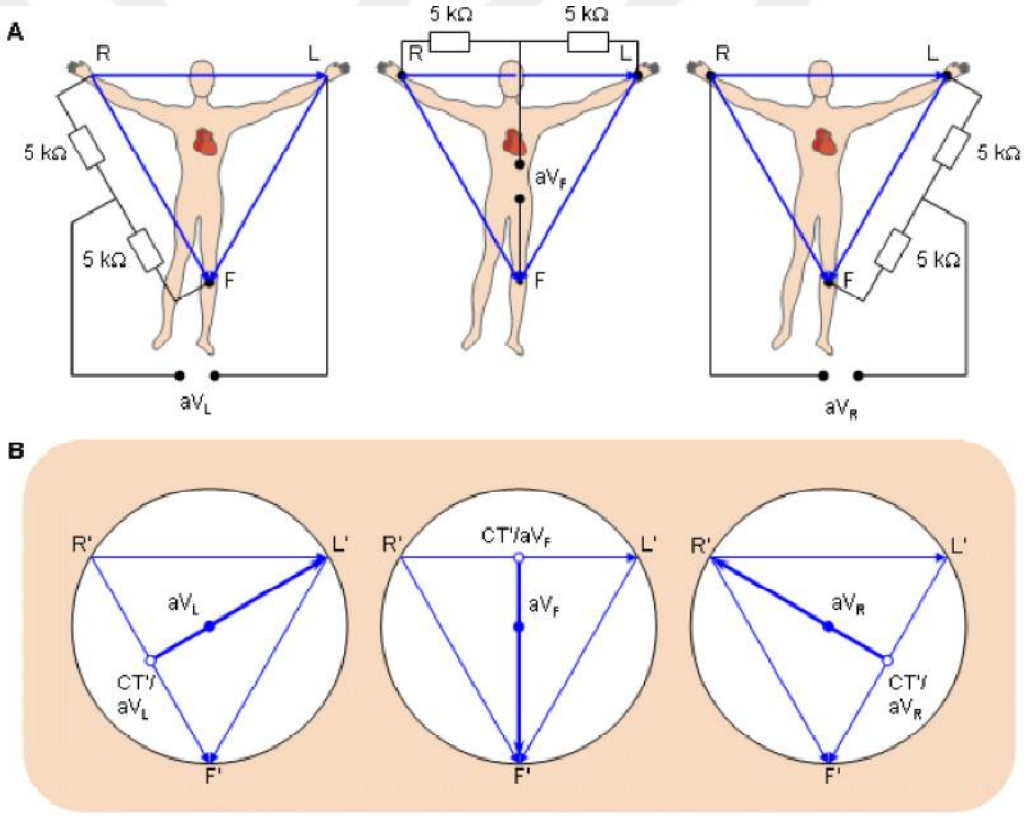


Figure. 1.16 The circuit of the Goldberger augmented leads and the location of the Goldberger lead vectors in the image space

As an example, the equation for the augmented lead aV_F is:

$$V_{aV_f} = \phi_F - \phi_{CT/aV_F} = \phi_F - \frac{\phi_L + \phi_R}{2} = \frac{2\phi_F - \phi_L - \phi_R}{2} \tag{1.19}$$

It is important to note that the three augmented leads are fully redundant with respect to the limb leads I, II and III.

In order to obtain another leads in 12-lead ECG, precordial leads were investigated by Wilson. For measuring the potentials close to the heart, Wilson introduced the precordial leads in 1944 [16].These leads, $V_1 - V_6$ are placed over the left chest as described in figure (1.17).

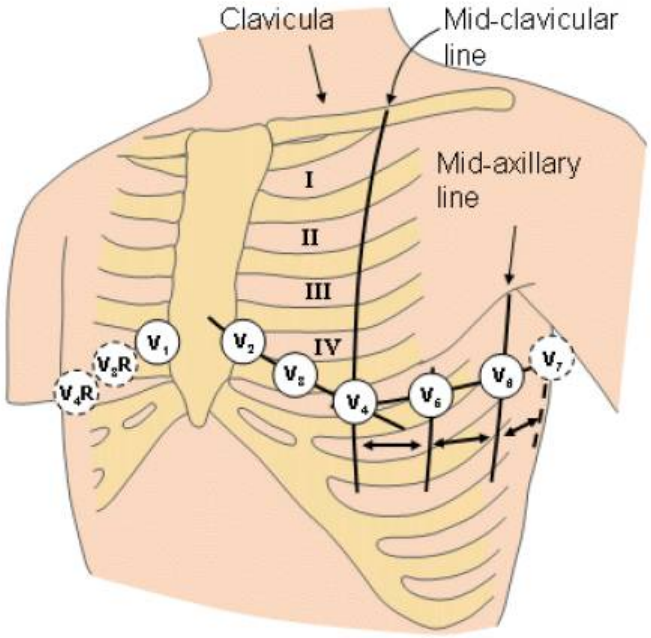


Figure. 1.17 Precordial Leads

The points V_1 and $V_2$are located at the fourth intercostal space on the right and left side of the sternum; V_4 is located in the fifth intercostal space at the midclavicular line; $V_3$is located between the points V_2 and V_4;V_5 is at the same horizontal level as V_4 but on the anterior axillary line; V_6 is at the same horizontal level as V_4 but at the midline.

12-Lead system has been completed by giving precordial, augmented and normal leads. However, modification must be necessary in order to remove artifacts or noise in ECG system. In exercise ECG, the signal is distorted because of muscular activity, respiration and electrode artifacts due to perspiration and electrode movements. The distortion due to muscular activation can be minimized by placing the electrodes on the shoulders and on the hip instead of the arms and the leg, as suggested by R. E. Mason and I. Likar (1966). The Mason-Likar modification is the most important modification of the 12-Lead system used in exercise ECG.

Now, the general information about ECG signal should be given to cover how it works. Over 90% of the heart's electric activity can be explained with a dipole source model

(Geselowitz, 1964) [17]. To evaluate this dipole, it is enough to measure its three independent components. In principle, two of the limb leads (I, II and III) could reflect the frontal plane components, whereas one precordial lead could be chosen for the anterior-posterior component. The combination should be sufficient to explain completely the electric heart vector.

However, in fact, the precordial leads detect also nondipolar components, which have diagnostic significance because they are located close to the frontal part of the heart. Therefore, the 12-Lead ECG system has eight truly independent and four redundant leads. The lead vectors for each leads based on an idealized (spherical) volume conductor are shown in figure (1.18). These figures are assumed to perform in clinical electrocardiography.

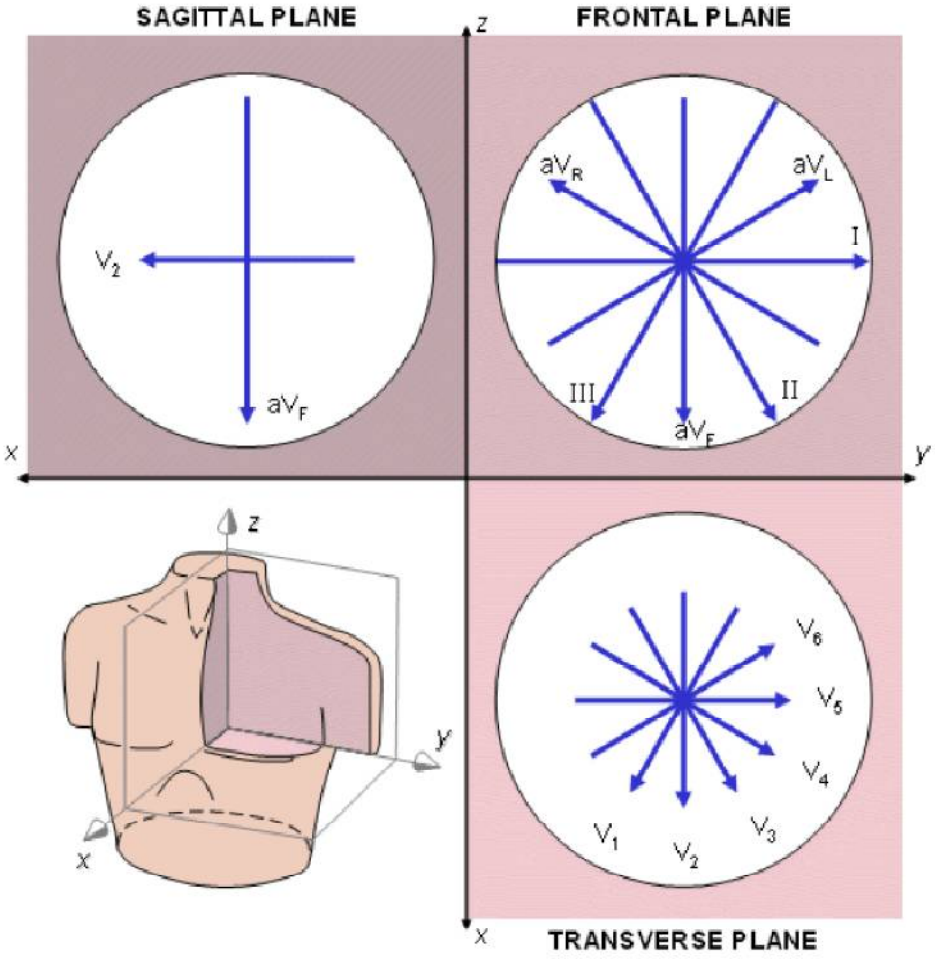


Figure. 1.18 The projections of the lead vectors of the 12-Lead ECG system in three orthogonal planes with assumptions

The main reason to obtain 12-Leads is that it enhances pattern recognition. This combination of leads gives the clinician an opportunity to compare the projections of the resultant vectors in two orthogonal planes and at different angles.

In summary, for the approximation of cardiac electric activity by a single fixed-location dipole, nine leads are redundant in the 12-lead system, as noted above. If we take into account the distributed character of cardiac sources and the effect of the thoracic surface and internal inhomogeneities, we can consider only the four of six limb leads as truly redundant.

Next section will discuss how the analysis of the electrocardiogram signals with neural network is made. As noted above, pattern recognition is the most important factor to diagnose any illness or abnormalities in the heart. Therefore, the understanding of the signal should be achieved effectively.

Heart structure is a unique system that can produce ECG signals independently via heart contraction and expansion. Normal healthy heart can be recognized by normal ECG signal while heart disorder or arrhythmias signals contain differences in terms of features and morphological attributes in their corresponding ECG waveform. Therefore, many methods have been investigated in order to evaluate heart signals with classes. Up to now, the analysis of the electrocardiogram signals have been achieved by using different pattern recognition approaches: template matching, statistical classification, syntactic or structural matching and neural networks. In this section, we will discuss about how well algorithm is and how it works.

Pattern recognition as a field of study was developed in the 1960. It is composed of very much interdisciplinary subject in the areas of statistics, engineering, artificial intelligence, computer science, psychology and physiology and so on. Then, researches were improved in accordance with the growth of knowledge-based systems in the 1970 and neural networks in the 1980. Nowadays, it is still being improved by the-state-of-the-art technology.

All of these techniques are important because there are some vital problems in a variety of engineering and scientific disciplines such as biology, psychology, medicine, marketing, computer vision, artificial intelligence and remote sensing. In order to recognize signals, given a pattern, its recognition and classification may consist of one of the following two tasks: 1) supervised classification in which the input pattern is

identified as a member of a predefined class, 2) unsupervised classification in which the pattern is assigned to a hitherto unknown class. The recognition problem here is being posed as a classification or categorization task, where the classes are either defined by the system designer or are learned based on the similarity of patterns [18]. These applications contain data mining, document classification, financial forecasting, organization and retrieval of multimedia databases and biometrics. That is to say, the patterns can be analyzed and recognized as signals, images, or plain tables of values.

In accordance with the improvement of pattern recognition, since 1903, the ECG was introduced to clinical medicine, the techniques have been developed rapidly in the record, processing and diagnosis of the ECG whether it is in the biomedical area or in engineering and it is accumulated that considerable experience from review is more important than before. ECG have an importance in the clinical diagnosis of the heart diseases. It provides many advantageous in order to find irregular pattern or illness in the heart. ECG is still a main research subject in the biomedical engineering [19]. Numerous research and work on analyzing ECG signals such as those by Conde (1994) and van Bemmel (1982) have been reported recently [20].

In ECG classification, the design of a pattern recognition essentially consists of the following three aspects: 1) data acquisition and preprocessing, 2) data representation and 3) decision making. However, these may cause some problems such as the choice of sensor, preprocessing techniques, representation scheme and decision making model. Also, learning from a set of examples is a vital and desired attribute of most pattern recognition systems. The four best known approaches for patter recognition are : 1) template matching, 2) statistical classification, 3) syntactic or structural matching and 4) neural networks.

Firstly, one of the simplest and approaches to pattern recognition is based on a Template matching [21]. Matching is the generic algorithm in pattern recognition, which is performed to determine the similarity between two entries of specified type. Several types of template matching have been performed.

One of the template matching is template cross-correlation. The signals are represented to be correlated if the shapes of the waveforms of two signals match one another. The correlation coefficient is a value that determines the degree of match between the shapes of two or more signals. A QRS detection technique designed by Dobbs et. al (1984)

performs cross-correlation [22]. This technique of correlating one signal with another requires that two signals be aligned with one another. Dobbs et al. describe two ways of implementing this. The first way of aligning the template and the incoming signal is by using the fiducial points on each signal. If the fiducial points on the template and the signal are aligned, then the correlation can be performed. Another implementation involves continuous correlation between a segment of the incoming signal and the template. A correlation is made between this signal segment and the template segment that has the same number of signal points. This technique does not require processing time to assign fiducial points to the signal. The template can be considered as a window that moves over the incoming signal one data point at a time. The value of the cross correlation coefficient always falls between +1 and -1. A value of +1 indicates that the signal and the template match exactly as mentioned earlier. This determines how well the shapes of the two waveforms under consideration match. The magnitude of the actual signal sample does not matter.

The other type of template matching is template subtraction. In this technique, a segment of the incoming ECG signal that corresponds to the QRS waveform is saved. This segment or template is then compared with the incoming ECG signal. Each point in the incoming signal is subtracted from the corresponding point in the template. When the template is aligned with a QRS waveform in the signal, the subtraction gives a value very close to zero. This algorithm has been used in where the template can be specified effectively.

Another approach in template matching is automata-based template matching. Furno and Tompkins (1982) investigated a QRS detector that is based on concepts from automata theory. The algorithm possesses some of the basic techniques that are common in many pattern recognition systems [23]. The ECG signal is first split into a set of predefined tokens, which represent certain shapes of the ECG waveform. The set of tokens that would represent a normal ECG is performed as input to the finite state automation. The finite state automation is essentially a state-transition diagram that can be implemented with if-then blocks. The sequence of tokens is fed into the automation. Therefore, the sequence of tokens must be derived from the ECG signal data. This is done by forming a sequence of the differences of the input data. Then the algorithm groups together those differences that have the same sign and also exceed a certain predetermined threshold level. The algorithm sums the differences in each of the groups

and associates with each group this sum and the number of differences that are in it. This QRS detector has an initial learning phase where the program approximately determines the peak magnitude of a normal QRS complex. Now, the algorithm teaches the finite state automation the sequence of tokens that make up a normal QRS complex. The number and sum values for a normal QRS complex are now set to a certain range of their respective values in the QRS complex detected.

Secondly, statistical classification should be discussed with both its advantageous and disadvantageous. The main goal of pattern recognition is supervised or unsupervised classification. In machine learning, classification becomes a problem of identifying to which of a set of categories, a new observation belongs, on the basis of a training set of data containing observations whose category membership is known. In this approach, some algorithms work only in terms of discrete data and require that real-valued or integer-valued data be discretized into groups.

In the statistical approach, each pattern is represented in terms of d features or measurements and is viewed as a point in a d-dimensional space. The goal is to select those features that allow pattern vectors belonging to different categories to occupy compact and disjoint regions in a d-dimensional feature space. The effectiveness of the representation space is found by how well patterns from different classes can be separated. In this method, the objective is to establish decision boundaries in the feature space which separate patterns belonging to different classes. The decision boundaries are determined by the probability distributions of the patterns belonging to ach class, which must either be specified or learned [25, 26]. Apart from this, the direct boundary construction approaches are supported by Vapnik's philosophy [27]: If you possesses a restricted amount of information for solving some problems, try to solve the problem directly and never solve a more general problem as an intermediate step. It is possible that the available information is sufficient for a direct solution but is insufficient for solving a more general intermediate problem.

Statistical pattern recognition [28, 29, 30] draws from established concepts in statistical decision theory to discriminate among data from different groups based upon quantitative features of the data. Examples of statistical feature extraction techniques include mean and standard deviation computations, frequency count summarizations, Karhunen Lo'eve transformations, Fourier transformation, wavelet transformations and Hough transformations. The quantitative features extracted from ach object for

statistical pattern recognition are organized into a fixed length feature vector where the meaning associated with each feature is determined by its position within the vector. The collections of feature vectors are passed to the classification task. Statistical techniques used as classifiers within the classification task include those based on similarity (template matching, k-nearest neighbor), probability (Bayes rule), boundaries (decision trees, neural network) and clustering (k-means, hierarchical).

Nandhini and Subhasini have presented five feature extraction methods, namely wavelet decomposition, edge detection, gray level histogram, fast fourier transform and mean-variance, and probabilistic neural network classification. An ECG image is classified by PNN using various feature extraction. Up to now, the wavelet decomposition gives a maximum accuracy compared to other feature extraction methods [31].

Thirdly, syntactical or structural matching is one of the important method to analyze ECG signals. The quantitative nature of statistical pattern recognition makes it difficult to discriminate among groups based on the morphological sub patterns and their interrelationships embedded within the data. This limitation provided the impetus for the development of a structural approach to pattern recognition that is supported by psychological evidence pertaining to the functioning of human perception and cognition. Object recognition in humans has been demonstrated to involve mental representations of explicit, structure oriented characteristics of objects [32, 33, 34, 35, 36], and human classification decisions have been shown to be made on the basis of the degree of similarity between the extracted features and those of a prototype developed for each group [37, 38, 39, 40, 41]. For instance, Biederman [42] proposed the recognition by components theory to explain the process of pattern recognition in humans: (1) The object is segmented into separate regions according to edges defined by differences in surface characteristics (luminance, texture, color), (2) each segmented region is approximated by a simple geometric shape, and (3) the object is identified based upon the similarity in composition between the geometric representation of the object and the central tendency of each group. Structural pattern recognition [43, 44, 45], sometimes referred to as syntactic pattern recognition due to its origin in formal language theory, relies on syntactic grammars to discriminate among data from different groups based upon the morphological interrelationships present within the data.

Feature vector contain a variable number of features in order to accommodate the presence of superfluous structures which have no impact on classification. Since the

interrelationships among the extracted primitives must also be encoded, the feature vector must either include additional features describing the relationships among primitives or take an alternate form such as a relational graph. This technique to extract structural features includes chain codes, piecewise linear regression and curve fitting which are used to generate primitives that encode sequential, time ordered relationships [46, 47].

Bandyopadhyay and Manna discussed syntactic pattern recognition techniques for the analysis of ECG and mentioned a standard three-channel ECG chart to provide immediate on-site ECG interpretation [48]. Trahanias and Skordalakis presented an application of the syntactic method to ECG pattern recognition and parameter measurement. This approach has been implemented and the performance of the resultant system has been evaluated using an annotated standard ECG library [49].

Finally, neural network is represented as the state-of-the-art technique in order to provide new and emerging applications such as data mining, web searching, retrieval of multimedia data, face recognition and cursive handwriting recognition require robust and efficient pattern recognition techniques.

The main characteristics of neural networks are that they have the ability to learn complex nonlinear input-output relationships, use sequential training procedures, and adapt themselves to the data [50]. The most commonly used family of neural networks for pattern classification tasks [51] is the feed-forward network, which includes multilayer perception and Radial-Basis Function (RBF) network [52], which is mainly used for data clustering and feature mapping.

ANN (artificial neural network) is an information processing paradigm that is inspired by the way biological nervous systems, such as the brain, process information. It consists of a large number of highly interconnected processing elements (neurons) working in unison to solve specific problems. In 2006, the artificial neural network method was performed for ECG pattern recognition. Four types of ECG patterns were chosen from the MIT-BIH database to be recognized, including normal sinus rhythm, premature ventricular contraction, atrial premature beat and left bundle branch block beat. ECG morphology and R-R interval features were performed as the characteristic representation of the original ECG signals to be fed into the neural network models.

The self-organizing mapping (SOM) network exhibited the best performance and reached an overall accuracy of 95.5%, and the back propagation (BP) and learning vector quantization (LVQ) network reached 92.5% and 91.5%. These result presents in [53, 54, 55]. Back propagation algorithm in a feed forward network is used for the feature extraction. Chazal and Reilly [56] presented a method for the automatic processing of the ECG for the classification of heartbeats is presented. In order to test this algorithm, 50000 beats and 22 recordings were used. Apart from these, [39] presents Artificial Neural Networks (ANN) has been used to classify the ECG arrhythmias. Different structures of ANN have been trained by arrhythmia separately and also by mixing these 10 different arrhythmias. They had an achievement to diagnose illnesses. Zhu et. al, presented the investigation of the use of artificial neural network for ECG abnormality detection in an ECG monitoring scheme was done [57]. Simulations are performed to explore how well neural networks can work after a short learning phase. The achievement rate is about 95%. Shanxiao and Guangying introduced the ECG pattern recognition method based on wavelet transform and standard BP neural network classifier. Experiment analyzeswavelet transform of ECG to extract the maximum wavelet coefficients of multi-scale firstly. Theexperimental result shows that the standard BP neural network classifier's overall patternrecognition rate is well [58]. Due to the fast nature of encryption/decryption process, F. Sufi et. alproposed the usage of multi-scroll chaos to encrypt ECG packets. ECG packets are beingencrypted by the mobile phones using the chaos key by patients' subscribed in tele-cardiologyapplications [59].

1.2. Objective of The Thesis

In this study, long QT syndrome is detected by novel pattern recognition algorithm with neural network in electrocardiograpy. Then, experts perform ablation process on the heart surface by using catheter ablation. It is important to determine correct diagnose for the patients' illness. Since it may be dangerous in wrong diagnoses. Therefore, correct recognition must be completed before intra-operative surgery.

1.3. Hypothesis

In this study, we propose a new method to recognize the pattern of QT segment based on Gaussian mixture model. Up to now, for detection of QT segment, many methods have been developed as mentioned above. However, no methods guaranteed accurate

QT segment measurements because of its variability and end difficulty in end point detection. Therefore, in order to attain high performance, we suggest to use mixture model based on probability. Using mixture model is an important to achieve pattern recognition because heart rhythm is non-stationary signal. Its shapes and amplitudes depends on time and no signal pattern cannot be matched perfectly to the other. It causes some problems such as training algorithm, deviations of signal rates and so on.

In this study, neural networks are used to model Gaussian mixture distribution as coefficients. It is the most vital part of this study because Gaussian mixture model can only be trained by using expectation maximization algorithm or MAP. However, given systems are much more complex than the model that GMM can create.

For these reasons, every Gaussian component should be transformed into coefficients in order to train by using back-propagation algorithm.

CHAPTER 2

HEART DISEASES

2.1. QT Syndrome

In cardiology, the **QT interval**is defined as a measure of the time between the beginning of the Q wave and the end of the T wave in the heart's electrical cycle. Actually, the QT interval can be represented as electrical depolarization and repolarization of the ventricles in the heart. Therefore, QT interval depends on the variation of the R-R interval.

The QT interval is most commonly measured in lead II for evaluation of serial ECGs with leads I and V5 being comparable alternatives to lead II. The accurate measurement of the QT interval is special since the end of the T wave is not always clear and usually merges gradually with the baseline. There are many methods to determine the end of the QT interval such as using threshold method that uses the end of the T wave is determined by the point at which the component of the T wave merges with the isoelectric baseline, tangent method in which the end of the T wave is specified by the intersection of a tangent line extrapolated from the T wave at the point of maximum downslope to the isoelectric baseline [60]. With the advancement of digital ECGs with simultaneous 12- channel recording, QT measurement may also be performed by the "superimposed median beat" method. In this method, a median complex is created for each of the 12 leads. Then, they are superimposed on each other and the QT interval is measured either from the earliest onset of the Q wave to the latest offset of the T wave or from the point of maximum convergence for the Q wave onset to the T wave offset [61].

However, in arrhythmias, some of the problems have an effect on the QT interval and its function in the heart. Abnormal intervals occur due to the different problems in the heart such as genetic causes [62], drug reactions [63], and pathological conditions [64].

Therefore, researchers defined different syndromes with QT interval abnormalities, short QT syndrome and long QT syndrome. They will be discussed next section deeply.

2.1.1. Short QT Syndrome

Short QT syndrome is a genetic disease of the electrical system of the heart. It can be diagnosed by a constellation of signs and symptoms. Apart from these, it is noticeable when doing ECG signal analysis. Especially, QT interval is consisted of 300 mS and small interval on the graph.

In order to determine short QT syndrome, several symptoms and signs can be evaluated by using some sort of techniques. Short QT syndrome can be diagnosed by examining loss of consciousness, mutations in KCNH2, KCNJ2 and KCNQ1 genes [65].The last genes can cause short QT syndrome. These genes control instructions for making proteins that act as channels across the cell membrane. In cardiac muscle, that is the key component of transporting ions in channels. These channels play critical roles in maintaining the heart's rhythm. When these genes are mutated, the activity of the channels is increased. Thus, QT interval is smaller than normal rhythm. Besides, short QT syndrome appears to have an autosomal dominant pattern of inheritance.

Short QT syndrome is associated with an increased risk of sudden cardiac death, most likely due to ventricular fibrillation.

As for its diagnosis, recent criteria have been reported of the Arrhythmia Research Laboratory [66]. There are five conditions to determine it: QTc in milliseconds, Jpoint-Tpeak interval, clinical history, family history and genotype.

QTc in milliseconds is an important measurement to diagnose short QT syndrome. According to the Arrhythmia Research Laboratory, QTc < 330 demonstrates highly risk for patients. Secondly, QTc < 350 is the second point to find short QT syndrome out. Finally, QTc < 370 is the last boundary to diagnose short QT syndrome. However, the currency of these values can be discussed because the measurements made by electrocardiography cannot give us absolute results about the electrical activity of the heart. Therefore, experts or doctors estimate how correct measurement is. The recognition algorithms earns an important because of that.

Jpoint-Tpeak is the second criteria to diagnose short QT syndrome. Reported results suggest that Jpoint-Tpeak is smaller than 120 milliseconds in order to be stabilized the heart. Otherwise, experts can suspect the short QT syndrome.

Another important factor is **clinical history** about the patient. There are some conditions that have an effect on occurring the short QT syndrome. Firstly, sudden cardiac arrest and polymorphic VT and VF are vital sources to be the short QT syndrome. Others, less important but cannot be neglected, are unexplained syncope and atrial fibrillation.

Fourthly, family history plays a critical role in the short QT syndrome. The degree in family possesses incremental effect on patients. Especially, first and second degree are important to be fallen short QT syndrome.

Finally, genotype may causes this illness because genetic effect is the main factor in short QT syndrome. Genotype positive, mutation of undetermined significance in a culprit gene can be included as cause effect.

The etiology of short QT syndrome has been discussed by researchers. A current hypothesis is that short QT syndrome is due to increased activity of outward potassium currents in phase 2 and 3 of the cardiac action potential. This bring on a shortening of the plateau of the action potential in phase 2, causing a shortening of the overall action potential.

In order to treat short QT syndrome, there are some methods being performed such as the implantation of implantable cardioverter-defibrillator (ICD), the use of antiarrhythmic agents, especially quinidline, may be of benefit in individuals with short QT syndrome due to their effects on prolonging the action potential and by their action on the I_k channels [67].

2.1.2. Long QT Syndrome

Long QT Syndrome (LQTS) is a rare inherited heart disease as delayed repolarization of the heart following a heartbeat increases the risk of event of torsades de pointes (TdP, a form of irregular heartbeat that originates from the ventricles). These events may cause palpitations, fainting, sudden death due to ventricular fibrillation.

This syndrome is named as QT because the appearances of the electrocardiogram on which a prolongation of the QT interval occurs. Normally, QT interval changes between 350 and 440 milliseconds [68].

LQTS can occur from mutation of one of several genes such as KCNQ1, KCNH2 and SCN5A [68]. These mutations lead to prolong the interval of the ventricular action

potential, thus lengthening the QT interval. Until now, twelve different LQTS have been discovered in order to classify disease and to treat them.

As an basic factor to occur this syndrome, it can be said that electrolyte imbalances and genetic mutations arise in ion channels [66]. All forms of LQTS contain an abnormal repolarization of the heart, which cause differences in the refractory period of the heart. **Refractory period** is span that muscle cells try to stabilize their action potential in cardiac reference. LQTS are believed to be due to reopening of L-type calcium channels during the plateau phase of the cardiac action potential. Since adrenergic stimulation can increase the activity of these channels. This is an explanation why the risk of sudden death in individuals with LQTS is increased during increased adrenergic states, especially since repolarization is impaired. **Adrenergic stimulation** is made by adrenergic receptors are a class of G protein-coupled receptors that are targets of the catecholamines, especially norepinephrine and epinephrine. These receptors generally stimulate the sympathetic nervous system. Therefore, the heart rhythm is affected by these receptor as increased heartbeat and irregular patterns. Normally during adrenergic states, repolarizing currents also are increased to shorten the action potential. In the absence of this shortening and the presence of increased L-type calcium current, after early after depolarizations may arise.

The delayed after-depolarizations are considered to be due to an increased Ca^{2+} filling of the sarcoplasmic reticulum which is responsible to receive electrical stimulation in muscles. This overload may cause spontaneous Ca^{2+} release during repolarization, causing the released Ca^{2+} to exit the cell through the $3Na^{+}/Ca^{2+}$ exchanger, which results in a net depolarizing current.

As for **diagnosis of LQTS**, it is a difficult mission for experts since 2.5% healthy population has prolonged QT interval, and 10-15% of LQTS patients have a normal QT interval [70]. Therefore, researchers can use a table called as "diagnostic score", calculated by assigning different points to various criteria. When patients have four or more points, the probability is high for LQTS [68]. There are seven criteria to diagnose long QT syndrome as the following paragraphs given.

Firstly, QTc should be bigger 480 milliseconds. However, it may be a risk for patients when QTc is in the range of between 460 and 470 milliseconds. Sometimes, for QTc, 450 milliseconds may be dangerous in male gender.

Secondly, torsades de pointes ventricular tachycardia causes long QT syndrome. This is an important because it produces an irregular pattern of electrical activity.

Thirdly, T wave alternans has an effect on patients because T wave amplitude may shift ion channels transformation between intracellular and extracellular domain. Apart from this, notched T wave in at least 3 leads may be cause effect of long QT syndrome.

The others are less important than the above reasons. Congenital deafness, family history and syncope may create distortion in the heart rhythm.

As for treatment in LQTS, those diagnosed with LQTS are usually suggested to avoid drugs that would prolong the QT interval further or lower the threshold for TDP [71]. Some of the published research suggest that arrhythmia termination and arrhythmia prevention can be performed in order to ill patients. In addition, the usage of ICD is considered to be a good treatment for long QT syndrome.

In some processes, LQTS can be treated by using **catheter ablation**. It is defined as the one of the state-of-the-art method. Catheter ablation is an invasive procedure used to remove or terminate a faulty electrical pathway from section of the hearts of those who are prone to developing cardiac arrhythmias such as atrial fibrillation, atrial flutter, supraventricular tachycardias (SVT) and Wolff-Parkinson-White syndrome.

Catheter ablation may be recommended for an arrhythmia that medicine can't control. The patient has faulty electrical activity in the heart that increases their risk of ventricular fibrillation and sudden cardiac death.

Catheter ablation is performed by advancing several flexible catheters into the patient's blood vessels. Electrical impulses are then used to induce the arrhythmia and local heating or freezing is used to ablate the abnormal tissue that is causing it.

CHAPTER 3

THE QT RECOGNITION ALGORITHM WITH LLGMN

3.1. QT Recognition

As mentioned pervious section, measurements of the width or duration of waves in the ECG are widely used to diagnose abnormal electrical conduction in the heart which causes myocardial damage and the risk of cardiac arrhythmias [72, 73]. Up to now, many methods for making such measurements, especially of the QT interval have been developed. Although, many algorithms have been tried to achieve measurement, they have been hampered by a lack of standardized databases containing a sufficiently large number of annotated heartbeats with manually-made measurements of waveform boundaries.

In these measurements, experts read ECG paper by using calipers either on sheet or computer screens. Therefore, generalized method is necessary to obtain diagnostic results. There is a rich literature documenting a wide variety of approaches to the problem of detecting QT interval [74,75,76,77]. Some of the algorithms have many advantages to detect abnormalities in the heart. W Zong et al. [78] used a curve length transform. Their advantageous are insensitivity to morphological variations of QRS complexes and T-waves and to ECG baseline wandering and its computational efficient. However, T wave amplitudes and morphologies depends on relative to normal electrocardiogram, so, T wave can changes in every time [79]. Qiuzhen Xue et al. [80] presented an algorithms by using least squares to the maximum slope of the T wave and an isoelectric line (LSI). In their method, to compute QT dispersion, they need to measure QRS complex onset and T wave offset . They realized that the variation of the

QRS onset from lead to lead is much smaller than that of the T offset, therefore, a global QRS onset was usually used. However, measurement of the T offset is more difficult owing to its flat pattern. As a result, several algorithms to locate the T offset have been developed. They divided the algorithms into two categories, namely, threshold-based algorithms and algorithms based on intersection of the slope and an isoelectric line. In the threshold based algorithm, the threshold can be adjusted a certain percentage of the T wave peak by examining the derivate and integral of it. Generally, it is used in manual measurement. The second type is based on the intersection of the maximum T wave slope after the final T wave peak with an isoelectric line in the TP segment.

Recently, a T wave complexity measurement based on principal component analysis (PCA) has been performed [81]. In this measurement, it uses whole T wave morphology information instead of distinct critical points, such as T offset and T peak, as in the QT interval dispersion algorithm which was originally proposed as an index of the spatial dispersion of ventricular recovery times (maximum QT interval minus minimum QT interval) [82]. They proposed two qualities to obtain good measurement: ability to differentiate between different groups of patients, normal and abnormal, and good reproducibility.

Alex DMITRIENKO et al. [83] demonstrated that the model-based method is the most effective QT analysis method that works for drugs inducing heart rate changes. Predefined QT correction formulas were considered to as unreliable when the investigational drug induces heart rate changes. They applied data-driven approaches by accounting for correlation among serial ECG measurements collected on the same subject and drug-induced heart rate changes. They compared the results in order to improve algorithm.

D Hayn et al. [84] presented an algorithm to make QT interval assessment, based on several databases such as PhyisoNet QT Database, the CSE Multilead Database and the PTB Diagnostic ECG Database. They combined previous method with their algorithm. Different channels were used to get information about cardiac rhythm and finally, the results were presented. It is a good approach because cardiac abnormalities should be diagnosed by experts. The existing database provide us to get information like comes from experts. It was the most useful algorithm in 2006.

In the study of McLaughlin et al. [85], they purposed to undertake a quantitative assessment of different automatic QT measurement techniques and investigate the influence of electrocardiogram filtering and algorithm parameters. For this purpose, four methods were performed: threshold crossing of the T wave, threshold crossing of the differential of the T wave, intercept of an isoelectric level and the maximum T wave slope and finally intercept of an isoelectric level and the line passing through the peak and the point of maximum slope of the T wave. They were almost interested in the morphology of ECG signal. As a result, mean and standard deviation of differences between reference and automatic QT measurements were compared for the four techniques. However, they did not recommend threshold crossing method because of poor quality.

Allan Murray et al. [86] presented to quantify the errors associated with manual measurement of QT intervals and to determine the source of errors. For this purpose, a randomized study of QT measurement plotted on paper in presentations with different noise levels, paper speeds, amplifier gains, and with or without next QRST complex to indicate the RR interval. They resulted that QT intervals measured were significantly longer with greater amplifier gain and at slower paper speeds. Neither the presence of noise nor the presence of a second QRST complex altered the mean QT measurements.

Langley et al. [87] suggested fully automated measurement for QT interval from 12 lead electrocardiogram. The presented algorithm determined the Q onset and T offset points from the average beat in each lead. In accordance with this, the QT interval was calculated from the median Q onset and T offset points. The difference between automatic and manual measurements was 48 milliseconds.

Christov and Simova [88] performed automated method for QT interval measurement. The presented algorithm includes QRS detection and ECG signal preprocessing allowing suppression of power-line interference, electromyographic noise and baseline drift guaranteeing accurate preservation of the QRS-onset and T-end offset. They had an achievement for the Challenge 2006 as the second best in Division 3.

To sum up all of the reasons mentioned, the effective algorithm is necessitated in order to diagnose illnesses in the heart. Therefore, we have chosen an algorithm based on Gaussian mixture model [89]. This algorithm was performed in order to recognize the movement of finger and hand. In addition, this algorithm was used to detect the change

of brain signal. However, no application is achieved by using LLGMN method in the pattern recognition of heart because heart signal has both stationary and non-stationary sections. Therefore, it is necessitated that sequential data processing is achieved to cover the heart sections.

Some investigators carried out EEG pattern classification by using backpropagation neural networks(NN) [90, 91]. The NN based on the error backpropagation learning have been frequently employed in various field, such as pattern classification and learning control [92]. These neural networks represent any nonlinear mapping between input and output patterns. However, there are some problems to use these networks because the networks need a large number of training data, learning iterations, and a large scale of structure.

Due to fact mentioned factors, in order to attain high classification performance and to improve the generalization ability of NN's, the present algortihm is proposed as a new type of the feedforward probabilistic NN based on the mixture model and the log-linear model of the probability density function.

In general, an input for a pattern classification problem can be considered as a random variable. In practice, there can be small variations in the measurements due to many causes such as noises, temperature fluctuations, non-stationary signal of heart. Therefore, the measurement is represented as a random variable and it is reasonable to the model the range of possible values of these information with an interval of real numbers. This is called as random variable [93]. In this study, the pattern classification problems reduce the estimation problem of probability density function(pdf) since the classification can be performed by using the Bayes' rule if a posteriori probability of the input pattern is obtained accurately.

In order to explain the Bayes' rule, we should give some definitions about probability. Firstly, sometimes, probabilities need to be reevaluated as additional information becomes available. Some events may depends on the others. Therefore, the probabilities can be revised to include this knowledge. This is stated as $P(B|A)$. This is called the conditional probability of B given A. If the conditional probability of an event B given an event A, denoted as $P(B|A)$, is

$$P(B|A) = \frac{P(A \cap B)}{P(A)} \; for \; P(A) > 0 \tag{3.1}$$

This formulation can be expressed by the following statements:

$$P(A) = (the\ number\ of\ outcomes\ in\ A)/n$$

$$P(A \cap B) = (the\ number\ of\ outcomes\ in\ A \cap B)/n$$

However, for some situations, there is no dependence between probabilities. In this condition, the conditional probability of $P(B|A)$ might equal $P(B)$.

$$P(A \cap B) = P(B|A)P(A) = P(B)P(A) \tag{3.2}$$

Therefore

$$P(A|B) = \frac{P(A \cap B)}{P(B)} = \frac{P(A)P(B)}{P(B)} = P(A) \tag{3.3}$$

Electrocardiogram signal cannot be considered as independence because all of the sections are formed according to the previous section. As a result, the probability that a condition was present has been a curiosity. Bayes' theorem is expressed as an equation or formulation in probability.

As the definition of conditional probability

$$P(A \cap B) = P(A|B)P(B) = P(B \cap A) = P(B|A)P(A) \tag{3.4}$$

This statement can be organized as following

$$P(A|B) = \frac{P(B|A)P(A)}{P(B)} \tag{3.5}$$

That is to say, every condition can be defined their previous condition and section in order to make a relation between them.

On the other hand, in probability, there are two important definitions. These are mean and covariance value. Mean value can be shown as the following equation in discrete analysis.

$$\mu_a = \bar{a} = \frac{1}{N}\sum_1^N a_n \tag{3.6}$$

where $\bar{a}$ is the mean value of a_n array. In order to classify signal or such array or matrix, mean value gives us estimation about which value characterizes the signal. However, some of the signals such as EMG, EEG, ECG contains many noises or artifacts. Therefore, in probability, it is defined to model relationship between the differences of signals as covariance value. It can be formalized in equation (3.7).

$$\sigma_{xy} = \frac{1}{N}\sum_{i=1}^{N}(x_i - \bar{x})(y_i - \bar{y}) \quad (3.7)$$

In this formula, the signal represents as the sum of many characteristic signals. As mentioned before, ECG signal is non-stationary, therefore, their values in time always vary due to physical condition of the heart. In order to model this signal, covariance matrix can be produced by using instantaneous values and their mean values. With this feature, biomedical signal can be characterized in order to estimate next section in the heart. As a result, covariance is a measure of how much two random variables change together.

In this section, firstly, general information about Gaussian mixture model is given to understand the mathematical basis of the algorithm. Next, in order to create an artificial neural network, training algorithm and its application on neural networks is discussed. In addition, it is demonstrated that the existing algorithm [89] cannot be performed on ECG signal because of the structure of ECG signal in neural networks. Then, we discuss a novel compare algorithm with adjustment function. Finally, the results are given in order to evaluate how effective our algorithm is.

3.1.1. Method

The algoritm is based on Gaussian Mixture Model (GMM). It is a parametric probbability density function represented as a weighted sum of Gaussian component densities. GMMs are commonly performed as a parametric model of the probability distributiin of continupus measurements or features in a biometric system, such as vocal-tract in a speaker recognition system.

GMM parameters can be estimated from training data using the iterative Expectation-Maximization (EM) algorithm or Maximum A Posteriori (MAP) estimation from a well-trained prior model. In this study, Expectation-Maximization algorithm is performed in order to create suitable distribution.

However, some related issues should be given in order to explain Expectation-Maximization. We begin out discussion with a very useful result called Jensen's inequality [94].

Let f be a function whose domain is the set of real numbers. Also, f is a convex function if $f''(x) \geq 0$ for all real numbers. If f is taken as vector-valued inputs, this can be generalized to the condition that its hessian H is positive semi-definite. If $f''(x) > 0$ for

all x, it can be said that f becomes convex. Jensen's inequality can then be stated as follows:

Let f be a convex function, and let X be a random variable.

$$E[f(X)] \geq f(EX) \tag{3.8}$$

Under this condition, if f is strictly convex, then $E[f(X)] = f(EX)$ holds true if and only if $X = E[X]$ with probability 1. In order to cover this theorem, the following figure can be proceed.

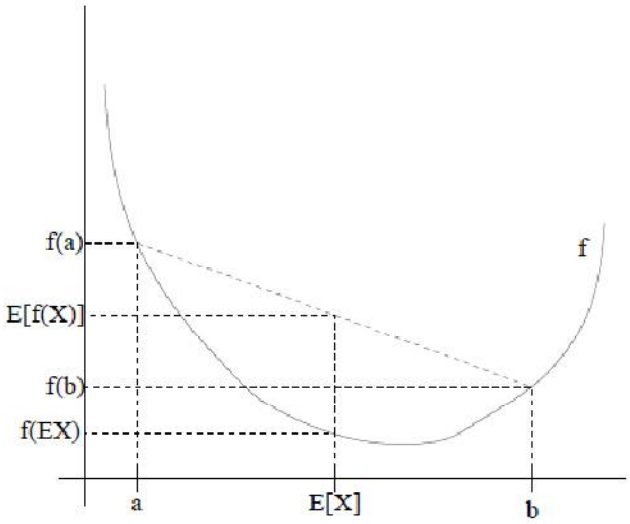


Figure. 3.1 The scheme for Jensen's theorem

It is seen that f is a convex function shown by solid line. Also, X is a random variable that has a 0.5 chance of taking the value a, and a 0.5 chance of taking the value b. It can be concluded that the expected value of X is given by the midpoint between a and b. That is, from our example, it must be the case that $E[f(X)] \geq f(EX)$. In addition, if f is concave, inequality can be reversed to apply on this type of function.

Now, EM algorithm can be explained effectively. Suppose that we have an estimation problem in which we have a training set $\{x^1, \dots, x^m\}$ consisting of m independent examples. We want to fit the parameters of a model $p(x, z)$ to the data where the likelihood is given by

$$l(\theta) = \sum_{i=1}^{m} \log p(x; \theta) \tag{3.9}$$

That is

$$l(\theta) = \sum_{i=1}^{m} \log \sum_{z} p(x, z; \theta) \tag{3.10}$$

where x represents training set, z denotes the latent variable and θ is a unknown parameter. z is a variable that are not observed but are inferred from other variables that are observed. In this algorithm, using latent variables is an advantageous because it reduces the dimensionality of data. When using latent variables, the model or maximization is easier to understand than more variables.

Normally, maximizing $l(\theta)$ might be difficult, therefore, it will be to instead repeatedly construct a lower-bound on l (E-step) and then optimize that lower-bound (M-step).

For each i, let Q_i be some distribution over the z's $(\sum_z Q_i(z) = 1, Q_i(z) \geq 0)$. We can write the following equation:

$$\sum_i \log(p(x^{(i)};\theta) = \sum_i \log \sum_{z^{(i)}} p(x^{(i)}, z^{(i)};\theta) = \sum_i \log \sum_{z^{(i)}} \frac{Q_i(z^{(i)}) p(x^{(i)}, z^{(i)};\theta)}{Q_i(z^{(i)})} \geq$$

$$\sum_i \sum_{z^{(i)}} Q_i(z^{(i)}) \log \frac{p(x^{(i)}, z^{(i)};\theta)}{Q_i(z^{(i)})} \tag{3.11}$$

In the last step of this derivation, Jensen's inequality is used. Logaritmic function is usually known as concave function since $f''(x) = -\frac{1}{x^2} < 0$ over positive real numbers. Now, Jensen's inequality can be performed on this problem.

$$f\left(E_{z^{(i)} \sim Q_i}\left[\frac{p(x^{(i)}, z^{(i)};\theta)}{Q_i(z^{(i)})}\right]\right) \geq E_{z^{(i)} \sim Q_i}\left[f\left(\frac{p(x^{(i)}, z^{(i)};\theta)}{Q_i(z^{(i)})}\right)\right] \tag{3.12}$$

where $z^{(i)} \sim Q_i$ subscripts above indicate that the expectations are with respect to $z^{(i)}$ drawn from Q_i. Therefore, for any set of distributions Q_i, equation (30) gives a lower-bound on $l(\theta)$. Many possible choices for the Q_i are found to be in the solution of the equation. It is an important part to choose correct Q_i.

To make the bound tight for a particular value of θ, we need for the step involving Jensen's inequality in our derivation above to hold with equality. For this to be true, the expectation are tkaen as a constant valued random variable. This can be described as the following equation.

$$\frac{p(x^{(i)}, z^{(i)};\theta)}{Q_i(z^{(i)})} = c \tag{3.13}$$

From the probability theorem, we know $\sum_z Q_i(z^{(i)}) = 1$, this tells us that

$$Q_i(z^{(i)}) = \frac{p(x^{(i)}, z^{(i)};\theta)}{\sum_z p(x^{(i)}, z^{(i)};\theta)} = \frac{p(x^{(i)}, z^{(i)};\theta)}{p(x^{(i)};\theta)} = p(x^{(i)}|z^{(i)};\theta) \tag{3.14}$$

Thus, it can be setted the Q_i to be the posteriori distribution of the $z^{(i)}'s$ given $x^{(i)}$ and the setting of the parameters θ.

Now, we can realize the expectation maximization algorithm. By using equation (30), lower-bound on the loglikelihood can be found in order to maximize Q_i. For M-step, we maximize equation (3.11) with respect to the parameters to obtain a new setting of the θ. Each steps is represented in equation (3.15) and (3.16).

$$Q_i\left(z^{(i)}\right) \coloneqq p\left(z^{(i)}\middle|x^{(i)};\theta\right) \tag{3.15}$$

$$\theta \coloneqq \text{argmax}_\theta \sum_i \sum_{z^{(i)}} Q_i\left(z^{(i)}\right) \log \frac{p\left(x^{(i)},z^{(i)};\theta\right)}{Q_i\left(z^{(i)}\right)} \tag{3.16}$$

These steps should be performed until the convergence point. However, we have to know that this algorithm will converge. We have to check that $l\left(\theta^{(t)}\right) \leq l\left(\theta^{(t+1)}\right)$ which shows EM always monotically improves the log-likelihood. Next θ is chosen explicitly to be

$$\text{argmax}_\theta \sum_i \sum_{z^{(i)}} Q_i\left(z^{(i)}\right) \log \frac{p\left(x^{(i)},z^{(i)};\theta\right)}{Q_i\left(z^{(i)}\right)} \tag{3.17}$$

and thus this formula evaluated at $\theta^{(t+1)}$ must be equal to or larger than the same formula evaluated at $\theta^{(t)}$.

Up to now, we have described how EM algorithm works and its meaning in convergence. In this study, GMM is fitted by using expectation-maximization algortihm for given variables such as covariance and mean value of signal. In GMM, the parameters are represented as $\phi, \mu \; and \; \Sigma$.

The E-step can be calculated as

$$w_j^{(i)} = Q_i\left(z^{(i)} = j\right) = P\left(z^{(i)} = j\middle|x^{(i)};\phi,\mu,\Sigma\right) \tag{3.18}$$

Here, $Q_i\left(z^{(i)} = j\right)$ denotes the probability of $z^{(i)}$ taking the value of j under the distribution Q_i.

In the M-step, it needs to maximize, with respect to our parameters ϕ, μ, Σ the quantity

$$\sum_{i=1}^{m}\sum_{z^{(i)}} Q_i\left(z^{(i)}\right)\log\frac{p\left(x^{(i)},z^{(i)};\phi,\mu,\Sigma\right)}{Q_i(z^{(i)})} =$$

$$\sum_{i=1}^{m}\sum_{j=1}^{k} Q_i\left(z^{(i)}=j\right)\log\frac{p\left(x^{(i)}|z^{(i)}=j;\mu,\Sigma\right)p\left(z^{(i)}=j;\phi\right)}{Q_i(z^{(i)}=j)} =$$

$$\sum_{i=1}^{m}\sum_{j=1}^{k} w_j^{(i)}\log\frac{\frac{1}{\frac{n}{(2\pi)^{\frac{n}{2}}}|\Sigma_j|^{\frac{1}{2}}}\exp\left(-\frac{1}{2}\left(x^{(i)}-\mu_j\right)^T\Sigma_j^{-1}\left(x^{(i)}-\mu_j\right)\right)\phi_j}{w_j^{(i)}} \tag{3.19}$$

Let's maximize this with respect to μ_l. If we take the derivate with respect to μ_l, we find

$$\nabla_{\mu_l}\sum_{i=1}^{m}\sum_{j=1}^{k} w_j^{(i)}\log\frac{\frac{1}{\frac{n}{(2\pi)^{\frac{n}{2}}}|\Sigma_j|^{\frac{1}{2}}}\exp\left(-\frac{1}{2}\left(x^{(i)}-\mu_j\right)^T\Sigma_j^{-1}\left(x^{(i)}-\mu_j\right)\right)\phi_j}{w_j^{(i)}} =$$

$$-\nabla_{\mu_l}\sum_{i=1}^{m}\sum_{j=1}^{k} w_j^{(i)}\left(-\frac{1}{2}\left(x^{(i)}-\mu_j\right)^T\Sigma_j^{-1}\left(x^{(i)}-\mu_j\right)\right) = \frac{1}{2}\sum_{i=1}^{m} w_l^{(i)}\nabla_{\mu_l} 2\mu_l^T\Sigma_j^{-1}x^{(i)} -$$

$$\mu_l^T\Sigma_j^{-1}\mu_l = \sum_{i=1}^{m} w_l^{(i)}\left(\Sigma_j^{-1}x^{(i)}-\Sigma_j^{-1}\mu_l\right) \tag{3.20}$$

If we set this equation to zero, we can find maximizing value at μ_l.

$$\mu_l := \frac{\sum_{i=1}^{m} w_l^{(i)}x^{(i)}}{\sum_{i=1}^{m} w_l^{(i)}} \tag{3.21}$$

Let's derive the M-step update for the parameter ϕ_j. Grouping together only the terms that depend on ϕ_j, we find that we need to maximize

$$\sum_{i=1}^{m}\sum_{j=1}^{k} w_j^{(i)}\log\phi_j \tag{3.22}$$

However, the sum of ϕ_j must be equal to one as rule of probability. In order to solve this constraint, we should construct the Lagrangian

$$L(\phi) = \sum_{i=1}^{m}\sum_{j=1}^{k} w_j^{(i)}\log\phi_j + \beta\left(\sum_{j=1}^{k}\phi_j - 1\right) \tag{3.23}$$

where β is the Lagrange multiplier. Taking derivatives

$$\frac{\partial}{\partial\phi_j}L(\phi) = \sum_{i=1}^{m}\frac{w_j^{(i)}}{\phi_j} + 1 \tag{3.24}$$

If it is setted to zero, we get

$$\phi_j = \frac{\sum_{i=1}^{m} w_j^{(i)}}{-\beta} \tag{3.25}$$

In order to demonstrate this equation is correct, $\phi_j \propto \sum_{i=1}^{m} w_j^{(i)}$. Using the constraint that $\sum_j \phi_j = 1$, we can find that $-\beta = \sum_{i=1}^{m}\sum_{j=1}^{k} w_j^{(i)} = \sum_{i=1}^{m} 1 = m$. In this

definitions, $w_j^{(i)} = Q_i\left(z^{(i)} = j\right)$ and since probabilites sum to 1. Therefore, M-step updates for the parameters ϕ_j can be given as follow:

$$\phi_j := \frac{1}{m}\sum_{i=1}^{m} w_j^{(i)} \tag{3.26}$$

Shortly, membership weight, mean and covariance values can be defined as the following formulas.

$$\alpha_k^{new} = \frac{N_k}{N},\ 1 \le k \le K \tag{3.27}$$

where N represents the number of all data points, K denotes the number of all mixture components. The mean value can be given in equation (3.28).

$$\mu_k^{new} = \frac{1}{N_k}\sum_{i=1}^{N} w_{ik} x_i, \quad 1 \le k \le K \tag{3.28}$$

Then covariance matrix is

$$\Sigma_k^{new} = \frac{1}{N_k}\sum_{i=1}^{N} w_{ik}(x_i - \mu_k^{new})(x_i - \mu_k^{new})^T, \quad 1 \le k \le K \tag{3.29}$$

The expectation maximization algorithm have been described in detailed in order to cover convergence operation in signal processing. Now, we will talk about gaussian mixture model to understand how it is necessitated for signal recognition.

As mentioned before, GMM is a parametric probability density function represented as a weighted sum of Gaussian component densities. It can be given as equation form

$$p(x|\lambda) = \sum_{i=1}^{M} w_i g(x|\mu_i, \Sigma) \tag{3.30}$$

where x is a D-dimensional continuous-valued data vector(i.e. measurement of features), $w_i, i = 1, \dots, M$ are the mixture weight and $g(x|\mu_i, \Sigma_i), i = 1, \dots M$ represents the component Gaussian densities. Each component density is a D-variate Gaussian function of the form,

$$(x|\mu_i, \Sigma_i) = \frac{1}{(2\pi)^{\frac{d}{2}}|\Sigma_i|^{\frac{1}{2}}} \exp\left(-\frac{1}{2}(x^* - \mu_i)^T \Sigma_i^{-1}(x^* - \mu_i)\right) \tag{3.31}$$

with mean vector μ_i and covariance matrix Σ_i. Remember that the mixture weights satisfy the constraint that $\sum_{i=1}^{M} w_i = 1$.

Knowing that Gaussian distribution shows the characteristic weight or mean value of data points given. However, Gaussian distribution has a constraint because of unique solution of data. Therefore, Gaussian mixture model can establish a model to split data

into sections by examining its mean and covariance value. This can be illustrated as the following figure.

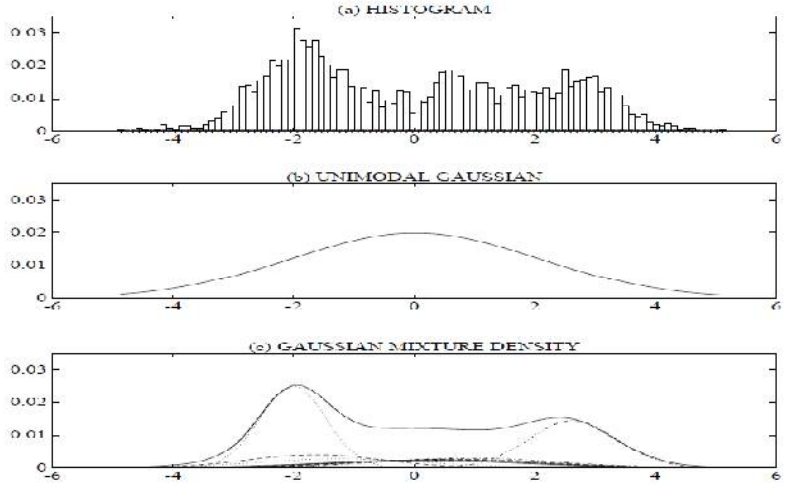


Figure. 3.2 Comparison of distribution modeling

In the first diagram, the given data is analyzed by using histogram method. It includes several sections. It is good for us to analyze deeply to the signal. However, variables which relates to the others can be lost because of many sections.

In the second diagram, unimodal gaussian distribution is given when using only a mean and variance value. When examining this diagram, there is only one point which can be inferred as meaningful for us.

In the third diagram, Gaussian mixture densities are represented as components with mean and covariance values. In this model, it contains several distribution with unique feature to the others. On the other hand, it is not complicated as much as histogram. We can infer data dispersion intutitively in order to classify data given.

Gaussian mixture model is an important part of this study to process heart signal because every ECG signal contains little differences to each other even if it is obtained from the same person. Therefore, it is an advantage of that the classification can be performed when the signal is non-stationary which means that it is time-dependent.

In the present study, a probability density function(pdf) is represented by the weighted sum of a finite number of components with Gaussian densities. Then the pdf estimation problem reduces to estimation of the parameters included in each component. A pdf $f(x)$ of the feature vector $X \in R^d$ is represented by GMM with K classes

$$f(x) = \sum_{k=1}^{K} \sum_{m=1}^{M_k} \alpha_{k,m} g\left(x; \mu^{(k,m)}, \Sigma^{(k,m)}\right) \quad (3.32)$$

$$\sum_{k=1}^{K} \sum_{m=1}^{M} \alpha_{k,m} = 1 \quad (3.33)$$

where $g\left(x; \mu^{(k,m)}, \Sigma^{(k,m)}\right)$ is the d-dimensional Gaussian distribution. M_k denotes the number of components of the class k, $\alpha_{k,m}$ denotes the mixture coefficient or the mixing proportion of each component $\{k, m\}$.

In ECG signal processing, components can be represented as the distributions of different section. For example, ECG signal has five fudicial points, P,Q,R,S and T. Every point can be considered as unique component. On the other hand, classes tell us what we work to recognize. Assume that you want to determine how frequent QRS peak occurs. For this purpose, you should establish two classes as one is logical positive and the other is logical negative. That is, we can set the state of the classes in order to obtain the section of the signal which we want to.

As mentioned before, the Bayes' rule have been given in order to cover the relation between two random variables. The Bayes' rule determines a specific class if a posteriori probability of the vector belonging to the class is larger than the ones of the other. When using GMM, the posteriori probability $P(k|x)$ can be given as

$$P(k|x) = \sum_{m=1}^{M_k} P(k, m|x) = \sum_{m=1}^{M_k} \frac{P(k,m)P(x|k,m)}{P(x)} \quad (3.34)$$

where $P(k,m)$ is a priori probability of the class k and the component m, which corresponds to the mixing coefficient $\alpha_{k,m}$; and $P(x|k,m)$ is the pdf of x agreed upon the class k and the component m. Then using gaussian mixture probability density function, the a posteriori probability, $P(k,m|x)$ can be expressed as

$$P(k,m|x) = \frac{P(k,m)P(x|k,m)}{\sum_{k'=1}^{K} \sum_{m'=1}^{M_k} \alpha_{k',m'} g\left(x; \mu^{(k',m')}, \Sigma^{(k',m')}\right)} = \frac{\alpha_{k,m} g\left(x; \mu^{(k,m)}, \Sigma^{(k,m)}\right)}{\sum_{k'=1}^{K} \sum_{m'=1}^{M_k} \alpha_{k',m'} g\left(x; \mu^{(k',m')}, \Sigma^{(k',m')}\right)} \quad (3.35)$$

That is, the pdf is approximated by the weighred sum of the Gaussian component.

Now, we introduce neural network to classify data coming from biomedical signal. In general definition, artificial neural networks (ANNs) are a family of statistical learning algorithms inspired by biological neural networks and are used to estimate approximate functions that can depend on a large number of inputs and are generally unknown. Warren McCulloch and Walter Pitts [95] invented a computational model for neural networks based on mathematics and algorithms. It is called as threshold logic. The

model paved the way for neural network research to split into two distinct approaches. One approach focused on biological processes in the barin and the other focused on the application ofneural networks to artificial intelligence.

Then, Donald Hebb [96] created a hypothesis of learning based on the mechanism of neural plasticity that is now known as Hebbian learning. It is typical unsupervised learning rule and its later variants were early models for long term potentiation in the brain.

Frank Rosenblatt [97] created the perceptron, an algorithm for pattern recognition based on a two-layer learning computer network using simple addition and substraction. After a while, Paul Werbos [98] presented backpropagation algorithm to train neural networks.

To sum up, neural networks, as used in artificial intelligence, have traditionally been viewed as simplified models of neural processing in the brain, even though the relation between this model and brain biological architecture is debated, as it is not clear to what degree artificial neural networks mirror brain function [99].

In this study, neural networks are used to model Gaussian mixture distribution as coefficients. It is the most vital part of this study because Gaussian mixture model can only be trained by using expectation maximization algorithm or MAP. However, given systems are much more complex than the model that GMM can create.

For these reasons, every Gaussian component should be transformed into coefficients in order to train by using back-propagation algorithm.

The published study [89] is an effective application of neural networks with Gaussian mixture model. The following paragraphs describe their method and its application.

In this study, the structure of neural network is chosen as feedforward containing three layers. First, the input feature vector $x \in R^d$ is prepocessed and converted into the modified input vector $X \in R^H$. There must be a transform to use neural networks because Gaussian mixture model creates a relation between input data. In order to show this transform, we should perform log-linearization on the signal.

When using the mean vector $\mu^{(k,m)} = \left(\mu_1^{(k,m)}, \dots, \mu_d^{(k,m)}\right)^T$ and the inverse of the covariance matrix $\Sigma^{(k,m)^{-1}} = [s_{ij}^{(k,m)}]$, the numerator of the right side of equation (3.35) can be represented as

$$\alpha_{k,m} g\left(x; \mu^{(k,m)}, \Sigma^{(k,m)}\right) = \alpha_{k,m}(2\pi)^{-\frac{d}{2}}\left|\Sigma^{(k,m)}\right|^{-\frac{1}{2}} \exp\left[-\frac{1}{2}\sum_{j=1}^{d}\sum_{l=1}^{j}(2 - \delta_{jl}) s_{jl}^{(k,m)} x_j x_l + \sum_{j=1}^{d}\sum_{l=1}^{d} s_{jl}^{(k,m)} \mu_j^{(k,m)} x_l - \frac{1}{2}\sum_{j=1}^{d}\sum_{l=1}^{d} s_{jl}^{(k,m)} \mu_j^{(k,m)} \mu_l^{(k,m)}\right] \quad (3.36)$$

where δ_{ij} is the kronecker delta: $\delta_{ij} = 1$ when $i = j$ and $\delta_{ij} = 0$ when $i \neq j$. If we linearize the right side of equation (55), we get

$$\varepsilon_{(k,m)} = \log\left(\alpha_{(k,m)} g\left(x; \mu^{(k,m)}, \Sigma^{(k,m)}\right)\right) = \beta^{(k,m)^T} X \quad (3.37)$$

where $X \in R^H$ and $\beta^{(k,m)} \in R^H$ can be defined as

$$X = (1, x^T, x_1^2, x_1 x_2, \dots, x_1 x_d, x_2^2, x_2 x_3, .. x_2 x_d, \dots, x_d^2) \quad (3.38)$$

$$\beta^{(k,m)} = \left(\beta_0^{(k,m)} \sum_{j=1}^{d} s_{j1}^{(k,m)} \mu_j^{(k,m)} \dots, \sum_{j=1}^{d} s_{jd}^{(k,m)} \mu_j^{(k,m)} - \frac{1}{2} s_{11}^{(k,m)}, -s_{12}^{(k,m)}, \dots, s_{1d}^{(k,m)}, \dots, -\frac{1}{2}(2 - \delta_{jl}) s_{jl}^{(k,m)}, \dots, -\frac{1}{2} s_{dd}^{(k,m)}\right)^T \quad (3.39)$$

$$\beta_0^{(k,m)} = -\frac{1}{2}\sum_{j=1}^{d}\sum_{l=1}^{d} s_{jl}^{(k,m)} \mu_j^{(k,m)} \mu_l^{(k,m)} - \frac{d}{2}\log 2\pi - \frac{1}{2}\log\left|\Sigma^{(k,m)}\right| + \log \alpha_{k,m} \quad (3.40)$$

and the dimension H is defined as $H = 1 + \frac{d(d+3)}{2}$.

All of the equations given above states that GMM distribution can be convertable from mean and covariance vector to coefficients in order to perform a neural network. For this purpose, modified input is generated because there is relationship between random variables in GMM. We can see that $\epsilon_{k,m}$ can be described as the product of the coefficient vector $\beta^{(k,m)}$ and the modified input vector $X \in R^H$ where the element of the vector $\beta^{(k,m)}$ is a nonlinear combination of the GMM parameters, such as the mixture coefficients, mean values, and standard deviations of the sample data, and the modified input vector X includes the product of the elements of the input feature vector.

By regarding the coefficient vector $\beta^{(k,m)}$ as the weight coefficients, the GMM can be incorporated as the network structure. However, the definition of $\beta^{(k,m)}$ indicates that each element of $\beta^{(k,m)}$ is constrained by the statistical properties of the parameter

$s_{i,j}^{(k,m)}$. This constraint may cause a difficult problem in the learning procedure: how to satisfy the constraints during the learning of the weight coefficients. In order to remove this difficulty, the new variable $Y_{k,m}$ and the new coefficient vector $w^{(k,m)}$ are introduced in this study as

$$Y_{k,m} = \epsilon_{k,m} - \epsilon_{K,M_k} = \left(\beta^{(k,m)} - \beta^{(K,M_k)}\right)^T X = w^{(k,m)^T} X \tag{3.41}$$

where the weight coefficient $w^{(k,m)}$ is defined as the difference between $\beta^{(k,m)}$ and $\beta^{(K,M_k)}$, and $w^{(K,M)} = 0$. Owing to this transformation, the weight coefficient $w^{(k,m)}$ can have any real number, so that there are no contraints in the learning procedure. Note that this transformation does not lead to any loss of information in spite of $Y_{K,M_K} = 0$ since the variable $\epsilon_{k,m}$ in (3.36) is redundant because of $\sum_{k=1}^{K}\sum_{m=1}^{M_k} P(k,m|x) = 1$. Then the a posteriori probability $P(k,m|x)$ of (3.35) can be computed as

$$P(k,m|x) = \frac{\exp(Y_{k,m})}{\sum_{k'=1}^{K}\sum_{m'=1}^{M_k}\exp(Y_{k',m'})} \tag{3.42}$$

By using the algorithm of each pdf and using the weight coefficient vector $w^{(k,m)}$, the a posteriori probability can be introduced with the use of the variables $Y_{k,m}$ which can be trainable.

Up to now, general information about neural network and its basis with GMM distribution have been explained in order to cover what is established. Next section will describe that training algorithm in neural networks. In this section, we will explicitly introduce its learning rule and selection of the teacher vector.

3.1.2. Training Algorithm

In this section, training algorithm to fix coefficient until convergence is described when GMM coefficients are created effectively. However, the neural network have to be established before applying training algorithm. Tsuji et al [89] illustrated this network as the following figure.

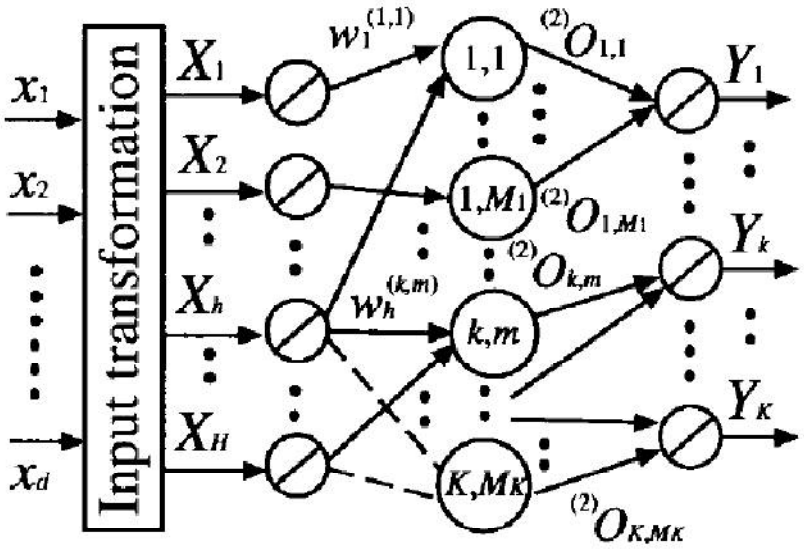


Figure. 3.3 The structure of neural network for LLGMN in [89]

In the above figure, the first layer consists of H units corresponding to the dimesion of X. In addition, identity function is performed to activate each unit. The relation between input and output in the first layer can be given as

$$I_j^{(1)} = X_j \tag{3.43}$$

$$O_j^{(1)} = I_j^{(1)} \tag{3.44}$$

where $I_j^{(1)}$ and $O_j^{(1)}$ represents the input and the output, respectively corresponding to the dimension of the system.

The second layer includes the same number of units as the total component number of the GMM $\sum_{k=1}^{K} M_k$. Each unit receives the output of the first layer weighted by the coefficient $w_h^{(k,m)}$ and the ouputs the a posteriori probability of each component according to equation (3.42). The equations for the second layer can be defined as

$$I_{k,m}^{(2)} = \sum_{h=1}^{H} O_h^{(1)} w_h^{(k,m)} \tag{3.45}$$

$$O_{k,m}^{(2)} = \frac{\exp I_{k,m}^{(2)}}{\sum_{k'=1}^{K} \sum_{m'=1}^{M_k} \exp I_{k',m'}^{(2)}} \tag{3.46}$$

where $w_h^{(K,M_k)} = 0$ because of difficulty problem in convergence. Equation (3.46) can be considered as a kind of the generalized sigmoid function.

Finally, third layer consists of K units corresponding to the number of classes and outputs the a posteriori probability of the class k. The relation between input and output can be represented as

$$I_k^{(3)} = \sum_{m=1}^{M_k} O_{k,m}^{(2)} \tag{3.47}$$

$$Y_k = I_k^{(3)} \tag{3.48}$$

As a result, we have gotten the neural network with trainable coefficients derived from GMM.

Now, the supervised learning should be applied on the system. The supervised learning is a process which system can be trained by teacher vector given. Assume that teacher vector $T^{(n)} = \left\{T_1^{(n)}, \dots, T_k^{(n)}, \dots T_K^{(n)}\right\}$ is given. As an convergence function for teaching, we use

$$J = \sum_{n=1}^{N} J_n = -\sum_{n=1}^{N} \sum_{k=1}^{K} T_k^{(n)} \log\left(Y_k^{(n)}\right) \tag{3.49}$$

and the training is applied until for every value is the same value of each training vector. Weight modification is performed by using Eq. (3.50).

$$\Delta w_h^{k,m} = -\eta \sum_{n=1}^{N} \frac{\partial J_n}{\partial w_h^{k,m}} \tag{3.50}$$

where η is the learning rate of neural network. The neural network is trained by using backpropagation rule. According to this rule, all of the inputs are taught by following equation until error between input and output equal to specified value.

$$\frac{\partial J_n}{\partial w_h^{k,m}} = \frac{\partial}{\partial w_h^{k,m}}\left(-\sum_{k=1}^{K} T_k^{(n)} \log\left(Y_k^{(n)}\right)\right)$$

$$= -\sum_{k=1}^{K}\left[\frac{\partial T_k^{(n)} \log\left(Y_k^{(n)}\right)}{\partial Y_k^{(n)}}\right] * -\sum_{k=1}^{K}\left[\frac{\partial\left(Y_k^{(n)}\right)}{\partial O_{k,m}^{(2)(n)}} \frac{\partial\left(O_{k,m}^{(2)(n)}\right)}{\partial I_{k,m}^{(2)(n)}} \frac{\partial\left(I_{k,m}^{(2)(n)}\right)}{\partial w_{k,m}}\right]$$

$$= \left(Y_k^{(n)} - T_k^{(n)}\right) \frac{O_{k,m}^{(2)(n)}}{Y_k^{(n)}} X_h^{(n)} \tag{3.51}$$

All of operations are continued until the differences between input and output are smaller than acceptable error specified by user. After all these steps, as a difference tool from LLGMN [89] method.

3.1.3 Tests

3.1.3.1 Gmm Algorithm and Back-Propagation Algorithm

In accordance with the above explanations, we should test algorithms given sequentially. In order to perform algorithm, firstly, we perform Gaussian mixture model with neural networks. Secondly, the back propagation algorithm are applied on the system. Thirdly, all of the results with graph will be given in order to compare how effective the standard algorithm is.

In the first place, we use the algorithm published [89] in order to show how effective it is in the ECG signal processing. However, the back-propagation rules are not included to the code because it increases stability of the network if your algorithm is not well-worked in your system. For testing the algorithm, an ideal ECG frame should be selected as the following figure.

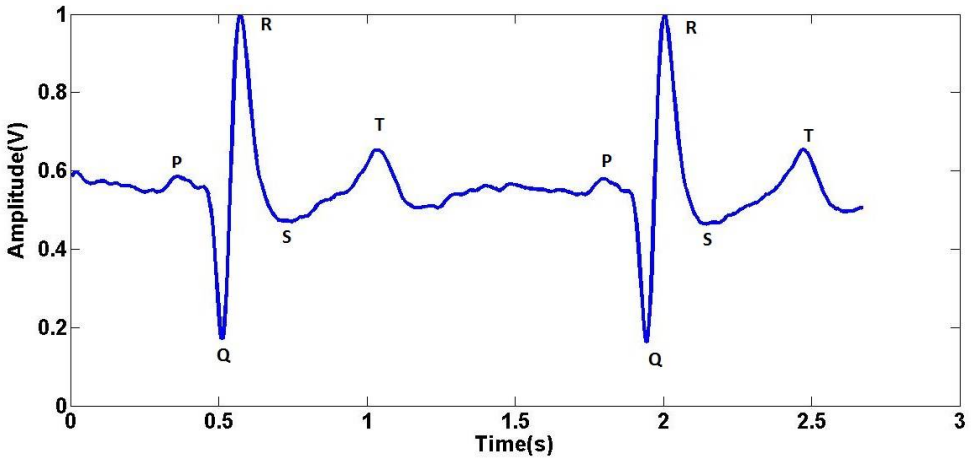


Figure. 3.4 An ideal ECG frame with typical features

This signal was obtained by novel ECG device manufactured by authors. When the signal can be obtained, we have to choose the section that we want to recognize by using the algorithm.

For this purpose, GMM algorithm is established by using the equations given above. The back-propagation algorithm is removed in order to demonstrate the effect of input which can be selected as both same and different to each other. So, training cannot be

performed. The following figures illustrate GMM algorithm with same input and different input.

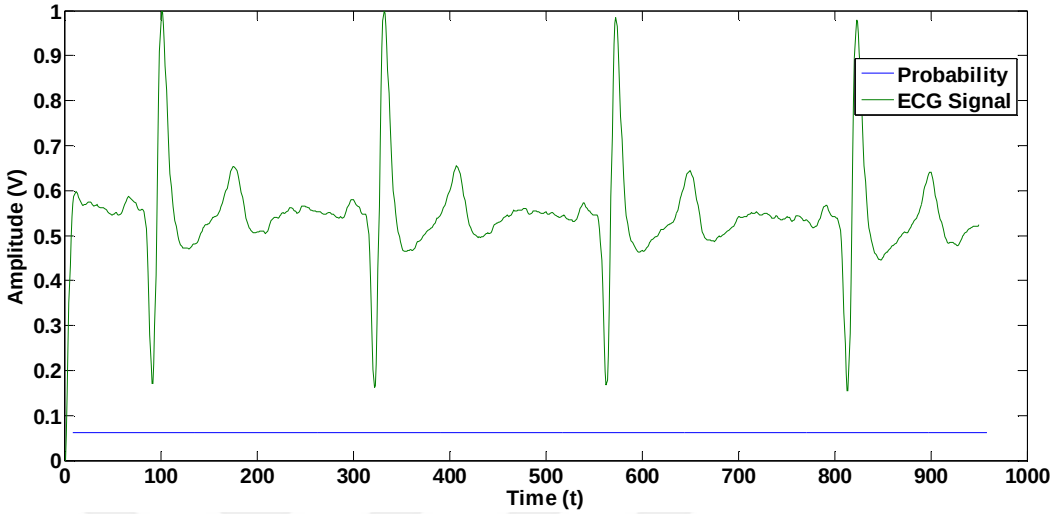


Fig. 3.5 QRS Recognition results with different input

Figure (3.5) demonstrates that feeding different input to the system does not work effectively due to some of the reasons. One of the reasons is that GMM algoritm produce expanding distribution because the input have a great range of values. Therefore, the algorithm supposes that input entried is an element of data given first. This can be illustrated as cluster structure in order to show how distribution data speard on the axis. This is given in figure (3.6).

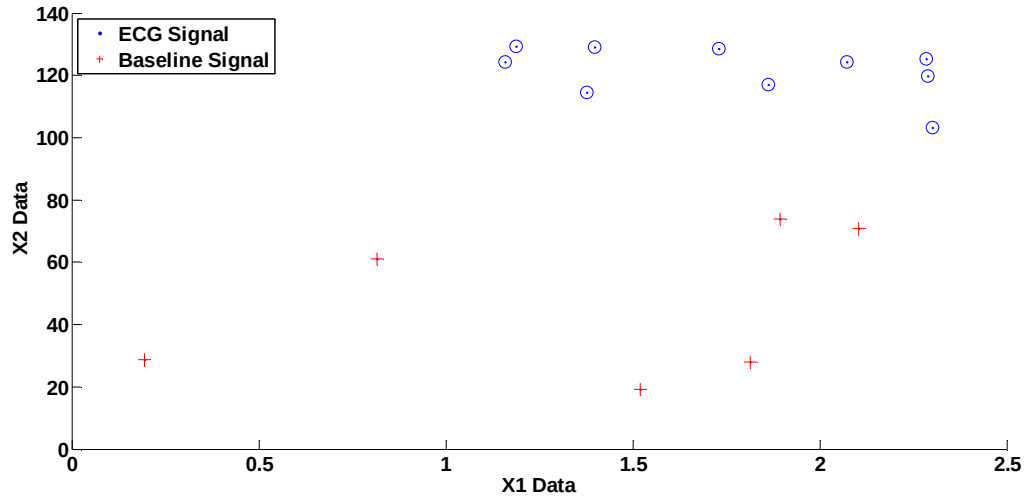


Figure. 3.6 The distribution of Data for different input

In figure (24), there are two different inputs independently when GMM is operated by using without back-propagation algorithm. In this state, the algorithm cannot be effectively applied because fitting parameters change QRS training values. Then, when creating distribution in accordance with these parameters, no data can be recognized by the algorithm.

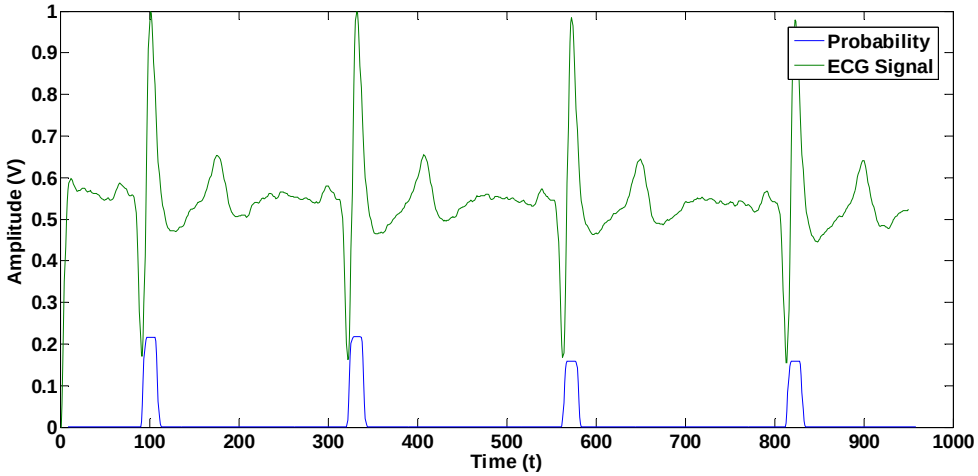


Figure. 3.7 QRS Recognition results with same input

On the other hand, for the same input with a little different values is performed effectively on the system. In figure (3.7), probability values is small because there is no correction threshold for the algorithm. However, this algorithm can be easily used to attain high performance in QRS complex classification. In order to show the spreading of data on the graph, figure (3.8) can be illustrated as follow.

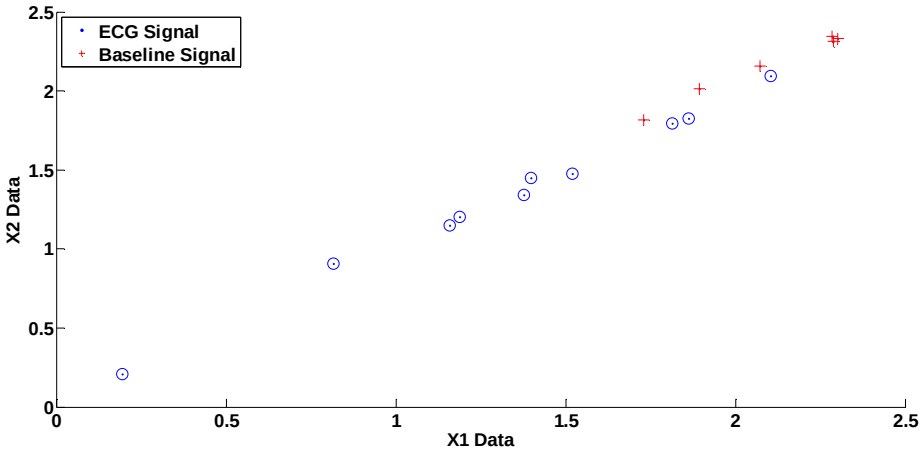


Figure. 3.8 The distribution of Data for same input

In this figure, ECG training data is dispersed as a line. Therefore, for any compare, the chance of successive recognition is more than the other situation. Tsuji et al. [89] used different inputs for their system to perform recognition on EEG signal. However, in this study, we cannot perform different inputs for the system because ECG signal has a unique pattern and its spreading is sequentially. In EEG and EMG, the value of amplitude is more important than duration or pattern because the activity of the muscle is the superposition of all the muscle fibers [100]. Due to these reasons, it can be concluded that the usage of same input for training the system is more convenient than the different input.

In addition, the coefficients which are created by one signal can be applied on different ECG signals. Figure (3.9) can be given as an example of that.

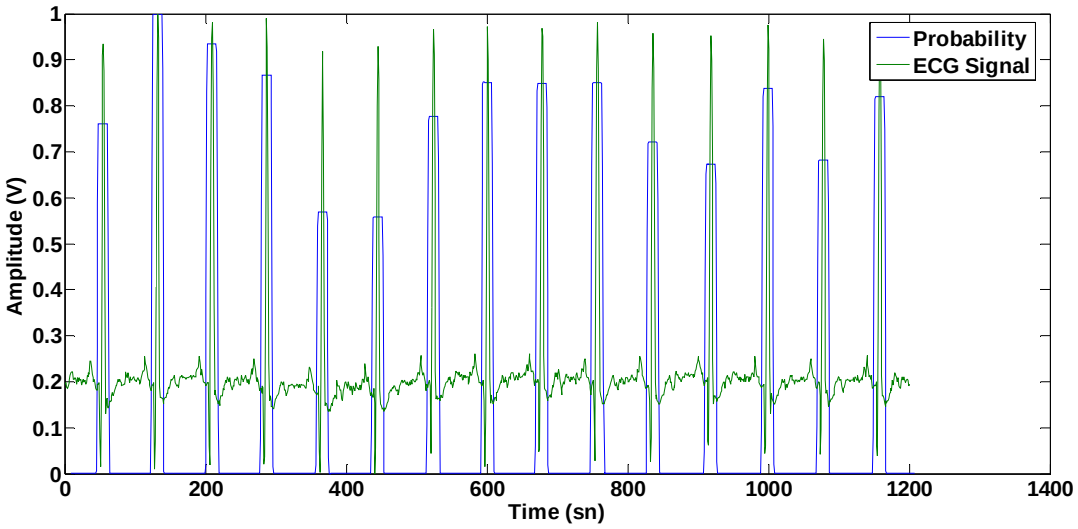


Figure. 3.9 QRS Recognition results with same input for different ECG signal

It can be said that GMM can be used to classify the other ECG signals effectively, however, there must be a condition that all of the inputs are similar to each other for QRS complex.

Now, the back-propagation rules are accounted for the neural network. For this purpose, MATLAB code is written to work appropriate with the neural network. When using back-propagation rule with GMM in neural networks, it can be given as the following diagram.

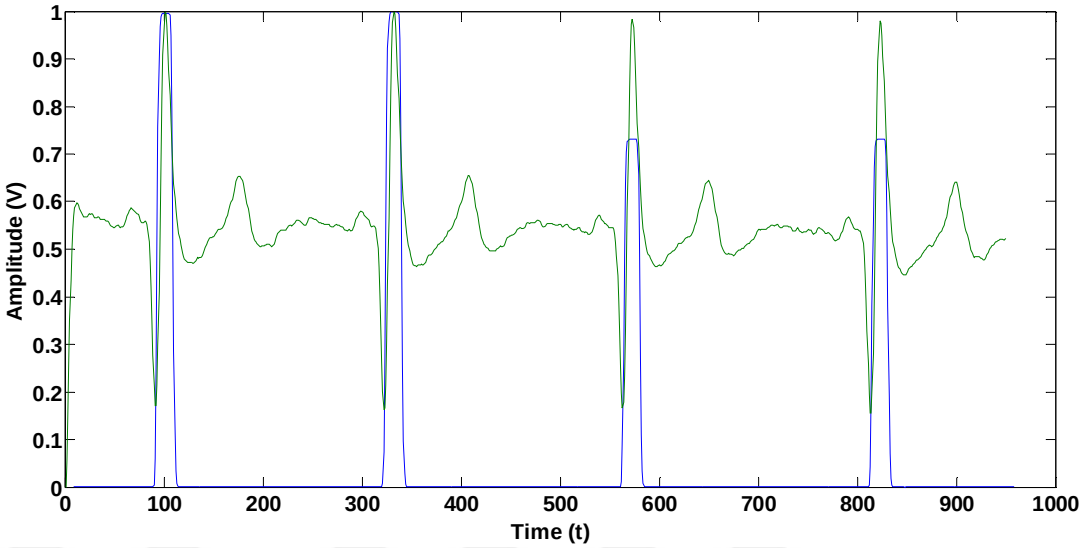


Figure. 3.10 An ideal QRS complex analysis with neural network

If the set of vector given is examined as a cluster, it can be illustrated as the same figure (3.5) because of the same training set. These algorithm perfectly analyze to the signal and its performance can be evaluated by applying on itself. We can also obtain result from the different ECG signal with the same coefficients. The following figure is illustrated for this purpose.

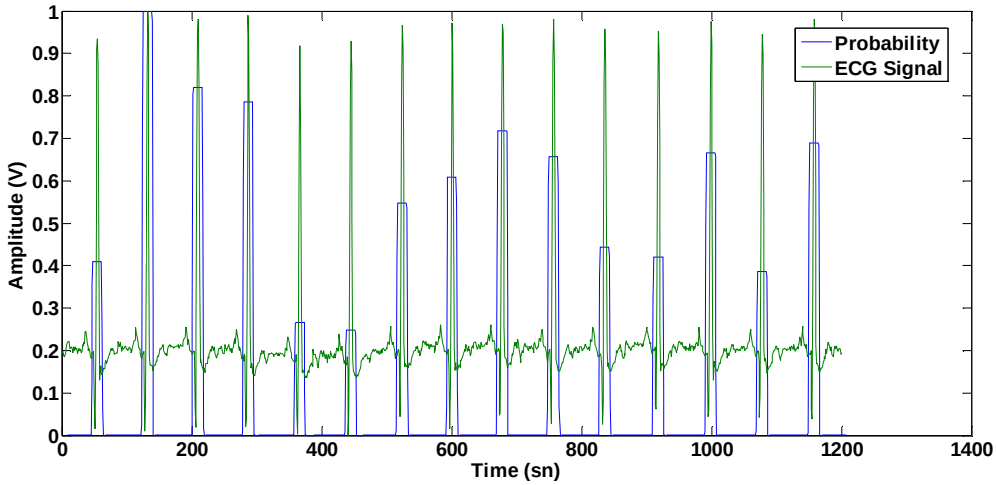


Figure. 3.11 An ideal QRS complex analysis with neural network for different signal

Figure (3.11) demonstrates that GMM with back-propagation works effectively when applying on QRS complex. Some of the QRS complex cannot be diagnosed about 100 percent but can be performed some sort of threshold in order to change their probability as 100 percent.

Finally, the novel algorithm for determination ECG pattern is introduced to attain high performance in neural networks. Our purpose defends that LLGMN algorithm cannot be performed effectively on ECG pattern due to some restrictions such as necessary of sequential data, the difference of input-output relation and so on.

The novel algorithm is based on Gaussian mixture model with back-propagation in neural network. In addition, we suggest a function to fix compare problem coming from sequential pattern form. What is more is that we introduce a compare algorithm for correction of the posteriori probability of ECG recognition.

On the other hand, we use teacher vector in both training and comparing algorithm separately. We observed different results when that was applied on the algorithm. Due to several factors such exponentiating outputs by teacher vector and changing input entry, the novel algortihm have become more applicable to detect signal abnormalities and the final points of the ECG sections such QT, QRS and PR segments.

For our algorithm, as distinct from LLGMN in [89], the training data are chosen as closely to each other. Normally, all of the training set should be selected as different to each other [89]. That may cause a problem to converge data set in Gaussian mixture model. Therefore, one of the problems for this study is to fix convergence problems in Expectation-maximization algortihm. Although, we faces with some of the problems, the novel algorithm can be applied on ECG pattern classification effectively.

In order to demonstrate the algorithm performance, firstly, we perform the algorithm to analyze QRS complex in different pattern of ECG signal. Secondly, P, Q, R, S and T waveforms are diagnosed by using our algorithm. Then, we present a section recognition to diagnose illness or abnormalities in the heart. Finally, we compare their results to the other algorithms.

3.1.3.2 The Novel Approach to Pattern Recognition of ECG

Up to now, many studies about QRS complex detection have been published by many researchers. QRS complex has an important feature to detect heartbeat. QRS complex is composed of three fiducial points but one of them is an important feature of detection of heartbeat. R point can be used to find heartbeat. Therefore, up to now, many studies have been published about its algorithm and process.

Shen *et al.* [101] investigated the feasibility of using the electrocardiogram (ECG) as a biometric for human identity verification. They used template matching as comparing

two signals which are similar to another one and a decision-based neural network which is a member of supervised learning family to identify individual ECG signal. They had an achievement about recognition and classification of ECG as an individual signal. However, they couldn't match ECG signal at the rate of %100 with one method, because they had to perform preprocess on the ECG signals. Israel *et al.* worked on the same pattern classification [102]. They focused on the relationship between feelings and ECG signals. For the classification of the signals, they performed standard linear discriminate analysis. The contingency matrix as a visualization for classification performance was also used. They compared to signals under different circumstances. Even though, they had an achievement to recognize individual pattern in ECG, they didn't identify heartbeats at the rate of %82. Chazal *et al.* [103] evaluated five beat classes recommended by ANSI/AAMI EC57:1998 standard. They applied a linear discriminant analysis on ECG data comes from MIT-DB arrhythmia. They used statistical classifier model and a large number of ECG data. Even though, they achieved the recognition in 50,000 heartbeats, training duration was very long. Also, they applied several filter on ECG signals. Therefore, the recognition rate of heartbeat couldn't become one hundred percent accurate. Andreao, *et al.* [104] implemented hidden markov model for ECG signal analysis. Gaussian probability density function and maximizing locally the likelihood were used effectively by them. Even though, beat detection performance was 99.79% and this method hadn't necessitate manual of labels for training, they had to use several methods to obtain high performance. Yu and Chen [105] performed ECG classification using probabilistic neural network and discrete wavelet transform. They provided good classification for ECG signals. Its recognition rate was about %99.65. Even though, it had a great pattern recognition rate, ECG data must be collected in sub bands produced by using a discrete wavelet transform. On the other hand, this method included some bad effects such as the noise on the classifier produced by probabilistic neural network and requirement to process ECG signals. Martis, *et al.* [106] published a mechanism consisted of two stage to classify of ECG signals using Gaussian mixture model (GMM). In this method, cardiac abnormality detection was performed using GMM. MIT-DB was used to obtain ECG arrhythmia. All of the obtained data were used to teach and validate the algorithm can work correctly. Sequentially, re-sampling, QRS extraction, linear prediction model, segmentation and principal component analysis (PCA) to reduce dimensionality were performed. GMM parameters were estimated using iterative expectation maximum

(EM). They had an achievement to recognize disease pattern classification at the rate of 99.7. Even though, it was achieved based on probabilistic method as GMM, there were many operation to reach a good classification. Saxena, *et al.* [107] used two wavelet transforms: one of them was used for QRS detection and the other was used for P and T wave detection. They evaluated the ECG signals comes from MIT/BIH database by which signals had an arrhythmia. There were several advantages to use the wavelet transform such as eliminating baseline wander, artifact and noise. Even though, they had a great recognition rate about QRS detection, they worked on virtual data. Apart from this, their algorithm gives a definite result regarding recognition of the signals. The other groups, Kim, *et al.* [108] performed ECG signal compression and classification algorithm based on quad level vector for ECG Holter system. The accuracy performance of the heartbeat detection was 100%. However, their accuracy rate decreased 95.63% in noise. Moreover, they had to compress ECG data and process it in this form due to designing for a Holter system.

In this paper, we have developed a new algorithm based on Gaussian mixture model and log-linearization. The proposed algorithm is composed of two sections: training and comparing. Training algorithm is similar to the log-linearized Gaussian mixture network presented by Tsuji [109] however, unlike to the Tsuji algorithm, input is used differently to achieve good classification in ECG signals. The Log-linearized Gaussian mixture network was first used to recognize EEG pattern classification by Tsuji. Latter, Tsuji *et al.* [110] developed a new method to construct an appropriate classification network. The present paper proposes a new algorithm to use in the recognition of ECG signals. The algorithm has many flexible features to attain high classification such as independent of signal frequency, necessitating a small data for training and short period of training time. Additionally, with the developed comparing algorithm, the output of the neural network can be analyzed by doctors or experts to detect heartbeat even if its output isn’t one hundred percent accurate.

In order to recognize QRS complex, the novel algorithm is performed on the ECG signal. Their result can be shown as the following figure.

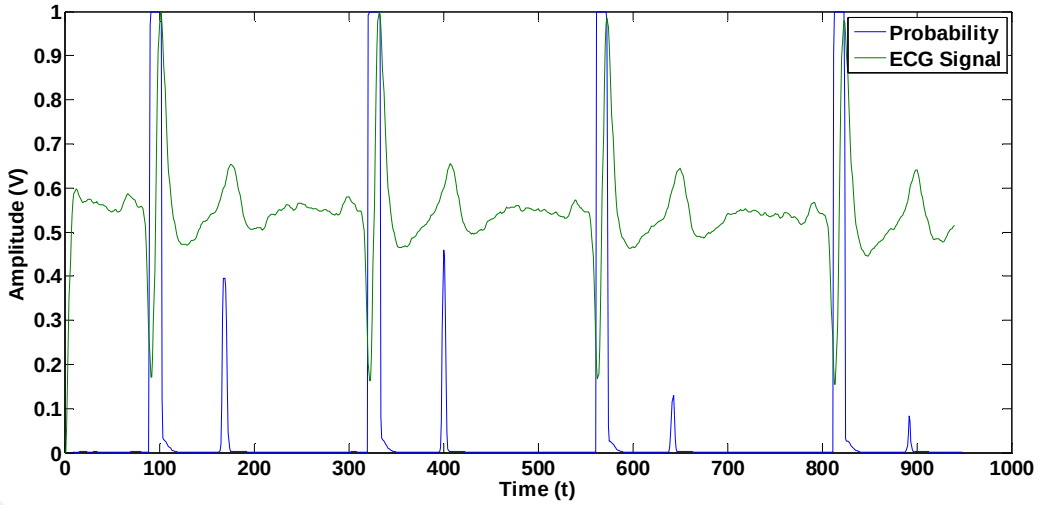


Figure. 3.12 QRS Complex Detection with Novel Approach

Figure (3.12) demonstrates that the novel approach to detect QRS complex is performed effectively. However, there are some error on the signal. One of the problems is T wave probability is increased at 40 percent because its shape is similar to the QRS complex. Also, the other problem is starting point shifting. Normally, neural network can give the beginning of the QRS complex. However, our algorithm is fixed by compare function when comparing algorithm is applied. Therefore, as a consequence of many experiment, we have found a relation between this shifting and correct position of QRS complex. This is given as the following equation.

$$T_{sp} = T_{tsp} + \frac{N_{tn}}{2} \tag{3.52}$$

T_{sp} represents the corrected starting point, T_{tsp} denotes the uncorrected starting point in time and N_{tn} is the number of training data set. Compare algorithm gives an output corresponding the proposed function. So, to find starting point correctly, it should be fixed by equation (3.52).

Now, we will describe the fixing function or compare function. In equation (3.53), it is shown.

$$Y_k^{(n)} = \prod_{i=1}^{N_{TN}} {Y_k^{(i)}}^{T_k^{(n)}} \tag{3.53}$$

In this equation, $Y_k^{(n)}$ represents the output for input given. $T_k^{(n)}$ is the teacher vector in order to fix the end and start points of output given. We can see that this formula creates

an output combining to the others in the range of the number of training data set. When applying this algorithm, fig. 36 can be obtained.

Although, as mentioned before, our algorithm gives two different output, one of them is positive result and the other is negative result. However, the standard method does not include positive or negative result because one of the input is desired characteristic and the other is undesired characteristic. Therefore, the algorithm should choose the output which will be used.

When applying the algorithm on different ECG signals, the results can be given represented as the following figure.

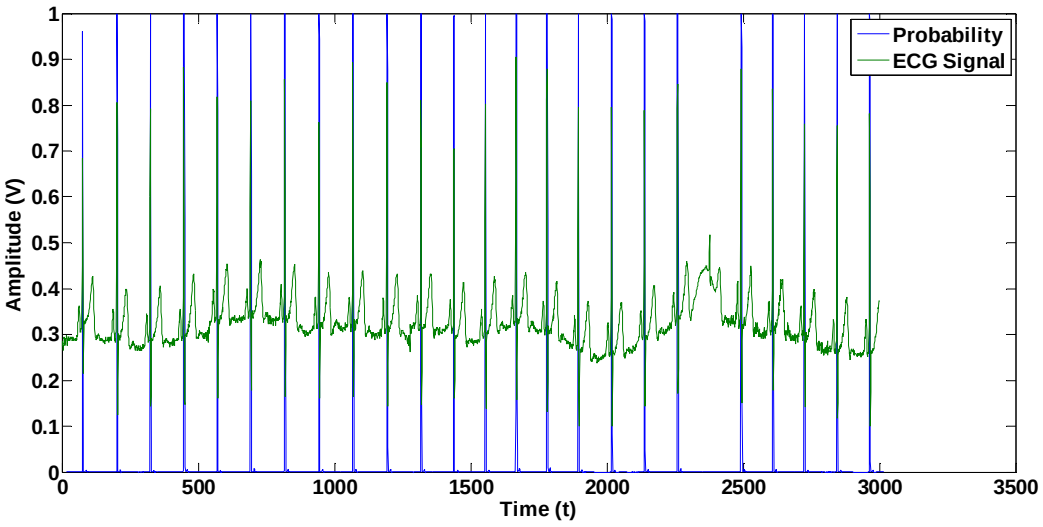


Figure. 3.13 QRS Complex Detection with different ECG signal

In this figure, QRS complex can be detected even if training data set is obtained from the different ECG signal. In this figure, the blue lines represent the probability of recognition and the green lines denote the ECG signal. There is one abrupt point in ECG signal between 2000 and 2500, but, it is an acceptable error for our results.

As mentioned before, QRS complexes have been analyzed effectively by using the novel method. Therefore, we try to detect another fiducial points of ECG such as P, Q, R, S and T wave. They are important detections because all of them become vital feature to diagnose the heart abnormalities.

When applying algorithm on P wave, the results can be given in figure 32.

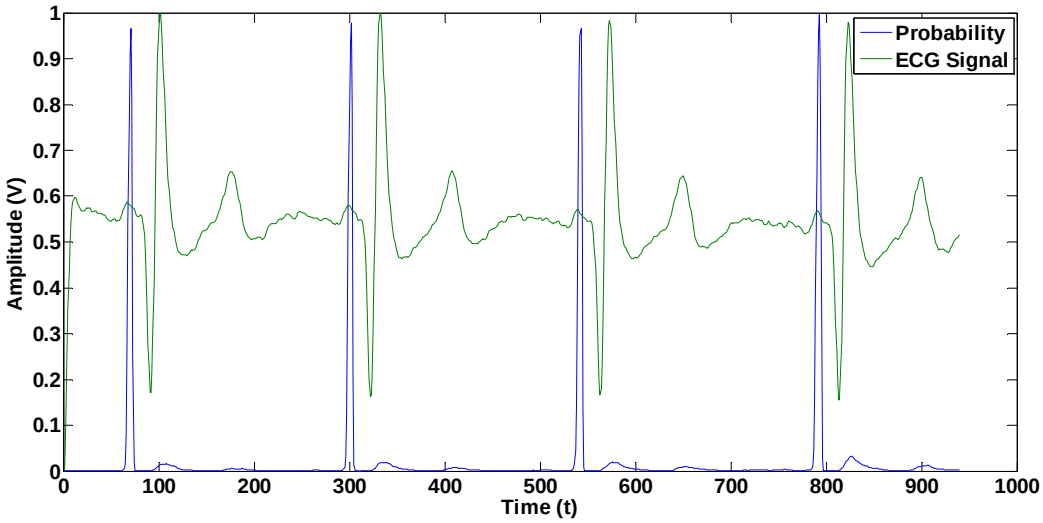


Figure. 3.14 P wave detection results

In figure (3.14), the head of P wave is fed to the system for training algorithm. The results are much more effective than the another algorithms. The next recognition for Q fiducial point is given as figure 33.

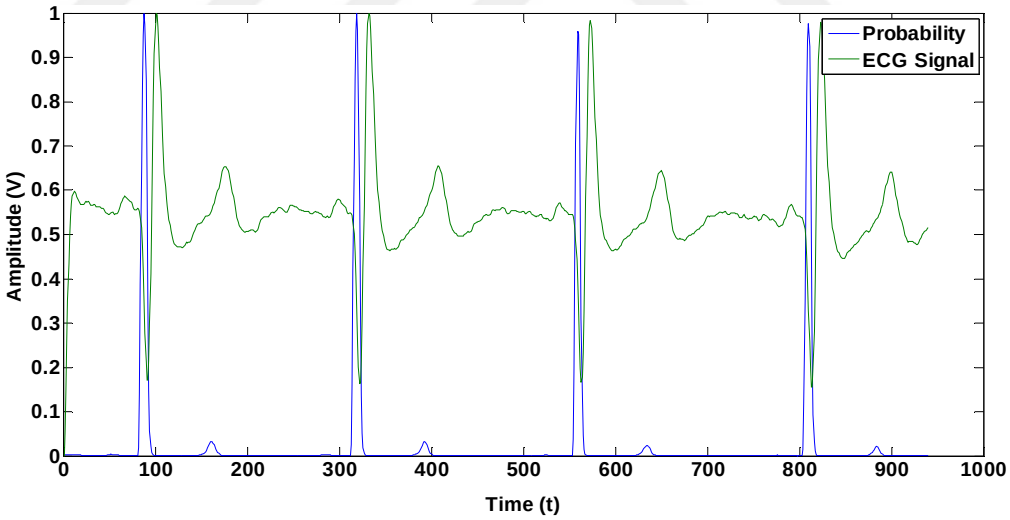


Figure. 3.15 Q wave detection results

When examining the above figure, the beginning of the Q wave is signed with the starting point of probability line (blue). In accordance with Q wave, S wave can be given as the following scheme.

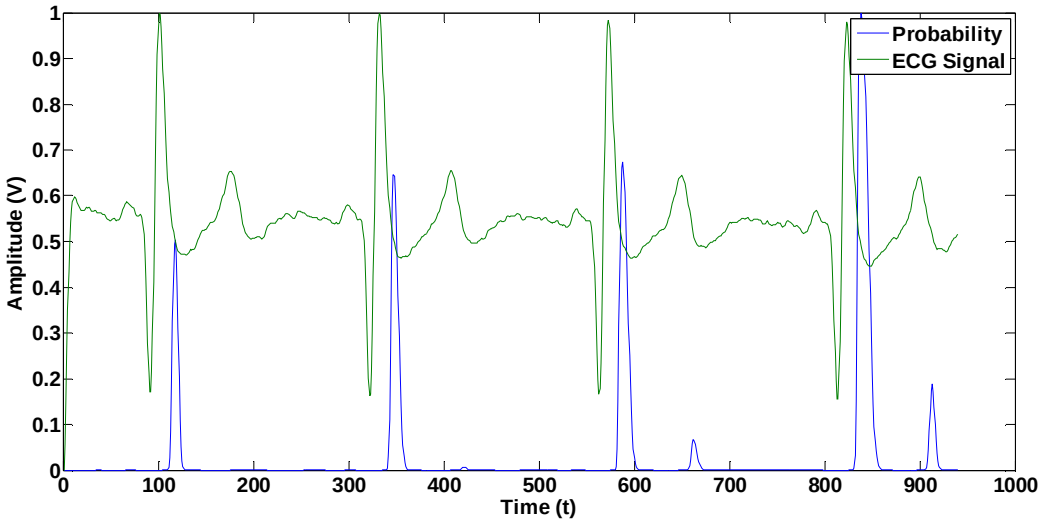


Figure. 3.16 S wave detection results

S wave detection contains some restriction for the novel approach because it is a convex function. If the algorithm is applied on the convex function, expectation-maximization algorithm cannot be converged to the these data set. Expectation maximization algorithm was performed by using concave methods, therefore, it couldn't converge like convex function even if back-propagation algorithm is used.

Up to now, the proposed algorithm has been performed effectively on ECG signal. Now, we investigate the algorithm in order to attain high performance and to cover their behaviours depending on ECG signal.

Firstly, QRS complex is chosen to examine their behaviours with the effects of cost function, convergence coefficient, teacher vector and compare vector. Many results are obtained in order to understand how convergence the algorithm is. Next sections disclosures their attributes.

3.1.3.2.1 Heartbeat Recognition

3.1.3.2.1.1 One-to-One Recognition

In one-to-one approach, the training data is selected unique signal with QRS complex. Then, the algorithm is trained by using the training data obtained by unique signal. Finally, the compare algorithm is performed for the same signal.

In the first place, the neural network can be generated as the following parameters:

Table 3.1 The characteristic parameters of convergence algorithm

J (cost function value)	0.1
η (learning rate)	0.01
Teacher Vector	[0.99 0.01]
Compare Vector	[0.5 0.5]

Cost function value is chosen 0.1 because converging error should be less than 0.1 for each data. Learning rate should be chosen less than 1 because all of the data given is fed to the system as normalized form. Teacher vector is selected as one of the vector is more dominant than the others because neural network only set their coefficients in accordance with the tendency of data in distribution. However, the values of compare vector should be equal to each other due to fact that two closer QRS complex is given to the neural network. The result is given as the following graph.

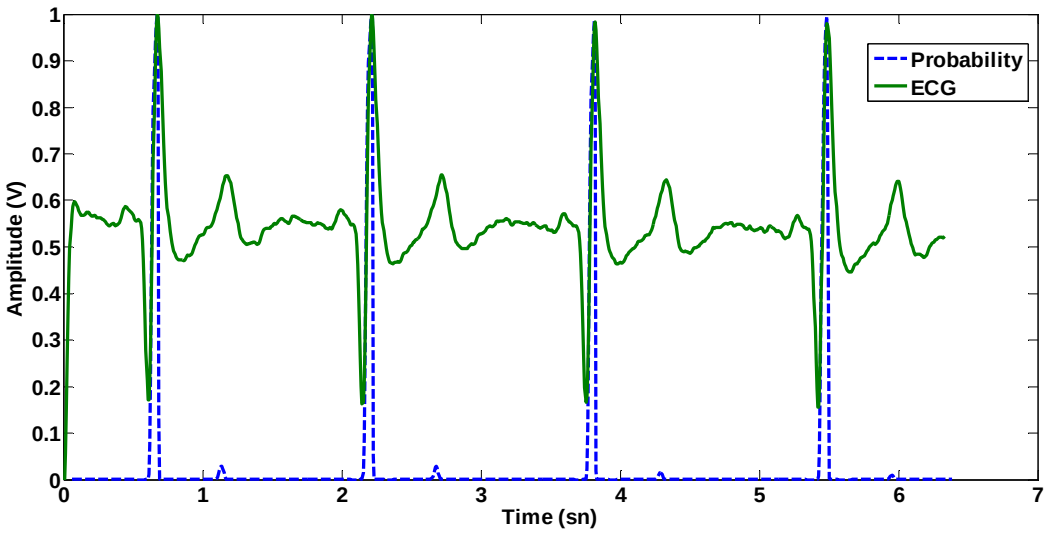


Figure. 3.17 QRS complex recognition with specified parameters

In fig. (3.17), it can be seen that QRS complex is effectively analyzed for the parameters given. Although, it can detect the QRS picks, there are some wave as dash line in the graph. The reason is that T wave is similar to the QRS complex when mean and covariance values of these signal are compared. Therefore, the neural network should be trained by changing their characteristic parameters given in table 1.

Firstly, we change cost function values in order to convergence at lowest error. The following table is explained the results coming from the experiment performed by changing cost function value. There are no difference for the other parameters in order to understand the effect of cost function value clearly.

Table 3.2 The recognition results for cost function values

Cost Function Value (j)	Pattern Recognition Result	Starting Point Detection (%)	Time Consuming (s)	Similar Shape Detection (%)
0.1	%100	%80	4	%3
0.01	%100	%85	6	%4
0.001	%100	%92	20	%7
0.0001	%100	%93	22	%9
0.00001	%100	%96	35	%13
0.000001	%100	%98	40	%16

In table (3.2), the value of cost function for one-to-one signal processing has no dominant feature in recognition of QRS complex. However, it is observed that the probability rates increases with low values of cost function. In addition, the starting point of QRS complex become more observable than high values of cost function. Also, due to the similarty of shape, T wave have become observable. On the other hand, time consuming is increased in accordance with decreasing cost value but doesn't cause significant change in time.

Therefore, cost function value is important to detect the starting point of QRS complex because any illnes in cardiac failure is determined by the interval of fiducial points.

That is, we obtain how cost value should be chosen in order to find the starting point of QRS and their location. Now, we examine the effect of changing learning rate η based on the following parameters in experiments.

Table 3.3 The characteristic parameters of convergence algorithm for learning rate

J (cost function value)	0.000001
η (learning rate)	0.1
Teacher Vector	[0.99 0.01]
Compare Vector	[0.5 0.5]

The experiments' results can be represented as the following figure to understand their effect mechanism on the neural network.

Table 3.4 The recognition results for learning rate changing

Learning Rate (η)	Pattern Recognition Result	Starting Point Detection (%)	Time Consuming (s)	Similar Shape Detection (%)
0.1	%100	%95	32	%13
0.01	%100	%99	41	%16
0.001	%100	%99,7	312	%20
0.0001	%100	%99,9	1624	%60

Table (3.4) demonstrates that learning rate directly affects time consuming badly because it significantly decreases the convergence of coefficient. Also, similar shapes such as P wave or T wave detection is increased when the learning rate is decreased. The reason is that covariance matrix is proportional to the square of signal value when the mean value is proportional to the signal value. If step number is augmented by decreasing learning rate, the neural network is more sensitive in proportional to the square of change, that is, the covariance matrix has more dominant than the mean value. Due to this reason, the optimum value of learning rate should be selected in order to recognize the specified pattern.

Apart from these, the pattern recognition is performed for all of the values of learning rate succesfully. In addition, starting point detection quality is promoted by decreasing learning rate because of the sensitivity of covariance matrix.

As for the change of teacher vector, it is an important issue for detection of heartbeat signal due to several reasons such as converging range, training level and so on. The table (3.6) represents the results of pattern recognition belonging to the change of teacher vector. The specifications for table 6 is given in table (5).

Table 3.5 The characteristic parameters of convergence algorithm for teacher vector

J (cost function value)	0.001
η (learning rate)	0.001
Teacher Vector	[0.9999 0.0001]
Compare Vector	[0.5 0.5]

Table (3.6) consists of 14 different results because teacher vector can be changeable in two separate directions.

Table 3.6 The recognition results for teacher vector changing

Teacher Vectors	Pattern Recognition Result	Starting Point Detection (%)	Time Consuming (s)	Similar Shape Detection (%)
[0.9999 0.0001]	%99	%100	340	%6
[0.999 0.001]	%100	%100	278	%0,2
[0.99 0.01]	%87	%99,7	248	%48
[0.9 0.1]	%97	%99,2	211	%15
[0.8 0.2]	%94	%97	178	%31
[0.7 0.3]	%92	%96	101	%29
[0.6 0.4]	%90	%94	62	%47
[0.5 0.5]	%100	%93	21	%0.03
[0.4 0.6]	%96	%92	24	%21
[0.3 0.7]	%98	%87	81	%3
[0.2 0.8]	%97	%84	98	%8
[0.1 0.9]	%89	%91	116	%40
[0.01 0.99]	%85	%93	143	%55
[0.001 0.999]	%82	%96	244	%78
[0.0001 0.9999]	%76	%98	298	%83

Table 6 demonstrates that if there are a big difference between teacher vector, time consuming is increased. When teacher vector are closer to each other, the good results can be obtained. Also, the reverse effect can be seen at the quality of performance even probability 1 and 2 are taken sequentially. That is, when the first coefficient of teacher

vector is bigger than the other, the probability 1 should be used in order to get the results correctly. At the extremities of teacher vector such as [0.9999 0.0001], the starting point of the QRS complex is more observable than the other situations. However, the other forms become observable due to certain points effect in compare function. When we examine the similar shape recognition performance, it has the smallest value in where the teacher vectors are closer to each other. In addition, probability of first output (probability 1) attains high performance in which the first component of teacher vectors is bigger than the other. Finally, the algorithm gives perfect results when the coeffecients of teacher vector are equal to each other.

The compare vector has an effect on the algorithm because it creates the outputs of the neural network appropriately. This cannot be included to training algorithm, that is, it cannot impress on training, it is related concerning the output of the neural network.

Table (3.7) gives us the effective parameters of algorithm under changing the compare vector.

Table 3.7 The characteristic parameters of convergence algorithm for compare vector

J (cost function value)	0.001
η (learning rate)	0.001
Teacher Vector	[0.9 0.1]
Compare Vector	[0.999 0.001]

In table (3.7), teacher vector is selected as [0.9 0.1]. The reason is that the time consuming is low in these values. In addition, the probability of first output is chosen as priori than the other. The following table represents the relation about changing compare vector in proportional to the quality of the neural network.

Table 3.8 The recognition results for compare vector changing

Compare Vectors	Pattern Recognition Result	Starting Point Detection (%)	Time Consuming (s)	Similar Shape Detection (%)
[0.999 0.001]	%34	%89	211	%94
[0.99 0.01]	%46	%91	211	%87
[0.9 0.1]	%67	%92.3	211	%47
[0.8 0.2]	%78	%92.7	211	%42
[0.7 0.3]	%82	%93.1	211	%31
[0.6 0.4]	%89	%94.2	211	%9
[0.5 0.5]	%98.9	%96.6	211	%1
[0.4 0.6]	%99.2	%97	211	%0.02
[0.3 0.7]	%92	%97.2	211	%17
[0.2 0.8]	%94	%97.7	211	%10
[0.1 0.9]	%96	%98.9	211	%4
[0.01 0.99]	%99.4	%99.4	211	%2
[0.001 0.999]	%99.7	%99.8	211	%1.4

The starting point is clear when compare vector is selected reversely with teacher vector. Time consuming is not affected by changing compare algorithm because it doesn't include training. When the compare vector is chosen proportionaly with teacher vector, the recognition is increased. However, the similar shape detection is promoted significantly. The most important issue is that if compare vector is equal to teacher vector, the signal is the same as original ECG signal. Additionaly, the starting point become more observable at the low values of compare vector.

Up to now, the algorithm has been evaluated in order to understand how the parameters have an effect on the performance of neural network. Next section, the algorithm trained

by unique QRS complex is applied on the other ECG signal in order to evaluate the results coming from both the same ECG signal and different ECG signal.

3.1.3.2.1.2 One-to-Another Recognition

In one-to-another approach, the algorithm is trained by unique QRS complex. Although, QRS complex is well-defined by using the neural network, there may be some problems when the neural network is applied on the different ECG signal. Therefore, the algorithm trained by unique QRS complex should be tested by doing some experiments on the different QRS complexes.

For these purposes, firstly, the neural network is teached by training data coming from unique QRS complex. In order to achieve this, the algorithm should be tried on the different ECG signals.

In the first place, the neural network is generated as the following table.

Table 3.9 The characteristic parameters of convergence algorithm for cost value

J (cost function value)	0.1
η (learning rate)	0.001
Teacher Vector	[0.99 0.01]
Compare Vector	[0.5 0.5]

The relating results are demonstrated in table 10.

Table 3.10 The recognition results for cost function value changing

Cost Function Value	Pattern Recognition Result	Starting Point Detection (%)	Time Consuming (s)	Similar Shape Detection (%)
0.1	%99,8	%98	15	%1.1
0.01	%99,92	%99.2	28	%0.7
0.001	%99,94	%99.7	35	%0.3
0.0001	%100	%98.7	47	%0
0.00001	%99.8	%96	76	%0
0.000001	%99.98	%94	117	%0

As different from one-to-one recognition, the probability should be corrected differently in order to attain high performance. As mentioned before, the half of the training number have to be added to the output in time axis. However, in one-to-another recognition, the correction number should be selected as the number of training data set. For evaluating performance, QRS complex is recognized effectively even if they are shortened or lengthened. In addition, QRS complex in large data set has been recognized perfectly than short number of training data. Time consuming is increased when the cost function values is decreased. It is noteworthy that starting point detection change is not proportional to decreasing cost function value. Finally, similar shape detection is not affected by chaning cost function value. The reason is that when the different ECG signal is classified by using unique QRS complex, the other shapes such as P, T wave cannot be diagnosed by the algorithm.

As for learning rate effect, the characteristic parameters are given in table (3.11).

Table 3.11 The characteristic parameters of convergence algorithm for learning rate

J (cost function value)	0.000001
η (learning rate)	0.1
Teacher Vector	[0.99 0.01]
Compare Vector	[0.5 0.5]

The results related to learning rate effect are shown as the following table 12.

Table 3.12 The recognition results for learning rate changing

Cost Function Value	Pattern Recognition Result	Starting Point Detection (%)	Time Consuming (s)	Similar Shape Detection (%)
0.1	%99,8	%99.1	15	%0.9
0.01	%99,98	%99.7	61	%0.4
0.001	%100	%99.96	122	%0.01
0.0001	%100	%100	197	%0.003

In testing learning rate effect, time consuming is increased in accordance with decreasing learning rate. Start point is much more clear than lesser values of learning rate. In addition, previously, we have given some definitions about negative and positive cost in the outputs of the neural network as probability 1 and 2. In this experiment, probability 1 and 2 are represented as negative and positive cost, respectively.

Teacher vector is a vital component to affect pattern recognition when evaluating different ECG signals. In the present algorithm, it directly changes the quality of start and end point detection of QRS complex. The values for testing the change of teacher vector is given in table 13.

Table 3.13 The characteristic parameters of convergence algorithm for learning rate

J (cost function value)	0.001
η (learning rate)	0.001
Teacher Vector	[0.9999 0.0001]
Compare Vector	[0.5 0.5]

The results are given in table (3.14).

Table 3.14 The recognition results for teacher vector changing

Teacher Vectors	Pattern Recognition Result	Starting Point Detection (%)	Time Consuming (s)	Similar Shape Detection (%)
[0.9999 0.0001]	%100	%100	116	%0.003
[0.999 0.001]	%100	%100	107	%0.007
[0.99 0.01]	%100	%99,7	105	%0.04
[0.9 0.1]	%100	%99,2	108	%0.09
[0.8 0.2]	%100	%97	111	%1
[0.7 0.3]	%100	%96	112	%1.3
[0.6 0.4]	%100	%94	103	%1.2
[0.5 0.5]	%100	%93	121	%1.12
[0.4 0.6]	%99.34	%92	118	%1.34
[0.3 0.7]	%99.65	%87	112	%1.16
[0.2 0.8]	%99.68	%84	114	%0.6
[0.1 0.9]	%99.87	%91	115	%0.33
[0.01 0.99]	%99.87	%93	119	%0.12
[0.001 0.999]	%99.91	%96	123	%0.11
[0.0001 0.9999]	%99.93	%98	126	%0.01

Table 14 demonstrates that there is no time consuming with changing teacher vector. When the highest difference between teacher vector components, starting point is detected perfectly. However, the end point of QRS complex is not easily determined when this condition occurs. On the other hand, it is noticed that end point is more clear when teacher vectors are chosen as similar to each other.

Finally, in order to test the effect of compare vector, their parameters are decided as the following table.

Table 3.15 The characteristic parameters of convergence algorithm for learning rate

J (cost function value)	0.001
η (learning rate)	0.001
Teacher Vector	[0.9 0.1]
Compare Vector	[0.5 0.5]

In table (3.15), teacher vector is selected as [0.9 0.1] because if teacher vector with highest difference is chosen, the neural network produces effective results.

Table (3.16) illustrates outcome of the algorithm.

Table 3.16 The recognition results for compare vector changing

Compare Vectors	Pattern Recognition Result	Starting Point Detection (%)	Time Consuming (s)	Similar Shape Detection (%)
[0.999 0.001]	%100	%100	108	%0
[0.99 0.01]	%100	%100	108	%0
[0.9 0.1]	%100	%100	108	%0
[0.8 0.2]	%100	%99.87	108	%0
[0.7 0.3]	%100	%99.72	108	%0
[0.6 0.4]	%100	%99.67	108	%0
[0.5 0.5]	%100	%99.54	108	%0
[0.4 0.6]	%100	%98.98	108	%0
[0.3 0.7]	%100	%98.43	108	%0
[0.2 0.8]	%100	%98.31	108	%0
[0.1 0.9]	%100	%98.04	108	%0
[0.01 0.99]	%100	%98.02	108	%0
[0.001 0.999]	%100	%98	108	%0

Table 16 illustrates that starting point is recognized perfectly, but has an effect on the detection of end point. It couldn't be determined by decreasing compability between teacher and compare vector. That is, when the teacher vector is equal to compare vector, it can give the perfect outcomes. Reversely, the present algorithm may not performed effectively.

Up to now, the hearbeat recognition has been performed effectively by discussing their advantageous and disadvantageous. The tables given above represent classification performance under different conditions.

Now, different patterns of ECG signals are struggled for classification. Firstly, QT segment should be recognized because it has an important to diagnose QT syndrome. For this purpose, we make an experiment in order to find out how it is affected by our parameters.

3.1.3.2.2 QT Segment Recognition

QT interval is the duration from the beginning of QRS complex to the end of T wave. Its properties about shape, amplitude is similar to QRS complex. Therefore, the algorithm may not be used effectively for detection of QT interval.

In the present study, we try to solve this problem by using template matching technique as mentioned before. Traditionally, template matching algorithm is classification algorithm which use template in order to find how much the evaluating pattern matches it. For this purpose, firstly, we should cover the problems of the present algorithm in QT interval analysis.

Normally, the ECG pattern can be identified easily for QRS complex when the correct coefficients are selected in the present algorithm. However, T wave is a kind of QRS complex because of its natural characteristic. In the heart, as mentioned before, a cycle of heart rhythm consists of atrioventricular and ventricular electrical activation. When the sinoatrial node is stimulated, atrium contracts and propagates the electrical current through the ventricular. Due to its electrical pathways, their electricity is similar to each other. Therefore, QRS complex and T wave is not easily separated during the heartbeat cycle.

In this study, the present algorithm performs to classify signal by comparing covariance and mean value. The reason is that when the fiducial points of ECG signal such as QRS complex, T wave is proceeded, the algorithm gives the different probabilities at different segments in ECG signal. However, there are some corruptive factors to recognize ECG signals. One of them is that the ECG signal is not always the same to the others. Sometimes, it is completely different when comparing normal heart rhythm. Secondly, the algorithm uses two inputs with same characteristic like QRS complex. If the algorithm receives two similar pattern with little difference, the algorithm produces

wrong results. In addition, some of the signals cannot be converged maximum likelihood point because of their similarity.

Therefore, we have decided to use template matching algorithm in order to differentiate the different sections of ECG. However, standard template algorithm requires the standard form of pattern when separating ECG sections. Due to these reasons, we transforms template matching from standard pattern into mean and covariance values of ECG signals. Normally, when the neural network is trained to recognize T wave, it can undeniably said that the algorithm gives high propababilites at the QRS complex because of the similarity of their shapes. As a result, we perform the covariance and mean vectors additively to classify the T wave in compare algorithm.

Applying formula can be written as the following equation:

$$Y = \begin{cases} y_1, \ \Sigma_{cds} - \Sigma_{tds} < \frac{\Sigma_{tds}}{TN} \\ e, \ \Sigma_{cds} - \Sigma_{tds} \geq \frac{\Sigma_{tds}}{TN} \end{cases} \tag{3.54}$$

In eq. (3.54), y_1 represents the first output of neural network trained by one, e denotes the small value but is not zero, Σ_{cds} and Σ_{tds} represents the covariance vector of compare data set and the covariance of training data set, respectively. Also, TN is the number of training data set. When this condition is supported for the neural network, the end of T wave can be recognized effectively. Figure 36 demonstrates the results of the classification algortihm for the end of T wave.

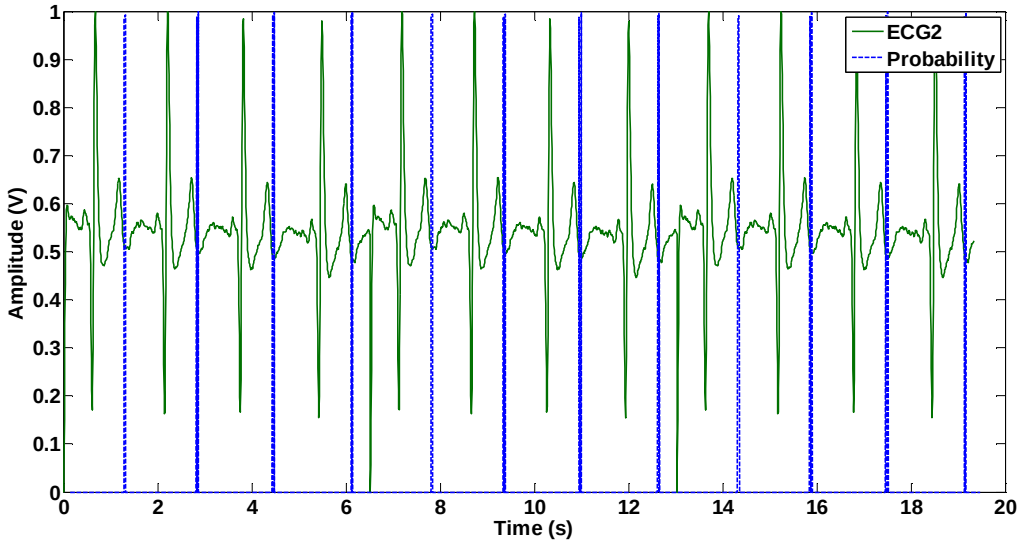


Figure. 3.18 Classification results for the end of T wave

When obtaining this results, cost function is selected as 0.01. Teacher vector is to be preferred as [0.99 0.01] because it gives us the oppurtunities both to attain high performance in recognition and to take a short time. It is known that when the patients are connected to the ECG monitor, the cardiac abnormalities should be analyzed effectively. Therefore, our parameters provide this feature.

In fig. (3.18), it is concluded that the normal cardiac rhythm can be effectively analyzed by using the present algorithm. In this picture, T wave is absolutely measurable and its classification can be performed effectively by the doctors. However, the doctors or experts can not diagnosed for the abnormalities frequently. Therefore, many of the ECG signals with QT segment should be analyzed in order to be sure that the present algorithm is worked well. For this purpose, eight separate ECG signals with different T wave are selected. All of them are obtained in PHYSIONET database [111]. PHYSIONET Databases submit us to evaluate different shapes of ECG signal which cannot be analyzed easily. The ECG signals obtained from the databases are selected from normal heartbeat because the algorithm should firstly be applied on them. In addition, the covariance matching should be performed on these data set in order to prove effectiveness of it.

In the first place, the dataset obtained by the novel ECG device is analyzed. When the pseudo is firstly evaluated, it can lead some problems due to fact that it is completely based on mathematical operations. The following figure is depicted the recognized dataset.

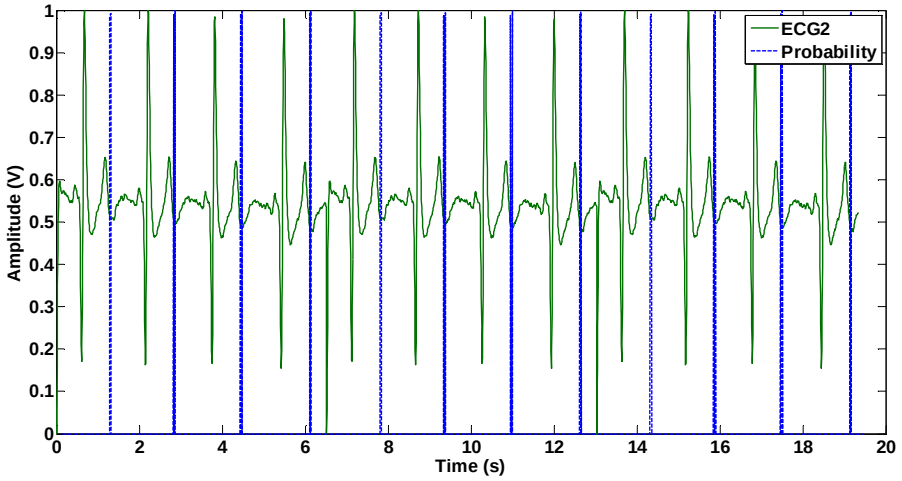


Figure. 3.19 Classification results for real ECG signal

In this experiment, the characteristic parameters of the algorithm are chosen as the following table.

Table 3.18 The characteristic parameters of the algorithm for QT recognition

J (cost function value)	0.00001
η (learning rate)	0.0001
Teacher Vector	[0.9999 0.0001]
Compare Vector	[0.9999 0.0001]

Table (3.18) demonstrates that the duration of the algorithm takes a long time because of its cost value and learning rate. In contrast to the mentioned method, the algorithm take teacher and compare vector parameters as both same and greater differences. In normal procedure, although teacher vector should be selected similar to the table parameters, compare vector parameters should be selected as closer to each other. The reason to choose similar to compare vector is that inputs are used differently in accordance with QRS complex classification. In this recognition process, there are two different data set which one of them is produced artificially at specified values from 0.99 to 1. The specified values have to be selected appropriate with the normalization rules. When doing this, the distributions of T wave and artificial data is spread over the plane as the following figure.

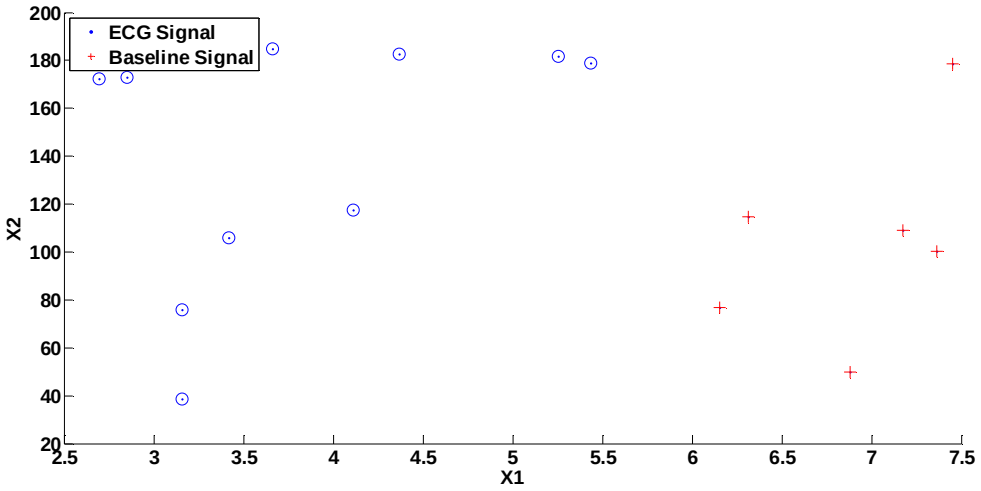


Figure. 3.20 Cluster diagram for T and Artificial Wave

Normally, we used inputs with the same but little difference QRS complexes in heartbeat recognition. However, in the classification of end of the T wave, we cannot perform previous distribution directly. The reason is that the end of T wave is concave function. This causes to prevent creating eliptic distribution in the T wave recognition. In order to create Gaussian distribution, expectation maximization algorithm based on jensen inequality was performed for initializing first coefficients of neural network. However, jensen inequality does not support the concave functions to convergence global minimum in the neural network, it only supports convex functions. Therefore, we produce artificial data in order to obtain real output. There must be provided some conditions that the artificial data are to be normalized and their values are in the range of between 0.99 and 1. When the neural network is teached, one input is the end of T wave and the other is artificial data.

Artificial data should be closer to the 1 because when the ECG data is normalized, all of the values changes from 0 to 1. However, due to the general characteristic of ECG signal, there are only some points which can converge to the maximum values of normalization. Therefore, when the artificial data are selected from 0.99 to 1, there are any corruption in the signal and its mean and covariance values can be decomposable.

In fig. (3.20), the present algorithm is performed effectively and there is no unrecognized pattern. In this figure, there are only twelve heartbeats which is shown. However, complete data consists of 2000 hearbeat.

In order to demonstrate the performance of the present algorithm, the table 19 is given below.

Table 3.19 The characteristic parameters of the algorithm for first QT recognition

J (cost function value)	0.00001
η (learning rate)	0.0001
Teacher Vector	[0.9999 0.0001]
Compare Vector	[0.9999 0.0001]
Back-Propagation Cost Function Calculation Type	Logaritmic
Training Number	16
Covariance Factor	2
End point effectivity	%99.962
Classification Performance	%99.92

In Table (3.19), cost function value is chosen as small as possible because it directly affects the convergence of the algorithm. However, there is a negative feature to increase time consuming because of using it. On the other hand, when the cost function value is smaller as much as, the algorithm is more general than the other situations. We can easily apply covariance factor to recognize T wave.

Secondly, learning rate has an effect on the coefficients of the algorithm because when the learning rate is used in its small value, the coefficients are converged better than the its bigger values. In addition, when the algoritm is trained, it never knows which coefficient can converge at the specified values. That is, during the training operation, the algorithm cannot know how their coefficients change. Therefore, learning rate is used at small values, the coefficients changes can be balanced for all of the parameters.

Thirdly, teacher vector has an important effect on converging due to several reasons. One of the reasons is that the algorithm should be worked with bigger diffrence in teacher vector parameters because we prove this idea in QRS complexes classification. When the teacher vector parameters are chosen with big difference between them, the

starting point detection quality is more valuable to detect the beginning of the QRS complexes. However, in T wave recognition, there are two different situations, time consuming and different input parameters. time consuming is increased when the teacher vector is used by big differences. Also, we performed QRS complexes classification under two QRS complexes input with little difference. However, T wave classification, there are two completely different input. Therefore, we have to establish this algorithm by providing the concave functions as mentioned before.

The other reason is that when the QRS complexes are tried to analyzed, teacher vector parameters should be submitted as closer to each other. In contrast to this idea, the end of T wave classification should be performed with highest difference in teacher vector because completely different input are used.

As mentioned before, compare vector is derived to obtain good classification performance in ECG pattern recognition based on Gaussian mixture model. Normally, LLGMN algorithm produces the outputs by using only their neural network. In this study, the ECG signal should be sequential in order to attain high performance and to cover the behaviour of the patterns such like T wave, QRS complexes. In QRS complex analysis, compare vector fixes the error at the beginning of QRS complex. When the compare vector parameters have big difference to each other, the starting point can be detected effectively. The reason to realize this advandageous is that we produced a function to organize the output of the algorithm given in equation (72). Then, we used this function to detect specified signal pattern which is used to train the system. That is, the neural network parameters is not only the output of training algorithm but also is dependent on the output of the comparing algorithm. To sum up, our algorithm generates one output by examining data set which have the number of training data. With the usage of compare function, we can change their response across the input as concave or convex. This is an important issue because when the data are evaluated as a group, the starting and end point is completely changed. Also, their raising values are different from the training algorithm. Therefore, in T wave recognition, compare vector parameters have a big difference with the other in order to detect the start and end points of it clearly.

Back-propagation cost function calculation is not included in QRS complex detection because their shape is more observable than the other type of signals due to mean and covariance values of it. However, it should be considered as an important parameter for

T wave recognition because of concave-convex problem. Logarticmic function represents the exponent to which another fixed value, the base, must be raised to produce that number. It always converge the fixed value depending on the base of it. If the cost function is normally chosen as the differences between the input and output, there may be produced big values of cost value. However, if we use the logaritmic function to converging operation, there will be two advantageous. One of them is that it never increases the specified maximum cost value. The other is that changing coefficient is bounded due to the feature of logaritmic function.

Training number is an important factor to affect on the quality of the output of the neural network. In ECG signal, some of the patterns like T wave, sometimes, can lengthen or shorthen. In order to attain high efficieny from the present algorithm, training number should be closer to the pattern signal which is evaluated. In addition, training number changes the mean and the covariance values of the neural algorithm. For QT experiment, we use 16 training data value which is completely determined by intuition of our observation.

Covariance factor has been explained in equation (73). Covariance factor is used to split pattern into different parts of characters. It means that when the pattern trains the neural network, there are many similarities in different heartbeats. Therefore, we presented a novel factor to correct the probability of the output. During classification, the outputs from compare vector are checked in order to know that there is any wrong pattern. When this is completed, the probability of recognition is more reliable than the other situation. For the current signal, the covariance factor is selected as 16 because the neural network was already trained by its T waves. When the algorithm is applied to another signals, this coefficient must be approriate with the condition that its value is smaller than the training number.

As a conclusion, the neural network produces perfect results for itself. The end point effectivity and classification performance are about %99.962, %99.92, respectively. For 2000 heartbeat, there are only two waveforms which cannot be identified because of their shape corruptions. These signals may occur due to changing probes or movement of arm.

Second signal is obtained from PHYSIONET database which represents the ECG signals to detect QT segment. In order to evaluate second signal, the characteristic parameters are chosen as the table 20.

Table 3.20 The characteristic parameters of the algorithm for second QT recognition

J (cost function value)	0.00001
η (learning rate)	0.0001
Teacher Vector	[0.9999 0.0001]
Compare Vector	[0.9999 0.0001]
Back-Propagation Cost Function Calculation Type	Logaritmic
Training Number	16
End point effectivity	%96.72
Classification Performance	%94.22

The result belonging to the second QT recognition, it is shown in figure 39.

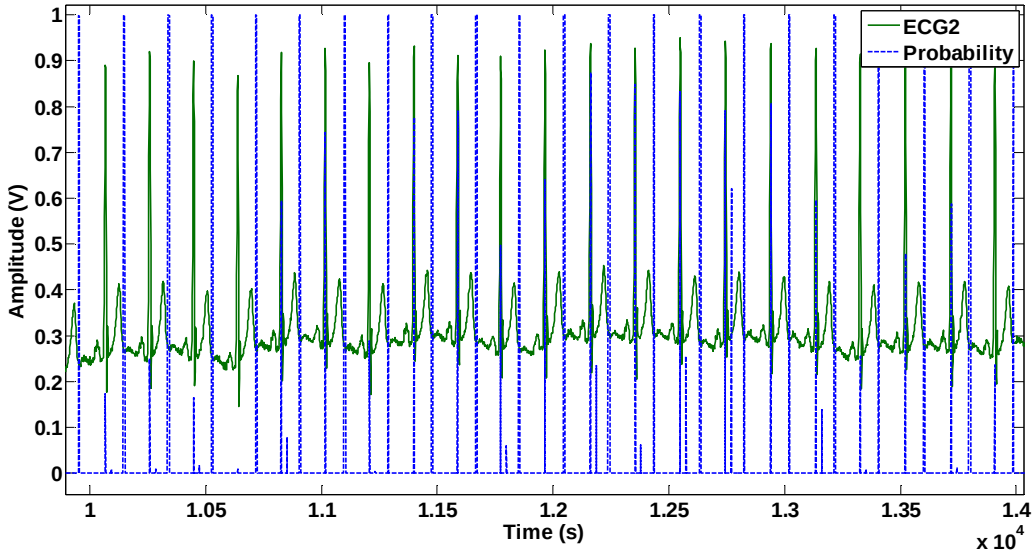


Figure. 3.21 Classification results for second (sel116) ECG signal

In PHYSIONET database, second QT signal is named as "sel116". Its the number of data is 225000. The neural network is trained by using real T wave given in figure

(3.21). The classification performance is about %94.22. This can be represented as a good result because the training data set don't include the current signal element. The end point effectivity is seen about %96.72. It can be said that when the algorithm uses the different training data set, it is more convenient to analyze the different ECG signals.

The experiment results should be discussed in order to cover how wrong it is. There are some regions with the different end of T wave. Also, some regions have a shape which is similar to the end of the T wave. In addition, some regions are different from the training data set completely. Due to the covariance factor, the algorithm gives the QRS complex because of unsuccessfully recognition. However, it is sourced that the unknown or different training data set was used to perform classification.

In order to investigate the recognition problems, we should examine the cluster diagram of it. The cluster diagram related to "sel116" is given in figure 40.

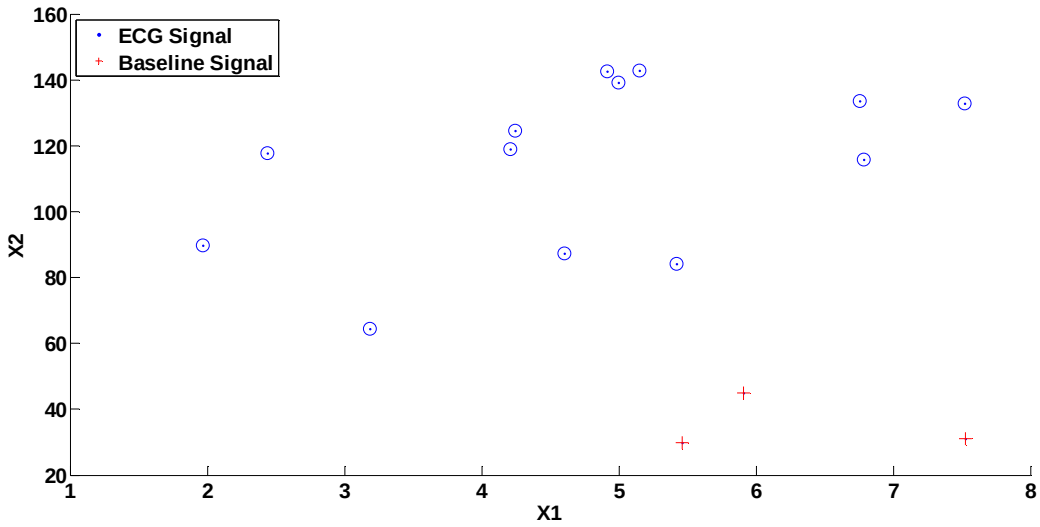


Figure. 3.22 Cluster diagram for T and Artificial Wave under sel116 training data set

Fig. (3.22) is similar to fig. (38), however, there are little differences between them because the training data have different characteristic on cluster diagram. Therefore, the algorithm cannot completely match the different ECG signal waveforms in fig. (3.18). It gives us a probability how similar the current signal waveform is to another.

On the other hand, we trained the algorithm by using its T wave.

Under training with itself data, the recognition results are illustrated in table (3.21).

Table 3.21 The characteristic parameters of the algorithm for second QT recognition with itself training data

J (cost function value)	0.00001
η (learning rate)	0.0001
Teacher Vector	[0.9999 0.0001]
Compare Vector	[0.9999 0.0001]
Back-Propagation Cost Function Calculation Type	Logaritmic
Training Number	16
Covariance Factor	16
End point effectivity	%99.11
Classification Performance	%99.93

Table (3.21) clearly demonstrates that when the training data set are chosen in the current signal, the classification performance becomes greater than the other situation. Although, table (3.21) results are better than the table (3.20), it is an acceptable classification around %90 to %95.

The third signal is obtained by PHYSIONET database. In order to analyze the signal, the parameters are selected appropriate with the following table.

Table 3.22 The characteristic parameters of the algorithm for third QT recognition

J (cost function value)	0.00001
η (learning rate)	0.0001
Teacher Vector	[0.9999 0.0001]
Compare Vector	[0.9999 0.0001]
Back-Propagation Cost Function Calculation Type	Logaritmic
Training Number	16
Covariance Factor	2
End point effectivity	%99.03
Classification Performance	%99.73

The algorithm can give a negative result with QRS complex and the beginning of the T wave. Due to the similarity between the current signal of T wave and training data, covariance factor should be selected as the number of training data. However, in some regions, the characteristic of T wave is different. Covariance factor data set should be chosen there in order to increase recognition compability. The results are illustrated as the following figure.

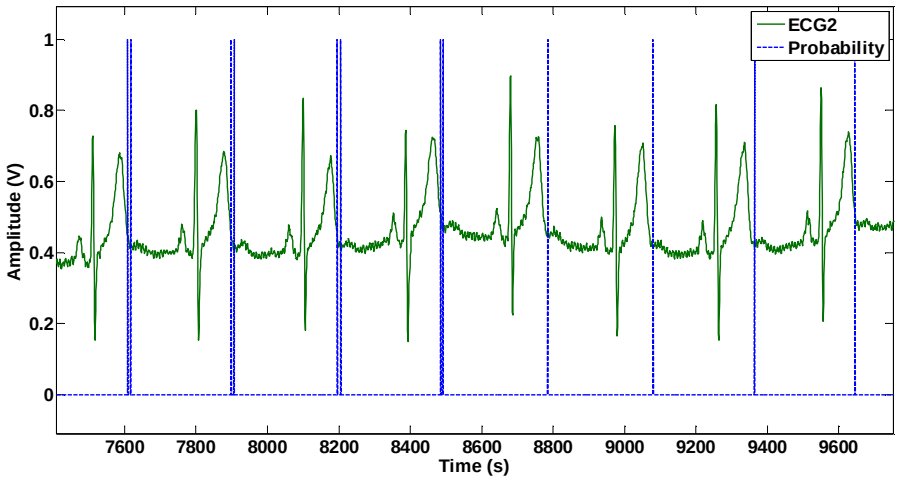


Figure. 3.23 Classification results for second (sel117) ECG signal

In Fig. (3.23), the end of T wave has been analyzed perfectly. Although, QRS complexes are not identified in the signal, there are some points in T wave as two one more raising probabilities. The reason is that T wave distribution at these points is corrupted by using covariance factor. This can be proved by demonstrating cluster diagram of the current signal.

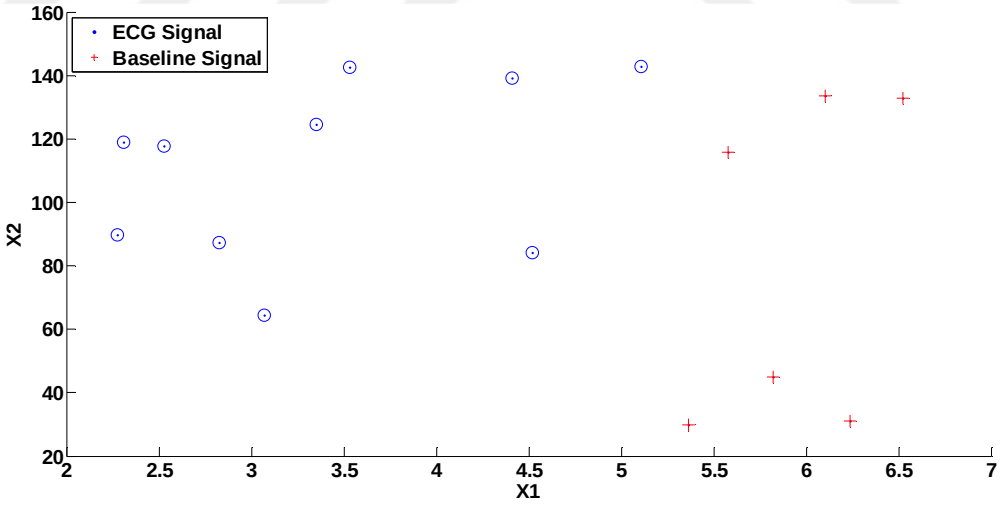


Figure. 3.24 Cluster diagram for T and Artificial Wave under sel117 training data set

When comparing Fig. (3.24), this distribution spreads over the plane more than Fig. (3.24). Therefore, some of the points to be determined as boundary are out of range. That is, the data are both observable and non-observable at the same time.

For the classification performance, their results are better than Fig. (38). It should be discussed carefully because when the algorithm is trained by using itself, the cluster

diagram expands and earn a new ability to recognize new patterns. The results coming from experiment which the algorithm is trained by itself are given as the following table.

Table 3.23 The characteristic parameters of the algorithm for third QT recognition

J (cost function value)	0.00001
η (learning rate)	0.0001
Teacher Vector	[0.9999 0.0001]
Compare Vector	[0.9999 0.0001]
Back-Propagation Cost Function Calculation Type	Logaritmic
Training Number	16
Covariance Factor	16
End point effectivity	%99.03
Classification Performance	%99.98

The classification performance has been increased by improving characteristic parameters. Covariance factor can be selected around the number of training data because the algorithm is trained by using values at the end of the T wave.

The another signal pattern obtained by PHYSIONET database is called as "sel123". It consists of 225000 data. The selected parameters are given in table (3.21).

Table 3.24 The characteristic parameters of the algorithm for fourth QT recognition

J (cost function value)	0.00001
η (learning rate)	0.0001
Teacher Vector	[0.9999 0.0001]
Compare Vector	[0.9999 0.0001]
Back-Propagation Cost Function Calculation Type	Logaritmic
Training Number	16
Covariance Factor	16
End point effectivity	%94.13
Classification Performance	%98.21

Table (3.24) results are obtained by using general training data coming from the real ECG signal. The classification performance is good because of the similarity of ECG probes. Therefore, the covariance factor can be selected as the number of training data. However, there are some observations to evaluate these results. When the covariance of current signals is chosen from the unsimilar T wave, the results can be improved. Secondly, covariance factor should be smaller than training number because the similarity of the signal is lesser than the real ECG signal. In addition, it can be said that end point effectivity is damaged due to several reasons. One of them is that the end of the T wave has two pick point. The algorithm cannot easily decide where the end of the T wave. Therefore, the algorithm needs to train its T wave end. We determine where the training data are obtained in order to attain high performance. It is important effect on recognition because when two pick points are teached in neural network, the present algorithm finds the final location of these two points. So, we decide to use first pick of the end of the T wave.

In order to demonstrate this idea to be stable for the present algorithm, the following figure represents the cluster distribution related to the training data.

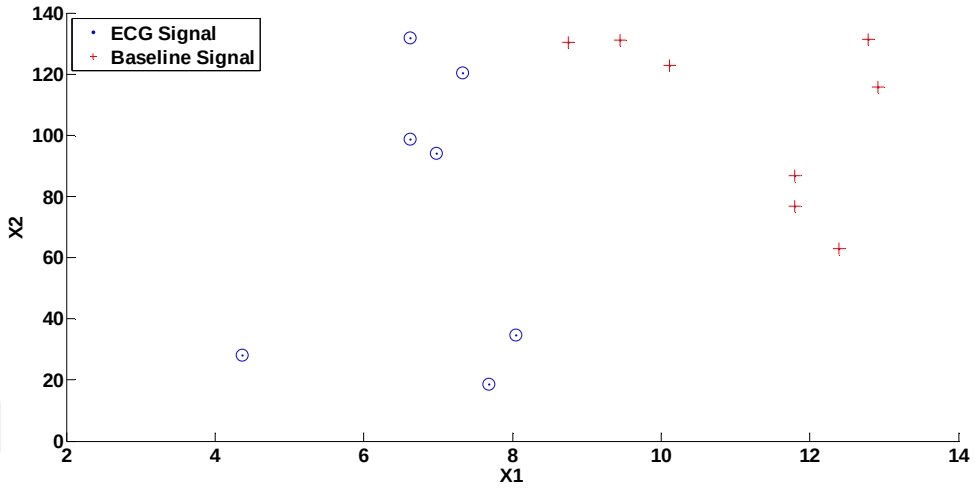


Figure. 3.25 Cluster diagram for T and Artificial Wave under sel123 training data set

In Fig. (3.25), the ECG signal consists of two different segments, up and down segments. Normally, the end of T wave falls down quickly which is represented in the figure as up section. However, two picks cause the training data to spread over the plane. That is, the detectable area of the end of the T wave expands, therefore, the algorithm resolution is degraded. In this region, every evaluating signal is considered as the end of the T wave. Although, there are some problems on this distribution, the results can be improved by changing the covariance factor.

The related results are explained in the table 25.

Table 3.25 The characteristic parameters of the algorithm for fourth QT recognition trained by itself

J (cost function value)	0.00001
η (learning rate)	0.0001
Teacher Vector	[0.9999 0.0001]
Compare Vector	[0.9999 0.0001]
Back-Propagation Cost Function Calculation Type	Logaritmic
Training Number	16
Covariance Factor	40
End point effectivity	%98.28
Classification Performance	%96.44

The results given in table (3.25) demonstrate that when the ECG signal has two picks at the end of the T wave, the classification performance diminishes even if their data are used to train the neural network. However, the detection of the end of the T wave is more detectable because training data are picked from the current ECG signal. In addition, the comparing algorithm results are organized by using different covariance factor. The reason is that when the distribution of training data is larger, the algorithm catches many signal patterns which are similar to the end of the T wave. Consequently, the covariance factor should be larger than the number of training data. Choosing covariance factor as larger does not lead any problem for the neural network because the end of the T wave is already recognizable due to expanding the cluster distribution.

Fifthly, the QT signal called "sel14046" obtained by PHYSIONET database is performed in order to get an achievement for the detection of the end of the T wave. Similarly, 225000 data were used to test the present algorithm.

The selected parameters are determined as the following table.

Table 3.26 The characteristic parameters of the algorithm for fifth QT recognition

J (cost function value)	0.00001
η (learning rate)	0.0001
Teacher Vector	[0.9999 0.0001]
Compare Vector	[0.9999 0.0001]
Back-Propagation Cost Function Calculation Type	Logaritmic
Training Number	16
Covariance Factor	40
End point effectivity	%97.21
Classification Performance	%28.82

Table (3.26) demonstrates that the present algorithm is not performed effectively on sel14046 data set. The reason is that there are some points which are recognized, but, generally, QRS complex is identified due to fact that QRS complex is much smaller than the T wave in this signal. Therefore, retraining should be done for this signal. In contrast to this, the end point effectivity at classified data set is not affected by changing classification performance because the recognized signals are already present and their characteristics are obtained perfectly due to the QRS complex - T wave incompability. The results are illustrated in figure (3.26).

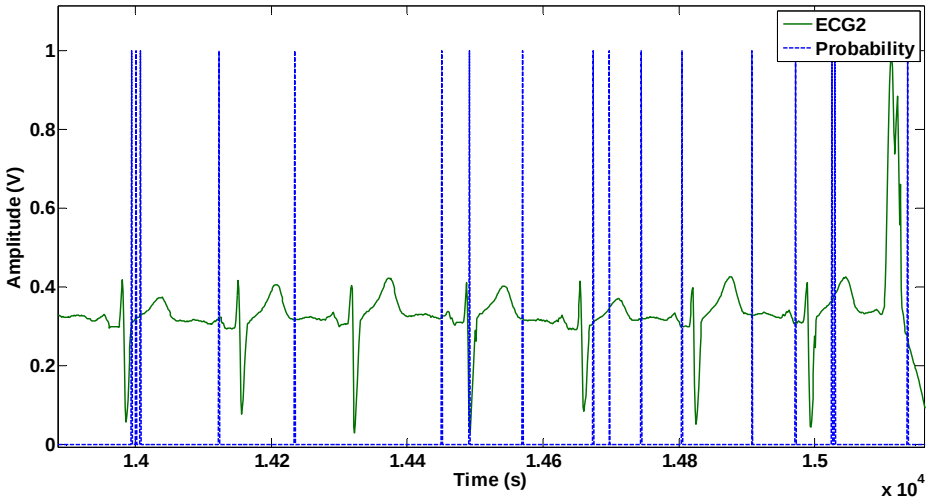


Figure. 3.26 QRS Complex - T wave incompability in sel14046

In Fig. (3.26), although QRS complex and T wave are classified, the algorithm should only determine the end of the T wave. The classification detects some points with raising in QRS complex but does not perform effectively on the T wave. In order to improve these results, we introduce the novel evaluation method for the determination of the specific pattern. Normally, the present algorithm produces the probability value in proportional to how the pattern is similar to the end of the T wave. However, QRS complex or P wave are analogous with the T wave.

Therefore, the outputs of the neural network should be improved in order to attain high perfomance in classification. As mentioned before, when the pattern of ECG is completely recognized, the neural network should be produced the probability about 100 percent. That is, the outputs can be conditioned by using the threshold. The following equation represents the procedure that should be applied on the probabilities.

$$P(o) = \begin{cases} 0, & o < Th \\ 1, & o \geq Th \end{cases} \tag{3.55}$$

In equ. (3.55), $P(o)$ represents the probability of the outputs in neural network, Th denotes the threshold value which is determined accordance with what the signal needs to be evaluated. Th value should be selected highly when the signal includes the many analogous patterns. T wave consists of two falling curve and a pick point. However, P and QRS complex is akin to this form. Therefore, we choose threshold value as 0.99. It is an important point to select threshold value. The reason is that if the ECG signal includes poor similar patterns, it may degrade the classification performance of the

neural network. The other reason to be important the selection of threshold value is that the neural network may not generate perfect results due to the differences of patterns such as T wave, P wave. Every fiducial point has a different characteristic depending on time even if the patient is same. As a result, when the threshold selection is made, two criteria should be examined, the similarity characteristic of fiducial waves and where the training data is obtained.

In sel14046 data set, the neural network is trained by using real T wave generated by the novel ECG device. Therefore, we could select the threshold value as high as possible in order to provide the stability of the neural network. On the other hand, the selection of the threshold value is appropriate with the another condition of the criteria because T wave has many common features of the other patterns of ECG.

Although, the classification performance is increased by changing this rule, covariance factor should be shifted because of increasing compability. Normally, when the covariance factor is chosen high, the neural network can suppress the similar forms of the ECG patterns such as QRS complex or corruptions created by noise. However, it has an impact to the recognition of the end of the T wave because every T wave has a specific feature at the same signal as mentioned before. Therefore, the covariance factor should be decreased in order to obtain the probabilites including many similar patterns from the ECG signal. If this is applied on the system, many outputs with high probabilities occur. However, the undesirable patterns cannot have probability with degree of 100 percent when the neural network is trained by using the characteristic parameters shown by table 26. Then, we split the patterns to use threshold value as desirable or undesirable.

After applying equation (74) on the neural network, the related results are given in table (3.27).

Table 3.27 The characteristic parameters of the algorithm for fifth QT recognition after applying the condition

J (cost function value)	0.00001
η (learning rate)	0.0001
Teacher Vector	[0.9999 0.0001]
Compare Vector	[0.9999 0.0001]
Back-Propagation Cost Function Calculation Type	Logaritmic
Training Number	16
Covariance Factor	1
End point effectivity	%92.81
Classification Performance	%84.67

Table (3.27) demonstrates that classification perfomance is highly enhanced even if the training data is not the subset of the processing signal. End point effectivity is good, however, the results indicate that the probabilities extend at the end of the T wave. It should be degraded the extension into one point. Covariance factor is selected as 1 becasue of the explained reasons above the table (3.27).

As for the usage of subset training data in current signal, the cluster diagram is depicted as the following figure.

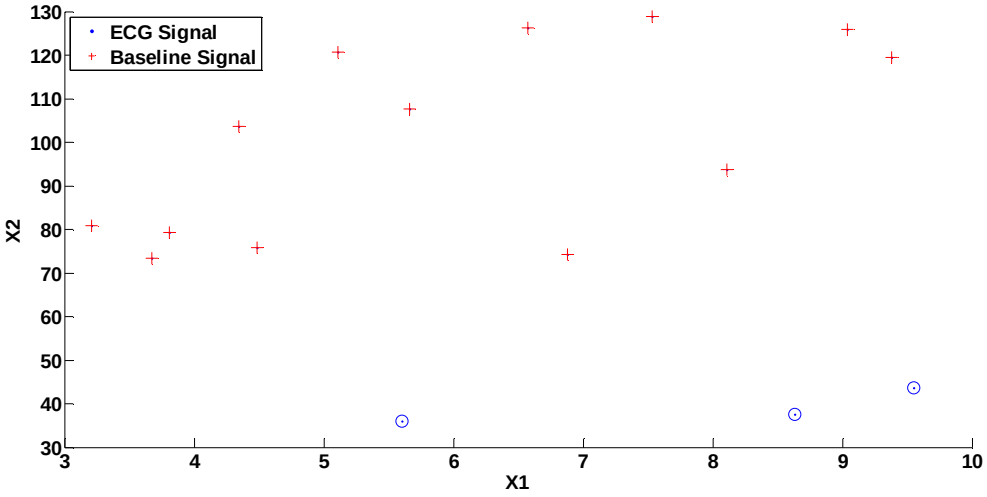


Figure. 3.27 Cluster diagram for T and Artificial Wave under sel14046 training data set

ECG signal distributes at low level of X2 variable, however, baseline or the generated signal is at high level of X2. When examining X1 distribution, two signals spread over the plane equally, however, baseline signal dominates to the ECG signal. This illustrates that when the neural algorithm is performed, the convergence area of baseline signal is bigger than the ECG signal. That is, the recognizable area or the effectivity of the classification is bounded.

We can deduce some ideas from the distribution of data in figure 44. Firstly, covariance factor should be lower values because the distribution is restricted under some area in the plane. On the other hand, the threshold value should be selected as higher value due to fact that when the neural network is compared by the comparing algorithm with high threshold value, the outputs reflects the certain points at the end of the T wave. The related figure is given in figure 46.

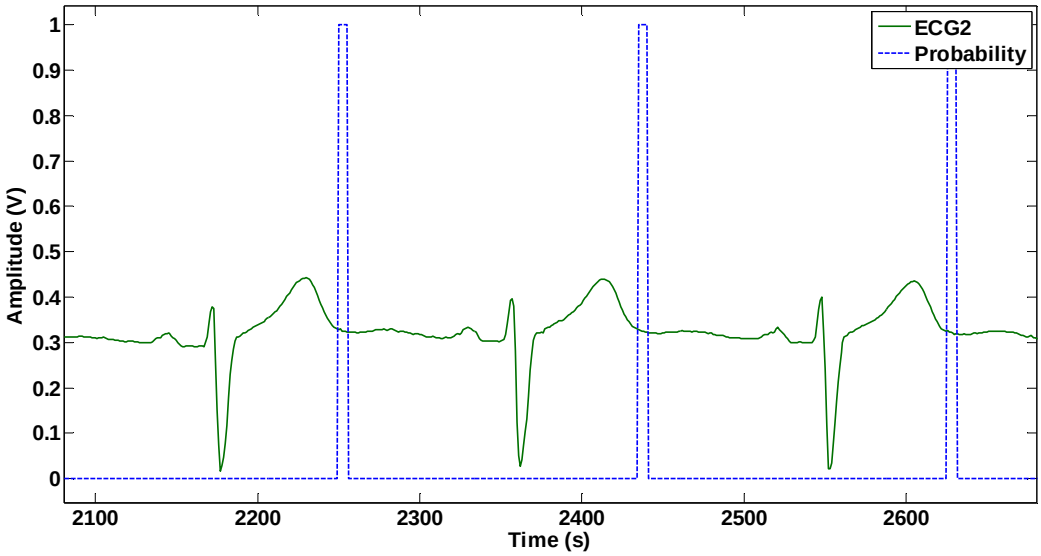


Figure. 3.28 Classification results for second (sel14046) ECG signal with the usage of subset training data of current signal

The algorithm can produce the absolute results when the comparing algorithm is reorganized. Threshold value removes the undesirable similarities such as QRS complex, P wave on the signal.

The responds related for the classification of the end of the T wave are given in table (3.28).

Table 3.28 The characteristic parameters of the algorithm for fifth QT recognition with the subset of training data after applying the condition

J (cost function value)	0.00001
η (learning rate)	0.0001
Teacher Vector	[0.9999 0.0001]
Compare Vector	[0.9999 0.0001]
Back-Propagation Cost Function Calculation Type	Logaritmic
Training Number	16
Covariance Factor	1
End point effectivity	%96.22
Classification Performance	%97.12

Table (3.28) indicates that when training neural network by using the subset of data in current signal, the classification performance is more effective than the usage of real ECG training data. Classification performance is about %97.12. This is a good score to analyze the ECG signal. On the other hand, the end point effectivity is quite enough to determine absolute point of the end of the T wave.

The other signal is named as "sel14157" obtained from PHYSIONET database. The sum of the data examined in neural network is 225000. This ECG signal has the different kind of the T wave. In this signal, T wave is located at the bottom of the isoelectric line. This is an important factor to process the signal. When the ECG signal is analyzed, the evaluation performance is reduced because of the difference between the mean values of current T wave and training T wave data.

The results can be represented as the following table.

Table 3.29 The characteristic parameters of the algorithm for sixth QT recognition with the subset of training data after applying the condition

J (cost function value)	0.00001
η (learning rate)	0.0001
Teacher Vector	[0.9999 0.0001]
Compare Vector	[0.9999 0.0001]
Back-Propagation Cost Function Calculation Type	Logaritmic
Training Number	16
Covariance Factor	16
End point effectivity	%73.23
Classification Performance	%94.32

The classification performance for sixth QT recognition is quite enough to recognize T wave pattern effectively. However, end point effecitivity is reduced because of the reasons explained above. In order to correct the results, covariance factor can be chosen as small as possible. However, the ECG signal cannot be defined completely. The classification illustration is given as the following figure in order to cover the problem.

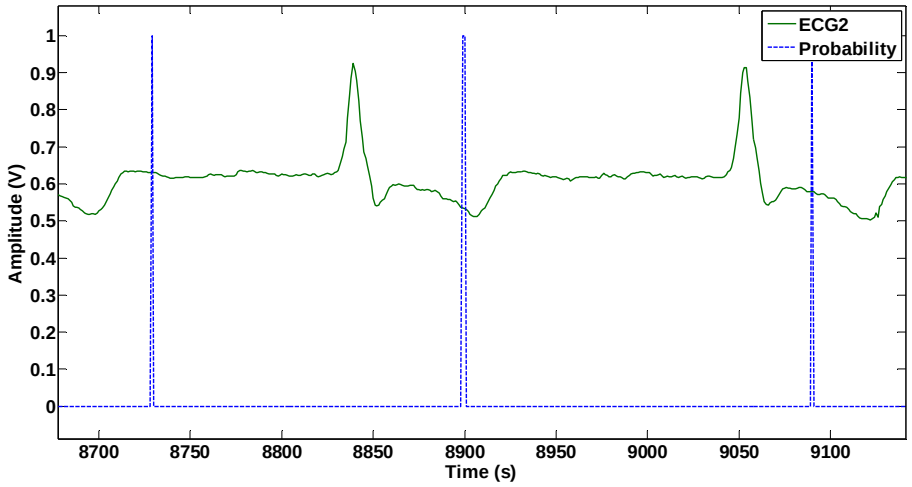


Figure. 3.29 The end of the T wave incompability in sel14157

In Fig. (3.29), the probabilities could detect the T waves but couldn't catch the end of the T wave effectively. In order to explain the related problem, the cluster diagram shown by figure (3.20), includes some errors such as incompability between the level of the T wave and lengthening T wave. When the neural network is trained according to the number of training data, the end of the T wave may not be detected usually. Therefore, we should organize the lengthened T wave in order to attain high efficieny in the present algorithm.

The lenghthened T wave should be tranformed into normal T wave by changing the sequence of the T wave data set.

Assume that a data set of T wave has 10 data to represent their pattern shape. The another pattern but different shape has 20 data. These values can be represented as the symbols n and m, respectively. n can be chosen as the number of training data. Otherwise, m denotes the number of current ECG signal which is being processed at the same time. The correction for compare algorithm to change the length of the T wave can be done by using the following formula.

$$ecg(fp{:}\frac{m}{n}{:}ep) \tag{3.56}$$

In equation (3.56), ecg is the current ECG signal which is being analyzed. fp and ep represent the final point and end point of the pattern processed by the compare algorithm. $\frac{m}{n}$ is used to scale the T wave whatever their length is. That is, when the neural network is trained by the specific number of data, the compare algorithm can be used flexibly to perform regardless of the number of training data. In addition, we mentioned the correction concerning the start location of the probabilites coming from the neural network. If this scaling function is used to the present algorithm in comparing section, the location of the start point is rearranged because of the change of data number. It can be represented in equation (3.57).

$$SP = TN + m - n \tag{3.57}$$

where SP is the starting point of the probability vector, TN is the training number of the data set, m is the number of the comparing data set and n is the number of trained data. When these functions are added to the code, the results are given in figure 48.

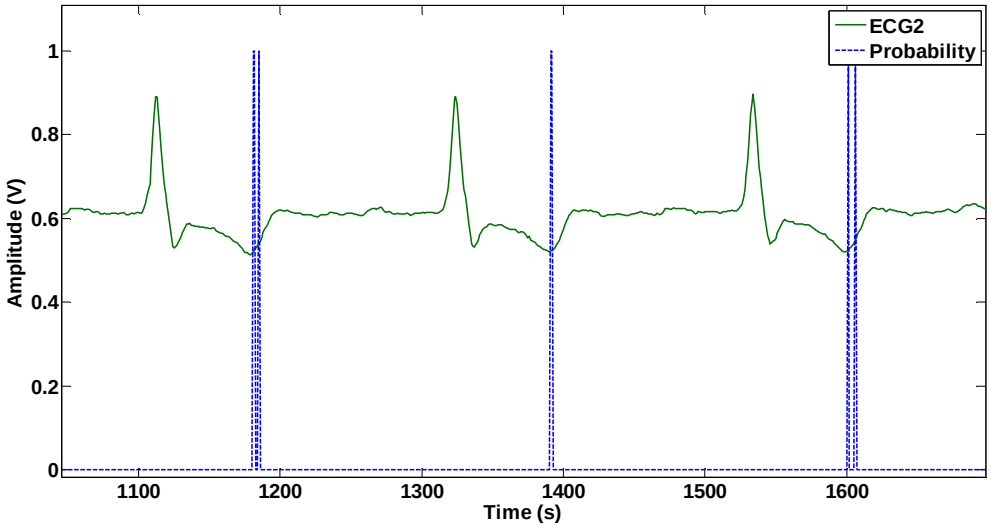


Figure. 3.30 Classification results for (sel14157) ECG signal with changing the lengthened data set

In Fig. (3.30), the results demonstrate that the processing ECG signal can be determined effectively when including the correction functions given above.

The related results is depicted as the following table.

Table 3.30 The characteristic parameters of the algorithm for sixth QT recognition after applying the correction functions

J (cost function value)	0.00001
η (learning rate)	0.0001
Teacher Vector	[0.9999 0.0001]
Compare Vector	[0.9999 0.0001]
Back-Propagation Cost Function Calculation Type	Logaritmic
Training Number	16
Comparing Number	25
Covariance Factor	16
End point effectivity	%98.12
Classification Performance	%95.19

In Table 30, a new parameter has been added to improve the results and to evaluate how it has an effect on the neural network. Comparing number should be selected by examining how many data the T wave has. In order to assess the performance, classification is higly improved by rearranging the T waves. The end point effectivity is enhanced remarkably when using the correction functions.

Although, the recognition quality is better in that situation, the neural network should be teached with the subset of the end of the T wave in order to cover the performance difference. For this purpose, the cluster diagram belonging to the subset of the end of the T wave is illustrated in figure (3.31).

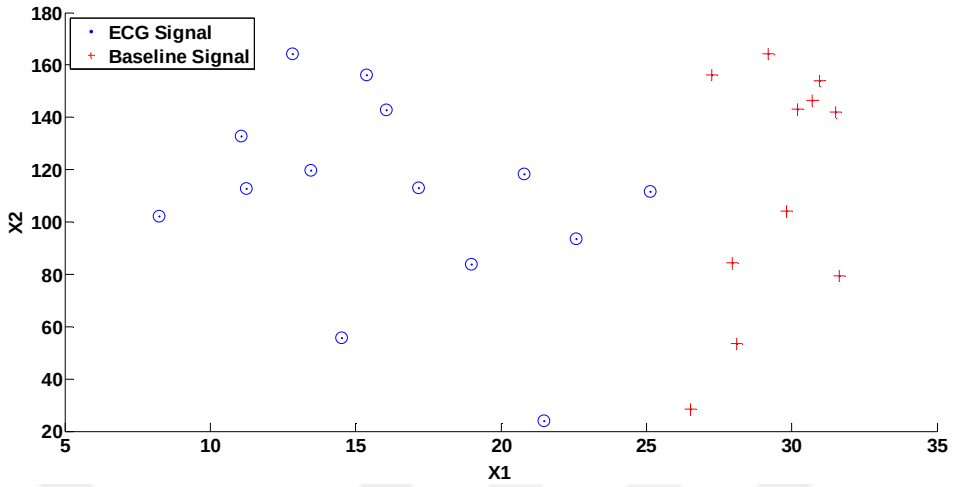


Figure. 3.31 Cluster diagram for T and Artificial Wave under sel14157 training data set

The cluster diagram demonstrates that T wave dominates the baseline signal because of the number of training data. However, the plane for recognition T wave has more oppurtunity to analyze T wave. Therefore, the present algorithm has become more insensitive to detect the end of the T wave, it also produces probabilities for QRS complex, P wave and the other fiducial points which are akin to the end of the T wave. The experiment results can be shown as the following figure.

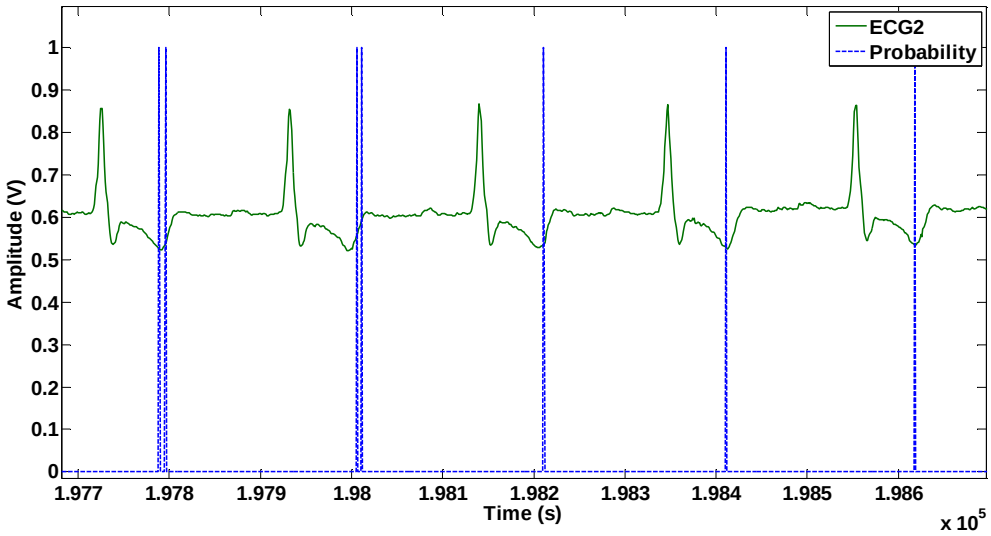


Fig. 3.32 Classification results for second (sel14157) ECG signal with the usage of subset training data of current signal

The concerned results are illustrated in Table (3.31).

Table 3.31 The characteristic parameters of the algorithm for sixth QT recognition with the subset of training data after applying the correction functions

J (cost function value)	0.00001
η (learning rate)	0.0001
Teacher Vector	[0.9999 0.0001]
Compare Vector	[0.9999 0.0001]
Back-Propagation Cost Function Calculation Type	Logaritmic
Training Number	25
Comparing Number	25
Covariance Factor	25
End point effectivity	%98.78
Classification Performance	%98.26

The classification performance is little enhanced but does not change their results effectively. The end point effectivity has become better than the other results. The reason is that the present algorithm is only trained by the subset of the training data which are selected at the processing ECG signal. In addition, Comparing and Training number are equal to each other due to that.

Up to now, several QT database signals have been evaluated in order to understand the effectivity of the present algorithm. However, there are complete different QT patterns from the QT shapes achieved above. One of them is sel14172 obtained by PHYSIONET QT database. Like the others, it consists of 225000 data set. In contrast to the others performed above, this signals has a characteristic shape with two picks at the end of the T wave. It can be illustrated as the following figure.

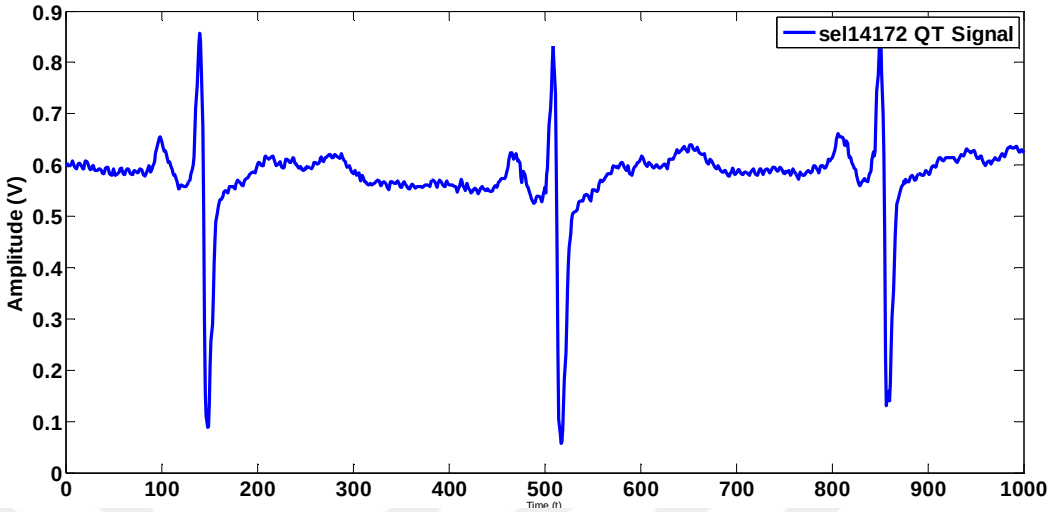


Fig. 3.33 The illustration of "sel14172" QT signal

The QT pattern shown in figure (3.33) is complete different from the QT pattern obtained by real ECG signal. Therefore, firstly, we apply the present algorithm by using the real ECG training data set in order to discuss the results of it.

When processing the neural network, the output of the present algorithm is illustrated in figure (3.34).

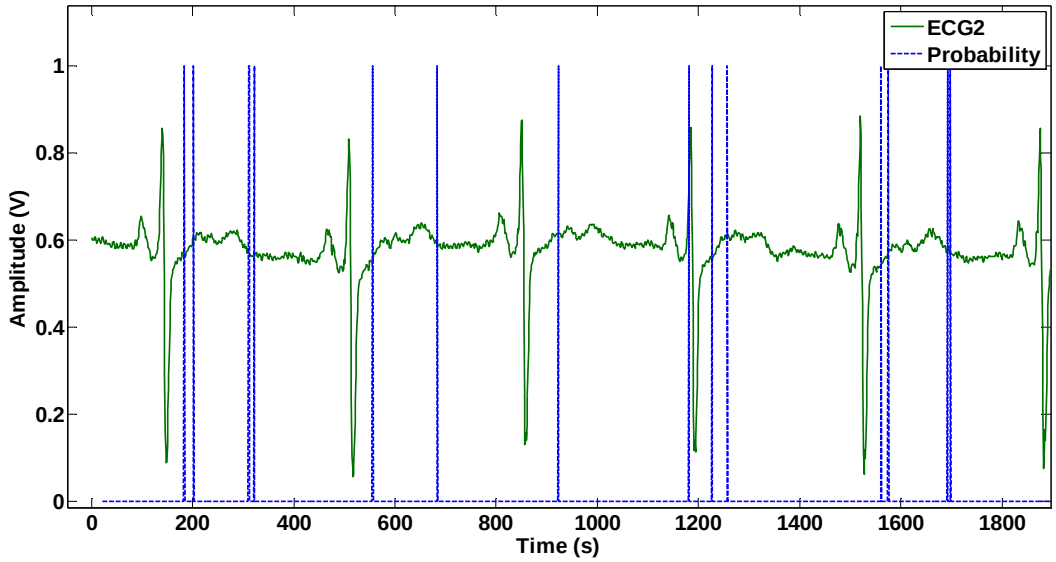


Figure. 3.34 Classification results for (sel4172) ECG signal

The results shown by figure (3.34) demonstrate that although, the present algorithm can have an ability to recognize the end of the T wave at some points, the false negative and false positive results occur at the beginning of the T wave and QRS complex. In order to

demonstrate the classification performance, Table (3.32) can be given with the characteristic parameters of the present algorithm.

Table 3.32 The characteristic parameters of the algorithm for sel14172 QT recognition

J (cost function value)	0.00001
η (learning rate)	0.0001
Teacher Vector	[0.9999 0.0001]
Compare Vector	[0.9999 0.0001]
Back-Propagation Cost Function Calculation Type	Logaritmic
Training Number	16
Comparing Number	16
Covariance Factor	40
End point effectivity	%89.02
Classification Performance	%11.23

The results indicate that the present algorithm is not enough to analyze this type of the QT signal. The classification performance is about 11.23 percent and the end point effectivity is about %74.02 because when the end of T wave is recognized, the probability outputs give correct locations where the T wave is ended. In addition, covariance factor should be discussed in this experiment because when the ECG signal has the differences between its T wave and real ECG T wave, it should be increased in order to attain high performance. However, covariance factor did not lead to a great change in classification performance. On the other hand, we have not yet applied to the neural algorithm to corrections functions. The reasons is that T wave includes two pick points, so, it must be reorganized to define the pattern of T wave in the current signal.

Before applying the correction function for the neural network, we investigate the characteristic of cluster distribution of the current signal training data set. It is an

important to determine how we can change the correction functions for the classification of the end of the T wave. The cluster diagram is given in figure (3.35).

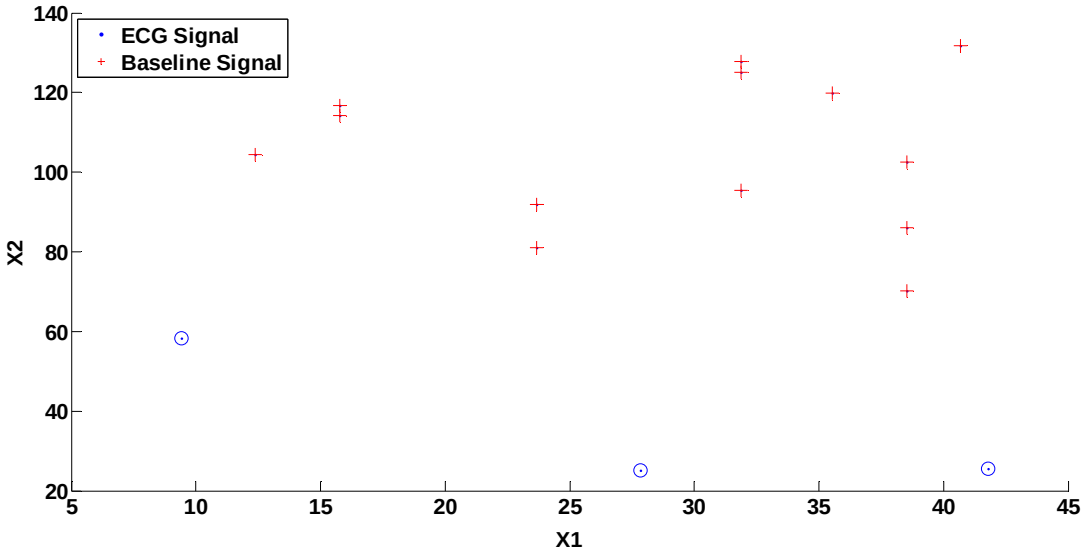


Fig. 3.35 Cluster diagram for T and Artificial Wave under sel14172 training data set

The cluster diagram shows that ECG signal has a wide range of X1 but short range of X2. It means that their characteristic features are meaningful with change of X2. On the other hand, there are only three points which distribute along X1 axis. The neural network collapses this range effectively when it is trained. Although, it covers the all of the area between X1 and X2 at the ECG signal, the neural network cannot easily decide which data represent the end of the T wave. The cluster diagram should be reaaranged in order to restrict the area of decision.

Although, the range of distribution is bigger in contrast to the number of recognizable points in cluster diagram, the back propagation algorithm restricts the area of decision by iteration.

Table (3.33) illustrates the results coming from the usage of subset of training data.

Table 3.33 The characteristic parameters of the algorithm for sel14172 QT recognition with the subset of training data

J (cost function value)	0.00001
η (learning rate)	0.0001
Teacher Vector	[0.9999 0.0001]
Compare Vector	[0.9999 0.0001]
Back-Propagation Cost Function Calculation Type	Logaritmic
Training Number	16
Comparing Number	16
Covariance Factor	40
End point effectivity	%84.12
Classification Performance	%79.41

The classification performance is enchanced by using the subset of the current signal as training data. When comparing the other experiments, the classification performance has poor results because of the shape of the T wave. The end point effectivity is degraded when the neural network is trained by using itself. The reason is that the present algorithm does not easily converge the end of the T wave because there are two picks waves like T wave.

The correction functions have not been applied on this experiment because the characteristic of the T wave in sel14172 differs itself from the experiment made. We cannot deduce specific rules or approach for this type of signal because the other experiments were made by approving that T wave has only pick and end point in ECG signal.

Finally, we make an experiment by using QT signal named as sel16265 obtained by PHYSIONET database. This signal are likely to real ECG signal but has little difference

with real signal. Its T wave shape is short and the time of period of this signal is shorten due to the recording frequency. When the present algorithm is tried to recognize on this signal, the results can be illustrated as the following figure.

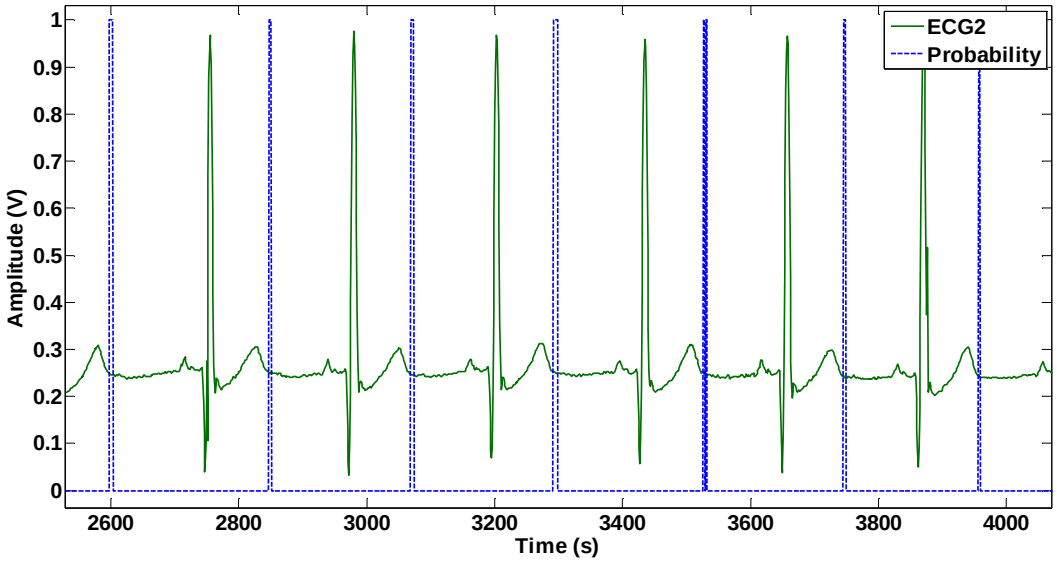


Figure. 3.36 Classification results for (sel6265) ECG signal

Figure (3.36) shows that the present algorithm can be analyzed the ECG signal given by using the training data of real ECG signal shown in figure 38.

The following table indicates the characteristic parameters of the neural network and classification performance.

Table 3.34 The characteristic parameters of the algorithm for sel16265 QT recognition with applying threshold

J (cost function value)	0.00001
η (learning rate)	0.0001
Teacher Vector	[0.9999 0.0001]
Compare Vector	[0.9999 0.0001]
Back-Propagation Cost Function Calculation Type	Logaritmic
Training Number	16
Comparing Number	16
Covariance Factor	5
End point effectivity	%99.12
Classification Performance	%96.44

Table (3.34) demonstrates that the neural network is enough to recognize the end of the T wave for the ECG signal given. The classification performance is about 96.44 percent and the end point effectivity is about 99.12 percent. Normally, it can be expected that the neural network would completely analyze the ECG signal because of the similarity between the current ECG signal and real ECG signal. However, in this experiment, sel16265 data set includes a different regions from the end of the T wave of real ECG signal. Therefore, the ECG signal classification could not pass 96.44 percent. In addition, covariance factor is chosen as 5 or small values of its range. The reason is that the neural network does produce rarely true negative signal patterns because of the similarity. Hence, covariance factor can be used in the range of small numbers in order to get a lot of information from the ECG signal about the end of the T wave. Also, threshold value is applied on the present results because when the covariance factor is small, there are only the regions which are detectable in order to find out the end of the

T wave due to the probability values. When the ECG signal is examined perfectly, the neural network gives a probability which is one. As a result, the results can be induced that the neural network is quite enough to analyze this type of the ECG signal.

On the other hand, we should look at the cluster diagram of the subset of the current ECG signal as training data. Figure (3.37) represents the cluster diagram of sel16265 data set.

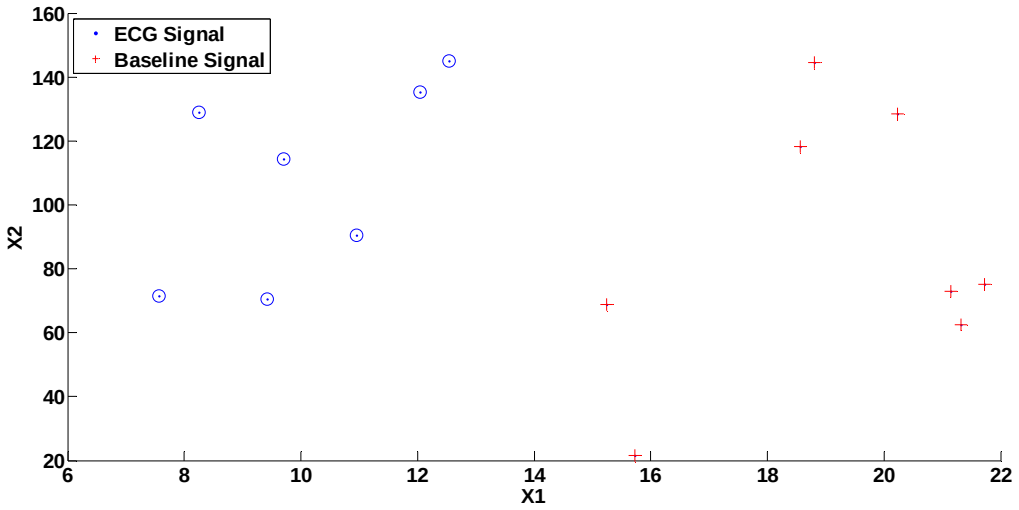


Figure. 3.37 Cluster diagram for T and Artificial Wave under sel16265 training data set

Figure 55 is similar to figure 38 given by real ECG signal training data. ECG signal distribution has deterministic form and it is easy to restrict the area of decision in this diagram. However, when the neural algorithm is trained by using the subset of the current ECG signal, the results are changed by due to two factors, covariance data set selection and the convergence characteristic of the neural network.

Before giving the reasons related to the performance of the neural algorithm, Table (3.35) should be given in order to evaluate the classification performance and the selection of its characteristic parameters.

Table 3.35 The characteristic parameters of the algorithm for sel16265 QT recognition by using the subset of the current ECG signal with applying threshold

J (cost function value)	0.00001
η (learning rate)	0.0001
Teacher Vector	[0.9999 0.0001]
Compare Vector	[0.9999 0.0001]
Back-Propagation Cost Function Calculation Type	Logaritmic
Training Number	16
Comparing Number	16
Covariance Factor	5
End point effectivity	%99.67
Classification Performance	%99.34

The classification performance is increased at the rate of 2.9 percent and the end point effectivity is about 99.67 percent. This is a perfect result for the present algorithm. Covariance data set in this experiment should be chosen at the unrecognizable section to enhance the compability of the present algorithm. The reason is that when the neural network outputs is compared by using the unrecognizable covariance data set, there is no loss of probability which represents the end of the T wave. In contrast to loss of data, the algorithm have an ability to recognize the T wave pattern which was not analyzed. Secondly, the convergence characteristic can be changed accordance with the selection of the training data set. Therefore, when the training data set is obtained from the current ECG signal, the convergence operation is more stable than the other situations.

CHAPTER 4

RESULTS AND DISCUSSION

In the present study, the novel approach to analyze the fiducial points of ECG signal especially QT interval is presented in order to attain high performance in classification achieved by neural network.

In first section, the study describes the anatomy of human to cover the concept of what we should measure from it. Then, the system required to obtain the ECG signal is given in order to understand the principles of the measurement of electrocardiography signal. Thirdly, the fundamentals of ECG signal are explained by supporting literature review. Its characteristic and behaviours in the face of measurement is described deeply. The heart muscles and its physiological features are given in parallel to the reflection of the ECG signal. Electrocardiographic basis and feature are disclosed in order to understand how we evaluate the ECG signal under some conditions such as the meaning of intervals. In order to make meaningful to the ECG signal, the classification algorithm review is made by demonstrating the type of it and the classification performance for this algorithm. Artificial neural network is described in this section because the present algorithm is worked based on the neural network mechanism. This section includes only the heartbeat recognition performance in classification because we did try to introduce the novel algorithm for the determination of the QT interval. Therefore, we selected the base point as QRS complex named as heartbeat in order to classify their characteristic by using the present algorithm. Especially, for first section, we only focus on which classification methods are used to perform the determination of the heartbeats in ECG signal.

The design of pattern recognition basically is comprised of the three aspects, data acquisition and preprocessing, data representation and decision making. The classification algorithm explained in this section consists of four different methods, template matching, statistical classification, syntactic or structural matching and neural network. First of them mentioned before is template matching algorithm published in [21] which performs the determination of the similarity between two entries of specified type like QRS complex, T wave matching. However, template matching algortihm has some restrictions to analyze the signal effectively. One of the restrictions is to find the general template because if there is no template, classification algorithm does not converge the wanted point. For this study, we cannot estimate what the ECG signal shape is, because the ECG signal is non-stationary signal. Secondly, statistical classification consists of supervised or unsupervised learning. Statistical pattern recognition is reported in [28, 29, 30], however none of them provide an effective solutions to classify the ECG signal. When one of the pattern is taken the evaluation of the ECG signal pattern, there is no guarantee to attain high classification performance because of the difference between the ECG signal qualities. In this study, we use the statistical methods including both supervised and unsupervised methods in order to train the system. However, the results obtained by the experiments demonstrates that the statistical method is not only enough to examine the ECG signal. Thirdly, we discussed the quantitative nature of statistical pattern recognition because it makes the algorithm to use the discrimination among groups sub patterns and their interrelationships embedded within the data. The selected articles published in [48, 49] were developed to syntactic method to ECG pattern recognition and parameter measurement. However, its convergence area is restricted with one statistical values which can be recognized to the system. Therefore, they do not easily control its convergence and apply on the ECG signal because of its non-stationary characteristic. Finally, the neural network is given in chapter 1 in order to cover the fundamentals of the present algorithm. [50, 51, 52] are explained to represent the samples of the ECG signal classification. Their classification performance changes in range of between 90 and 95 percent for heartbeat recognition. However, in the present algorithm, the results demonstrate that the heartbeat recognition with any kind of the ECG signal is in the range of between %97 and %99.2. In some cases, the heartbeat recognition could be completely recognized without any failure.

In second section, in order to explain the physiological problems in the heart, QT syndrome is explained. We make two subsection in this chapter, short and long QT syndrome. We mentioned the general idea of the QT syndrome and what we need to know the physiological basis of it. Normally, the QT interval should be measured correctly in order to understand that people have an abnormalities in the heart.

In the third section, we tried to figure out how the QT segment can be determined by the novel algorithm and how we can improve the present algorithm. We used the gaussian mixture model to charaterize the ECG signal given for QRS complex and QT segment. As mentioned before, Gaussian mixture model is based on the mixture of covariance and mean values of the ECG signal. It can represent the ECG signal as its mean and covariance values. Therefore, we firstly used LLGMN method published in [89] which is a probabilistic method with neural network to analyze the EEG and EMG signals. However, the general characteristic of LLGMN algorithm cannot give us an oppurtunity to analyze the ECG signal because the ECG signal has an sequential patterns. In EEG and EMG, there is no sequence pattern after the normalization and filtration of the data processed.

Due to these reasons, we introduce the novel pattern recognition algoritm for the ECG signals in order to analyze the fiducial points of it. We create the gaussian mixture model to use the mean and covariance values of the ECG signal trained. Then, we transform Gaussian mixture parameters into neural network coefficients from the mean, probability coefficient and covariance value. Then, we performed the transformation explained in [89]. However, when the LLGMN is applied, we realize that it cannot be effectively worked due to the sequential pattern format. Also, when the ECG signal is normalized, many pick and fall curves occurs. It is a big problem to process the LLGMN because when the EMG and EEG signal is normalized after filtration, there is no fall and pick points more than one. In addition, for EMG and EEG signal, the training data set of LLGMN are chosen as the highest points on the graph.

For these reasons, we develop a new probabilistic method based on gaussian mixture model with neural network described in [89]. For the evaluation, we present a new compare algorithm in order to the incompability of sequential data in ECG. On the other hand, normally, for the signal recognition in neural network, two input should be given to the neural network differently. As different from [89] in heartbeat recognition, the present algorithm is achieved by feeding two similar QRS complexes but little

differences. The reason is that when the two different input are fed into the neural network, the outputs cannot be understandable. On the other hand, due to the usage of Gaussian mixture model, there could be a problem to use two similar input because when the input are closer to each other expectation maximization algorithm is not be worked effectively because of converging the mean and covariance value through zero.

In accordance with the explanations mentioned above, we only apply the gaussian mixture model parameters without training data. When the neural network coefficient is determined, all of the coefficients are performed in compare algorithm with its characteristic function named as compare function. The compare algorithm outputs in heartbeat recognition arise only at the QRS complex section but low probabilities. That is, we detect the QRS complexes to train the neural network with two similar QRS complexes as different from LLGMN.

Secondly, we train the neural network with initial values coming from the transformation supported by Gaussian mixture model. The results become more clear than the usage of Gaussian mixture model coefficient. Then, we try the neural network in order to understand that how parameters affect on the results. Four different parameters are chosen to understand the change of the quality of the neural network, teacher vector, learning rate, cost function value and compare function. Normally, two of them are used in [89], however, the others are produced to increase the quality of the outputs in compare algorithm. When the neural network is trained under changing four parameters, the effects of characterization in parameters is determined. Also, we reach the perfect classification in heartbeat recognition about 100 percent whatever the ECG signal is different from the training data.

Thirdly, we try to analyze the ECG signal at the end of the T wave in order to determine the QT interval. As mentioned before, QT interval is examined in order to diagnose the short and long QT syndrome. However, at the end of the T wave, Jensen inequality is not effectively performed because of convex-concave incompability. In order to fix it, we produce covariance matching, covariance corretions and data alignment technique which are develop by the authors. Then, we apply the threshold value for the output of the compare algorithm because the correct probabilities is always about 100 percent. When applying all of the functions and conditions, the end of the T wave becomes observable for the compare algorithm.

In order to demonstrate the classification performance, eight different ECG signal with different T waves are analyzed by the present algorithm. The number of all of the data tried is about 2000000. The performance classification changes in accordance with the several conditions. One of them is choosing the training data set. When the training data set are selected as the subset of the current ECG signal, the performance is better than the other situation. Second of them is using the covariance factor. When the covariance factor is chosen as the signal type, we realize that it should be same with the number of training data if the current and training signal is similar to each other. While the training signal is different from the covariance factor, the covariance factor should be smaller than the training number. However, the threshold value should be applied to the current signal in order to obtain only probability with 100 percent.

As a conclusion, the present study have developed the novel algorithm for the detection of QT interval. When examining the results, the present algorithm performance is in the range of between 96 and 99.96 percent accuracy. When comparing with the QRS complex recognition, the present algorithm with QT correction functions can be used perfectly.

REFERENCES

[1] Williams, P.L., and Warwick, R. (eds.) (1989): Gray's anatomy, 37th ed.,Churchill Livingstone, Edinburgh

[2] Netter, F.H., (1971). Heart, The Ciba Collection of Medical Illustrations, Ciba Pharmaceutical Company, Summit, N.

[3] Ruch, T.C., and Pattan, H.D.(1982). Physiology and Biophysics, 20th ed, W.B. Saunders, Philadelphia.

[4] Hodgkin, A.L., Rushton W.A. (1946). "The electrical constants of a crustacean nerve fiber", Proc. R. Soc. , B133: 444-79

[5] Kleber, A.G., and Riegger C.B. (1986). "Electrical Constants of arterially perfused rabbit papillary muscle", J. Physiol. (Lond.) 385: 307-24

[6] Waller, A.D. (1887). A demonstration on man of electromotive changes accompanying the heart's beat. J. Physiol. (Lond.) 8:229-34.

[7] Ader, C. (1897). "Sur un nouvel appareil enregistreur pour cables sousmarins", Compt. rend. Acad. Sci. (Paris) ,124: 1440-2.

[8] Einthoven, W., Fahr G., de Waart A (1913). "Uber die Richtung und die Manifeste Grosse der Potentialschwankungen immennschlichen Herzen und uber den Einfluss der Herzlage auf die form des Elektrokardiogramms". Pflüger Arch. ges.Physiol. 150: 275-315.

[9] Scher, A.M., and Young A.C. (1957). "Ventricular depolarization and the genesis of the QRS". Ann. N.Y. Acad. Sci. 65: 768-78.

[10] Ruch, T.C., and Pattan H.D.(1982). Physiology and Biophysics, 20th ed, W.B. Saunders, Philadelphia.

[11] Sokolow, M. and Lyon, T.P. (1949). "The ventricular complex in left ventricular hypertrophy as obtained by unipolar precordial and limb leads". Am Heart J., 37:161-186.

[12] Wilson, F.N., Macleod, A.G., Barker, P.S. (1931). "Potential variations produced by the heart beat at the apices of Einthoven'striangle". Am. Heart J. 7: 207-11.

[13] Wilson, F.N., Johnston F.D., Macleod A.G., Barker P.S. (1934). "Electrocardiograms that represent the potential variations of a singleelectrode". Am. Heart J. 9: 447-71.

[14] Goldberger, E. (1942a). "The aVL, aVR, and aVF leads; A simplification of standard lead electrocardiography". Am. Heart J. 24:378-96.

[15] Goldberger, E. (1942b). A simple indifferent electrocardiographic electrode of zero potential and a technique of obtainingaugmented, unipolar extremity leads. Am. Heart J. 23: 483-92.

[16] Wilson, F.N., Johnston, F.D., Rosenbaum, F.F., Erlanger, H., Kossmann, C.E., Hecht, H., Cotrim, N., Menezes, de Olivieira R., Scarsi, R.,Barker P.S. (1944). "The precordial electrocardiogram. Am. Heart J.", 27: 19-85.

[17] Geselowitz, D.B. (1964)."Dipole theory in electrocardiography.", Am. J. Cardiol. 14(9): 301-6.

[18] Basu J.K., et al.(2010). "Use of Artificial Neural Network in Pattern Recognition", International Journal of Software Engineering and Its Applications, 4(2):23-34

[19] Yang S. and Yang G.,(2010). "ECG Pattern Recognition Based on Waveletc Transform and BP Neural Network", ISNNS2010,4(2):246-249

[20] Foo, S. Y., Stuart, G., Harvey B., (2002). "Neural network-based EKG pattern recognition",Engineering Applications of Artificial Intelligence ,15:253-266

[21] Dobbs, S. E. (1984). "QRS detection by template matching using real-time correlation on a microcomputer", Journal of Clinical Engineering, 9:197-212

[22] Dobbs, S. E.(1984). "QRS detection by template matching using real-time correlation on a microcomputer", Journal of Clinical Engineering, 9:197-212

[23] Furno, G. S. and Tompkins,(1982). "QRS detectionusing automata theory in a battery powered microprocessor system", IEEE Frontiers of Engineering in Health Care, 3:155-158

[24] L. Devroye, L. Gyorfi, and G. Lugosi (1996). "A Probabilistic Theory of Pattern Recognition", Springer-Verlag, Berlin

[25] R.O. Duda and P.E. Hart(1973). "Pattern Classification and Scene Analysis", John Wiley & Sons, New York

[26] V.N. Vapnik,(1998)."Statistical Learning Theory", John Wiley & Sons, New York

[27] Richard, O. Duda, Peter E. Hart, and David E. Stork (2001)." Pattern Classification", John Wiley & Sons, New York

[28] Keinosuke (1990)."Introduction to Statistical Pattern Recognition", Academic Press,Boston

[29] Anil, K. Jain, et al.(2000). "Statistical Pattern Recognition: A Review", IEEE Transactions on Pattern Analysis and Machine Intelligence, 22(1):4-37

[30] Martin, J. Uttner (1997)."Evidence-Based Pattern Classification: A Structural Approach to Human Perceptual Learning and Generalization",Journal of Mathematical Psychology, 41(3):244-259.

[31] Irving, Biederman (1987). “Recognition-by-Components: A Theory of Human Imageunderstanding”, Psychological Review, 94(2):115-147

[32] Martin, J. Uttner (1997). “Evidence-Based Pattern Classification: A Structural Approach to Human Perceptual Learning and Generalization”,Journal of Mathematical Psychology, 41(3):244-259

[33] David, Noton(1970). “A Theory of Visual Pattern Perception”. IEEE Transactions on Systems Science and Cybernetics, 3:349-357

[34] Stephen K. Reed (1974). ”Structural Descriptions and the Limitations of Visual Images”,Memory & Cognition, 1(2):329-336

[35] Stephen, K. Reed and Jeffrey A. Johnsen (1975).”Detection of Parts in Patterns and Images”,Memory& Cognition, 3(5):569-575

[36] John, R. Anderson (1991). “The Adaptive Nature of Human Categorization Psychological Review”, 98(39):409-429

[37] Barbara, Hayes-Roth and Frederick Hayes-Roth (1977)."Concept Learning and the Recognition and Classification of Exemplars". Journal of Verbal Learning and Verbal Behavior, 16(3):321–338

[38] Stephen, K. Reed (1972).“Pattern Recognition and Categorization”,Cognitive Psychology,3(3):382-407

[39] Amos, Tversky (1977).”Features of Similarity”,Psychological Review, 84(4):327-352

[40] Barbara, Tversky and Kathleen Hemenway(1984).”Objects, Parts, and Categories” ,Journal of Experimental Psychology: General, 113(2):169-193

[41] T. Pavlidis, “Structural Pattern Recognition”(1977).Springer-Verlag, Berlin

[42] K. S. Fu (1982). “Syntactic Pattern Recognition and Applications”, Prentice-Hall, Englewood Cliffs, New Jersey

[43] Rafael, C. Gonzalez and Michael G. Thomason, (1978).“ Syntactic Pattern Recognition: An Introduction”.Addison-Wesley,Reading, Massachusetts

[44] T. Pavlidis, (1977). “Structural Pattern Recognition”.Springer-Verlag, Berlin

[45] Edward, R. Dougherty.,(1992). “An Introduction to Morphological Image Processing”,SPIE, Optical Engineering Press, Bellingham, Washington.

[46] Charles, R. Giardina and Edward R. Dougherty,(1988).”Morphological Methods in Image and Signal Processing”,Prentice- Hall, Englewood Cliffs, New Jersey

[47] Bandyopadhyay,(1990). “Diagnosis of ECG Diagnosable Diseases Syntactic Pattern-Recognition Approach”.International Journal of Electronics, 68:915-924

[48] Trahanias, P. and Skordalakis, E. (1990), ”Syntactic Pattern-Recognition of the ECG”, IEEE Transactions on Pattern Analysis and Machine Intelligence, 12:648-657

[49] Sarkaleh, M.K. and Shahbahrami A. (2012), “Classification of ECG Arrhythmias Using Discrete Wavelet Transform and Neural Networks”,

International Journal of Computer Science, Engineering and Applications (IJCSEA),2(1):193-199

[50] Jain, A.K., J. Mao, and K.M.Mohiuddin,(1996). “Artificial Neural Networks:A Tutorial”,1(1):31- 44

[51] T.Kohonen,(1995). “Self-Organizing Maps”, Springer Series in Information Sciences, Berlin,30:44-67

[52] Raushan Ara Dilruba, Nipa Chowdhury, Farhana Ferdousi Liza, Karmakar,K.C.,(2006). “Data pattern recognition Using neural network with back propagation training”, 4(5):451-455

[53] Philip, de Chazal, Maria O'Dwyer and Richard B.Reilly,(2004). “Automatic Classification of Heartbeats Using ECG Morphology and Heartbeat Interval Features”, 5(2):1196 - 1206

[54] S. H. El-Khafif and M. A. El-Brawany, (2013).“Artificial neural network-based automated ECG signal classifier,” ISRN Biomedical Engineering, 1:66-72

[55] P. de Chazal and R. B. Reilly,(2003). “Automatic Classification of ECG Beats Using Waveform Shape and Heart Beat Interval Features”, 4(2):269-272

[56] Yuksel, Ozbay. and Bekir, Karlik.,(2001). “A Recognition of ECG Arrhythmias Using Artificial Neural Networks”, 22(2):1680-1683

[57] K.Zhu, P. D. Noakes and A.D.P. Green,(1991). “ECG Monitoring with Artificial Neural Networks”,4:205 - 209

[58] Shanxiao Yang, Guangying Yang, (2010). “ECG Pattern Recognition Based on Wavelet Transform and BP Neural Network“ , Proceedings of the International Symposium on Networking, 44:246-252

[60] Panicker, GK, Karnad DR, Natekar, M, Kothari S, Narula, D., Lokhandwala, Y. (2009). "Intra- and interreader variability in QT interval measurement by tangent and threshold methods in a central electrocardiogram laboratory". J Electrocardiol 42 (42(4)):348–52.doi:10.1016/j.jelectrocard.2009.01.003.PMID 19261293.

[61] Salvi, V., Karnad, D.R., Panicker, G.K., Natekar, M., Hingorani, P., Kerkar, V., Ramasamy A, de Vries M, Zumbrunnen T, Kothari S, Narula D.(2011). "Comparison of 5 methods of QT interval measurements on electrocardiograms from a thorough QT/QTc study: effect on assay sensitivity and categorical outliers".,J Electrocardiol, 44:96–104

[62] Arking DE, Pfeufer A, Post W, Kao WH, Newton-Cheh C, et al. (2006) A common genetic variant in the NOS1 regulator NOS1AP modulates cardiac repolarization. Nat Genet 38: 644–651.

[63] Leitch A, McGinness P, Wallbridge D, (2007). "Calculate the QT interval in patients taking drugs for dementia." BMJ, 1:335:557.

[64] C.M. Armstrong, G. Cota, (1999). "Calcium block of Na+ channels and its effect on closing rate", Proc Natl Acad Sci USA, 96(7):4154–4157

[65] P. Bjerregaard, I. Gussak, (2005). "Short QT syndrome: mechanisms, diagnosis and treatment", Nat Clin Pract Cardiovasc Med, 2:84-77

[66] Gollob, M.H., Redpath, C.J., and Roberts, J.D. (2011). "The short QT syndrome: proposed diagnostic criteria.", J Am Coll Cardiol. 57:802–812

[67] Gaita F, Giustetto C, Bianchi F, Schimpf R, Haissaguerre M, Calo L, Brugada R, Antzelevitch C, Borggrefe M, Wolpert C.(2004). "Short QT syndrome: pharmacological treatment". J Am Coll Cardiol.,43:1494 –1499

[68] Levine E, Rosero SZ, Budzikowski AS, Moss AJ, Zareba W & Daubert JP (2008). "Congenital long QT syndrome: considerations for primary care physicians"., Cleve Clin J Med,75:591–600.

[69] Viskin S. (1999). "Long QT syndromes and torsade de pointes.",Lancet 354:1625–1633

[70] Moric-Janiszewska E, Markiewicz-Łoskot G, Loskot M, Weglarz L, Hollek A and Szydlowski L,(2007). "Challenges of diagnosis of long-QT syndrome in children"., Pacing Clin Electrophysiol. 30:1168–1170

[71] D.W. Abramson, D.K. Quinn, T.A. Stern,(2008). "Methadone-associated QTc prolongation: a case report and review of the literature Prim Care Companion", J Clin Psychiatry, 10:470–476

[72] M.E. Nygards and L. Siirnmo,(1983). “Delineation of the QRS complex using the envelope of the ECG,” Med. Rid Eng. Comput., 21:528-547

[73] The CSE Working Party, (1985). “Recomendations for measurement standards in quantitative electrocardiography,” European Heart Jour,al, 6:815-825

[74] Laguna P, Jané R, Caminal P. (1994). "Automatic detection of wave boundaries in multilead ECG signals: validation with the CSE database.", Computers and Biomedical Research, 27(1):45-60.

[75] Li, C., Zheng C., and Tai C., (1995). "Detection of ECG characteristic points using wavelet transforms.", IEEE TBME, 42(1):21-28

[76] Martinez JP, Almeida R, Olmos S, Rocha, AP, and Laguna P.(2004). "A wavelet-based ECG delineator: evaluation on standard databases.", IEEE TBME, 51(4):579-581.

[77] Zhang, Q., Illanes Manriquez, A., Medigue, C., Papelier, Y., and Sorine, M.,(2005). "Robust and efficient location of T-wave ends in electrocardiogram.", Computers in Cardiology, 32:711-714.

[78] Zong, W, M, Saeed., T, Heldt.,(2006). "A QT Interval Detection Algorithm Based on ECG Curve Length Transform",Comp. in Card., 1:44-48

[79] McLaughlin, N. B., Campbell, R.W. F., Murray, A.(1996). "Accuracy of four automatic QT measurement techniques in cardiac patients and healthy subjects",Heart, 76:422-426

[80] Quizhen, Xue, Shankara, Reddy, (1996). "Algorithms for Computerized QT analysis", Journal of Electrocardiology 30:121-134

[81] Napolitano, C., Diem, L., Paganini V. et al(2002). "Principal component analysis identifies abnormal complexity of repolarization in post myocardial infarction patients.", J Am Coil Cardiol,74:56-77

[82] Malik M, Batchvarov VN, (2000). "Measurement, interpretation and clinical potential of QT dispersion.", J Am Coll Cardiol,;36:1749-1766.

[83] Alex Dmıtrenko, Brian P. Smith, (2002). "Analysis of the QT interval in clinical trials", Drug information Journal, 36:269-279

[84] Hayn, D., Kollman, A. Schreier, G., (2006)."Automated QT interval Measurement from Multilead ECG signals", Computers in Cardiology, 33:381-384

[85] McLaughlin N.B, Campbell R.W.F, Murray A, (1995),"Comparison of automatic QT measurement techniques in the normal 12 lead electrocardiogram.", Br Heart J., 74:84-89.

[86] Alan Murray, Neil B McLaughlin, John P Bourke, J Colin Doig, Stephen S Furniss, Ronald W F Campbell,(1994). "Errors in manual measurement of QT intervals", Br Heart_J,71:386-390

[87] Langley, P., Smith, F.E. , King, S.T., Zheng, D., Haigh, A.J., Murray, A., (2006). "Fully Automated Computer Measurement of QTInterval from the 12-Lead Electrocardiogram", Computers in Cardiology, 33:345−348.

[88] II, Christov1., II, Simova2., (2006). "Fully Automated Method for QT Interval Measurement in ECG", Computers in Cardiology,33:321−324.

[89] Toshio, Tsuji, Osamu, Fukuda, Hiroyuki, Ichinobe, Makoto, Kaneko, (1999), "A log-linearized Gaussian mixture network and its application to EEG pattern classification", IEEE Trans Syst Man Cybern C Cybern,29(1):45-67

[90] Wu, F.Y., Slater J.D., Honih, L.S. and Ramsey, R.E.,(1993). "A neural network for event-related potential diagnosis", Computational Biol. Machine, 23(3):251-264

[91] Schaltenbrand, N., Lengelle, R., and Macher J.P.,(1993), "Neural network model: Application to automatic analysis of human sleep", Computational Biomed.Res.26(2):157-171

[92] RumelHart, D.E. and McClelland, J.L., Parallel Distributed Processing, Explorations in the Microstructure of Cognition,(1986),MIT Press,Cambridge

[93] Montgomery, D.C. and George C. Runge,(2006), Applied Statistics and Probability for engineers, fifth edition, John Wiley&Sons, New York

[94] Jensen, J. L. W. V. (1906). "Sur les fonctions convexes et les inégalités entre les valeurs moyennes". Acta Mathematica 30 (1): 175–193

[95] McCulloch, Warren; Walter Pitts (1943). "A Logical Calculus of Ideas Immanent in Nervous Activity". Bulletin of Mathematical Biophysics **5** (4): 115–133.

[96] Hebb, Donald (1949). The Organization of Behavior. : Wiley, New York

[97] Rosenblatt, F. (1958). "The Perceptron: A Probalistic Model For Information Storage And Organization In The Brain". Psychological Revie. 65(6): 386–408

[98] Werbos, P.J. (1975). Beyond Regression: New Tools for Prediction and Analysis in the Behavioral Sciences, MIT Press, Cambridge

[99] Carpenter, G.A., Ross, W.D., (1995). "ART-EMAP: A neural network architecture for object recognition by evidence accumulation", IEEE Transactions on Neural Networks, 6:805–818

[100] Carlo J. De LUCA,(1976) "Physiology and Mathematics of Myoelectric Signals", IEEE Trans. On. Biomed. Eng., 26(6):45-66

[101] Shen, T. W. , Tompkins W. J. and Hu Y. H., (2002). "One-lead ECG for identity verification", Proc. 2nd Joint EMBS/BMES. 1:62-63

[102] Steven, A. Israela, John M. Irvineb, Andrew Chengb, Mark D. Wiederholdc, Brenda K. Wiederholdd,(2005).”ECG to identify individuals”, Pattern Recognition, 38:133 – 142

[103] Philip, de Chazal, Member, IEEE, Maria O’Dwyer, and Richard B. Reilly, Senior Member, IEEE, (2004). ”Automatic Classification of Heartbeats Using ECG Morphology and Heartbeat Interval Features”, IEEE Trans. On. Biomed. Eng, 51(7):133-151

[104] Rodrigo, V. Andreao, Bernadette Dorizzi, Jerome Boudy, (2006). ”ECG signal analysis through hidden markov models”, IEEE Trans. On. Biomed. Eng 53(8):67-88

[105] Sung-Nien, Yu, Ying-Hsiang Chen,(2007). ”Electrocardiogram beat classification based on wavelet transformation and probabilistic neural network”, Pattern Recognition Letters,28:1142–1150

[106] Roshan, Joy Martisa, Chandan Chakrabortya, Ajoy K. Raya,b, (2009). “A two-stage mechanism for registration and classification of ECG using Gaussian mixture model”, Pattern Recognition,42:2979-2988

[107] Saxena, S.C., Kumar, V., Hamde, S.T., (2002). “Feature extraction from ECG signals using wavelet transforms for disease diagnostics”, International Journal of Systems Science,33(13):1073–1085

[108] Hyejung Kim, Refet Firat Yazicioğlu, Patrick Merken, Chris Van Hoof, Hoi-Jun Yoo, (2010). “ECG signal compression and classification algorithm with quad level vector for ECG holter system”, IEEE Trans. on info. tech. in biomed., 14(1):556-578

[109] Toshio, Tsuji, Osamu, Fukuda, Hiroyuki, Ichinobe, Makoto Kaneko,(1999), ”A log-linearized Gaussian mixture network and its application to EEG pattern classification”, IEEE Trans. on. sys.,man,and cyber- part C, app. and rev. 29(1):56-88

[110] M. Okamoto, K. Shima, Y. Matsubara, T. Tsuji,(2008). “Pattern discrimination method with a boosting approach using hierarchical neural trees”, J. Systems and Control Engineering, 222:78-88

[111] Goldberger, A.L., Amaral, L.A.N., Glass L., Hausdorff JM, Ivanov PCh, Mark RG, Mietus JE, Moody GB, Peng C-K, Stanley HE(2000). "PhysioBank, PhysioToolkit, and PhysioNet: Components of a New Research Resource for Complex Physiologic Signals.", Circulation,101(23):215-220

CURRICULUM VITAE

PERSONAL INFORMATION

Name Surname	: Mehmet İŞCAN
Date of birth and place	: 16.05.1991 / Tekirdağ
Foreign Languages	: English
E-mail	: miscan@yildiz.edu.tr

EDUCATION

Degree	**Department**	**University**	**Date of Graduation**
Undergraduate	Mechatronic Engineering	Yıldız Technical University	18.06.2013
High School	Teacher School		12.06.2009

WORK EXPERIENCE

Year	**Corporation/Institute**	**Enrollment**
2012	Yıldız Technical University Central Lab	2010
2013	Alarge Alıç Ağacı Mak. Elek. Ar-Ge San.	2012

	Tic. Ltd. Şti	
2016	Yıldız Technical University Mechatronic Engineering	2014

PUBLISHMENTS

Conference Papers

1. Mehmet İşcan; Cüneyt Yilmaz; Faruk Yiğit, " Arrhytmic and Non-Arrhytmic Heartbeat Classification based on Gaussian MixtureModel", DOI: 10.1109/EBBT.2016.7483686, Pages 1 - 4, 2016

2. Mehmet İşcan; Cüneyt Yilmaz; Faruk Yiğit, " T-wave end pattern classification based on Gaussian mixture model", DOI: 10.1109/SIU.2016.7496149, Pages 1953 - 1956, 2016

3. Mehmet İşcan, Faruk Yiğit, Cüneyt Yilmaz," Heartbeat Pattern Classification Algorithm Based on Gaussian Mixture Model", Inter. Symp. on Med. Meas. and App., Italy,2016

Projects

1. Vacum Coating Device Design, Supported by Coordinatorship of Scientific Research Projects, YTU, 2013

2. T Wave Alternans Test Device Design and Its Software Application, Supported by the Minister of Science, Industry and Technology,Turkey, Grant No: TGSD.0493.2015.

AWARDS

1. Tübitak 1601, Entrepreneurship Academy, June, 2014

2. Third Prize with Vacum Coating Device Design, "Sanayi Odaklı Bitirme Projeleri Yarışması", Tübitak, July2013

3. Graduate Ranking Second in Class, Bachelor's Degree, YTU, July, 2013